Flow characteristics of groundwater systems: An investigation of hydraulic parameters

by

Khahliso Clifford Leketa

THESIS

Submitted in the fulfilment of the requirement for the degree of

Master of Science

In the Faculty of Natural and Agricultural Sciences

Institute for Groundwater Studies

University of the Free State

Bloemfontein

May 2011

Supervisor: Prof. G Steyl

Declaration

I, Khahliso Clifford Leketa declare that; this thesis hereby submitted by me for the Master of Science Geohydrology degree in the Faculty of Natural and Agricultural Sciences, Institute for Groundwater Studies at the University of the Free State is my own independent work. The work has not been previously submitted by me or anyone at another university. I furthermore cede the copyright of the thesis in favour of the University of the Free State.

Khahliso Clifford Leketa

2008052298

Acknowledgements

No one has ever done anything great alone.

I would therefore want to acknowledge the following people for their contribution and assistance in the period of my study:

Water Research Commission of South Africa and Prof G. Steyl for financial assistance during the period of my study. Without financial assistance, this study could have been but a dream. Hence I pass my sincere thanks to them.

Government of Lesotho through the National Manpower Development Secretariat (NMDS) for the academic assistance since the commencement of my Tertiary education in 2004,

Director of Water Affairs (Lesotho) Mr Mokake Mojakisane and Mr Thabiso Mohobane (senior engineer and boss) for standing against all odds that hindered me to further my studies in 2009 but opened new channels for me to get sponsorship to study further,

My Supervisor Prof. Gideon Steyl for his massive study guidance through my research, always making sure that the study environment is conducive and that all material is available from mere stationary (pens) to study permit and medical aid. Thank you Prof!

Prof. Gerrit Van Tonder for his inspiration and meaningful ideas on the appropriate field procedures to follow in order to meet the study objectives,

Field work operations were made possible by the involvement of my colleagues Funnie de Lange (PhD Student), Modreck Gomo (PhD Student), and Teboho “Shakes” Shakhane (fellow MSc student). Without their support and strong passion for field work, none of these could have happened,

The whole of IGS family (Institute for Groundwater studies):

- Lorinda Rust for her motherly love , Mr Peter Mokgobo and Mrs Dora du Plessis for being there,
- Dr Danie Vermeulen, Dr Rainier Dennis, Dr Ingrid Dennis, Prof Gerrit Van Tonder, Prof Gideon Steyl for their academic advice and Mr Eelko Lukas for his assistance with WISH program.

Mathilde Luise “Lulu” Pretorius (MSC student in Environmental Management at UNISA and UFS-soil science department) for the assistance with soil analysis and particle distribution,

My Pastors, (Mr) Festus and (Mrs) Sikhanyisile Ndlovu for their encouragement on my studies and always motivating me to aim higher in life,

Most of all my family:

My late Grandma (Maphomolo E Tjapela) who used to wake me up for secondary school in the morning and telling me “haho khomo ea boroko” which means, “there is no reward for sleeping”. She taught me that education is a key to success!

My mother, two sisters and late father who have been supporting me through my studies all the way, I love you and I thank God almighty for you!

Last but most importantly, the Lord Jesus Christ my saviour. Without Him being on my side, I can’t tell how I would have survived. *I never would have made it without Him*.

He who thinks it is impossible should not discourage the one doing it-Chinese proverb.

He who said it cannot be done was suddenly interrupted by the one who just did it.

Contents

Declaration i
Acknowledgements ii
Contents iv
List of Figures vii
List of Equations x
List of Tables xi
1 INTRODUCTION 1
1.1 Purpose of the study 1
1.2 Scope of the study 1
1.2.1 Aim 1
1.2.2 Specific objectives 2
1.3 Thesis structure 2
1.4 Site description 3
1.4.1 Location of site 3
1.4.2 Climate 4
1.4.3 Vegetation, land, and water uses 5
1.4.4 Topography and hydrology 8
1.4.5 Geology 12
1.5 Conclusion 13
2 INVESTIGATION APPROACH AND RESEARCH METHODOLOGY 14
2.1 Introduction 14
2.2 Desktop study 15
2.3 Fieldwork 15
2.3.1 Site inspection study and drilling 15
2.3.2 Water level monitoring 16
2.3.3 Hydraulic tests 16
2.3.4 Tracer tests 19
2.3.5 Hydrochemistry and environmental isotope sampling and analysis 20
2.4 Data interpretation 21
2.4.1 Hydrochemistry analysis 21
2.4.2 Environmental isotope analysis 25
2.4.3 Aquifer parameters 28

2.4.4 Recharge 30
2.4.5 Groundwater flow direction 32
2.5 Conclusion 34
3 GEOLOGY 35
3.1 Introduction 35
3.2 Regional Karoo geology and hydrogeology 35
3.3 Site geology 39
3.3.1 Desktop study 40
3.3.2 Visual land surface inspection 40
3.3.3 Drilling 45
3.3.4 Unconsolidated surface soil matter-Soil analysis 49
3.4 Conclusion and geological conceptual model 54
4 BOREHOLE CONSTRUCTION, NETWORK DESIGN, AND FLOW BEHAVIOUR 57
4.1 Introduction 57
4.2 Network design and borehole construction 57
4.3 Natural groundwater behaviour on site 60
4.3.1 Change of Water level with time 60
4.3.2 Natural recharge and discharge 62
4.3.3 Groundwater flow direction 64
4.4 Conclusions 68
5 HYDRAULIC CHARACTERIZATION 70
5.1 Introduction 70
5.2 Aquifer tests/pumping tests 70
5.2.1 Slug test 70
5.2.2 Constant discharge test 72
5.3 Tracer tests 75
5.3.1 Point dilution test 75
5.4 Conclusions 77
6 CHEMICAL CHARACTERIZATION AND ISOTOPE ANALYSIS 78
6.1 Introduction 78
6.2 Hydrochemistry characterization 78
6.2.1 Macro elements data analysis 79
6.2.2 Trace element data analysis 83

6.3 Environmental isotope analysis 84
6.3.1 Non-radioactive ^{18}O and ^{2}H 84
6.3.2 Radioactive tritium 86
6.4 Conclusion 89
7 CONCLUSIONS AND CONCEPTUAL MODEL 91
7.1 Introduction 91
7.2 Conclusion 91
7.2.1 Geology 91
7.2.2 Groundwater flow behaviour, discharge and recharge 92
7.2.3 Aquifer parameters 92
7.2.4 Hydrochemistry 92
7.3 Conceptual model 93
8 REFERENCES 97
9 APPENDIXES 101
9.1 Appendix A: Geology 101
9.2 Appendix B: Hydraulic tests 109
9.3 Appendix C: Natural Groundwater Behaviour 115
9.4 Appendix D: Chemistry 117
Summary 120

List of Figures

Figure 1-1: Location of the Krugersdrift study site in Free State, South Africa 4
Figure 1-2: Change in rain fall in year 2010 to Jan 2011..... 5
Figure 1-3: Large pumps drawing water from the Modder River on the opposite side of the river 6
Figure 1-4: Water requirement for irrigation and urban use in the Modder River catchment (Kinyua, et al. 2008, p. 242). 7
Figure 1-5: The Oryx that live on the western side..... 7
Figure 1-6: Land use summary and geological features. 8
Figure 1-7: Modder River catchment drainage showing the pans and tributaries that constitute the catchment. (Department of Environment and Tourism; 2001).....10
Figure 1-8 : Topography of the Modder River catchment (addapted from Kinyua et al. 2008)....11
Figure 1-9: The elevation contour map of the study area showing two points and their elevations. 12
Figure 1-10: Typical rounded pebbles and gravel obtained during drilling in all boreholes at varying depths.....13
Figure 2-1: Flow Diagram-Research Approach 14
Figure 2-2: Spatial distribution of sites that were sampled. 20
Figure 3-1: The simplified geological map of South Africa showing the approximate location of the study area. (www.geoscience.org.za).....37
Figure 3-2: Matrix and fracture flow in Karoo aquifers (adapted from Fourie, FD, 2003). 38
Figure 3-3: Photograph of micro fractures in 0.25mm quarts grains, from a core sample of the campus Test Site. (Botha *et al*, 1998). 39
Figure 3-4: Calcrete outcrops on the land surfaces. 41
Figure 3-5: Geological profile on the river banks of the Modder River adjacent to the study site. 41
Figure 3-6: Vertical cross-section of the geology that makes the river bank.....42
Figure 3-7: Clay caused as a result of excessive weathering of shale. 42
Figure 3-8: Spring water seeping through the shale layers 43
Figure 3-9: The Mudstone river bed and the position of the weir relative to the mudstone mass. 44
Figure 3-10: Dolerite dyke across the river bed. 44
Figure 3-11: Percentage composition of soil in six soil classes.....52
Figure 3-12: percentage composition of the soil samples in three class separations 52
Figure 3-13: Soil textural triangle used for determination of soil type on site.....53

Figure 3-14: The production of CO2 from the reaction of dilute HCl and Carbonates in the soil. 54
Figure 3-15: Air percussion drilling machine in action on site 45
Figure 3-16: Geological samples and logging showing BH10 geology profile 47
Figure 3-17: Elevation comparisons of geology and hydrogeological features. 49
Figure 3-18: Geological Conceptual model of the study area (Not drawn to scale). 56
Figure 4-1: The aerial view of the boreholes that were drilled on site showing the river flow direction 57
Figure 4-2: Sanitary seal of the boreholes. 58
Figure 4-3: Theodolite and staff used for surface elevation survey 59
Figure 4-4: Screening of PVC casings for borehole construction. 59
Figure 4-5: Sketch of the Borehole casing as performed on-BH10 60
Figure 4-6: The correlation of water-levels with surface elevations 61
Figure 4-7: Change of groundwater water levels with time for the 6 months period 61
Figure 4-8: Seepage zone along the river bank. 63
Figure 4-9: Yield measurement technique that was followed 64
Figure 4-10: Groundwater flow direction as determined on triangle 1. 65
Figure 4-11: Groundwater flow direction as determined from boreholes BH10, BH11 and BH12. 66
Figure 4-12: Groundwater flow direction determined from a bigger triangle 1 67
Figure 4-13: Groundwater flow direction versus change in topography (green dashed arrows are groundwater flow direction; black dotted arrows are topography slope direction). 68
Figure 4-14: Summary of groundwater flow direction on site 69
Figure 5-1: Correlation between recession time vs. borehole yields (representing BH10) 71
Figure 5-2: The comparison of estimated yields among slug tested boreholes. 72
Figure 5-3: Cooper Jacob plot for pumping duration for determination of Transmissivity in BH10 73
Figure 5-4: Recovery plot for BH10 73
Figure 5-5: Estimated Transmissivity values from constant rate test. 74
Figure 5-6: Standardized decay of EC concentrations for BH12 point dilution 76
Figure 6-1: Piper diagram of all the sampled hydrochemistry data 79
Figure 6-2: Durov diagram of all the sampled hydrochemical data 80
Figure 6-3: SAR diagram of all sampled hydrochemistry data 82
Figure 6-4: STIFF diagrams for all the sampled hydrochemistry data 83
Figure 6-5: Bar graph of all the trace elements data 83

Figure 6-6: $\delta^{18}O$ versus $\delta^{2}H$ for groundwater in the alluvium aquifers. 84
Figure 6-7: $\delta^{18}O$ versus $\delta^{2}H$ plot for shallow and deep boreholes 85
Figure 6-8: Correlation of tritium with pH of sampled sites 89
Figure 6-9: Correlation of chloride concentrations with EC values. 90
Figure 7-1: Geological conceptual model of the study area showing how geology changes from inland to the river. 93
Figure 7-2: Conceptual model seepage flow through gravel and shale formations on the site. ..94
Figure 7-3: Conceptualized groundwater flow in the study system. 95
Figure 7-4: Summary of hydraulic parameters (spatial distribution of transmissivity and Darcy velocity over the study area as obtained from Cooper Jacob plots). 96

List of Equations

Equation 2-2: Calculation of δ notation on isotope concentrations. 25
Equation 2-3: Global Meteoric Water Line 27
Equation 2-4: Transmissivity as product of hydraulic conductivity and aquifer thickness. 28
Equation 2-5: Logan equation for determination transmissivity. 28
Equation 2-6: A qualified guess estimate of transmissivity. 28
Equation 2-7: Specific discharge (Darcian velocity) 30
Equation 2-8: Darcy velocity equation. 30
Equation 2-9 : Hydraulic gradient determination. 33
Equation 5-1: Electric conductivity-concentration standardizing equation. 75
Equation 5-2: Darcy velocity equation by Drost et al (1968). 76

List of Tables

Table 2-1: Some Environmental isotopes used in hydrogeological studies (Appelo *et al.*, 2005) 26
Table 2-2: Hydraulic conductivities of some rock types and unconsolidated matter (Brassington, 1998) 29
Table 3-1: Water strikes and depths of boreholes 48
Table 3-2: Percentage composition of sampled soil showing six fractions 51
Table 3-3: Percentage composition of soil in three soil classes 52
Table 4-1: The construction information of the boreholes including the positions of the water strikes. 58
Table 5-1: Slug test results.....71
Table 5-2: Transmissivity values obtained from the constant rate tests. 74
Table 5-3: Geometric means of Darcy velocities obtained from point dilution test. 77
Table 6-1: Irrigation water type based on EC values (from IGS laboratory). 80
Table 6-2: Irrigation water type based on SAR values (from IGS Laboratory). 81
Table 6-3: Tritium concentrations and groundwater aging. (William, 2000).....87
Table 6-4: Tritium concentrations in groundwater.....88

List of Abbreviations

Mamsl	meters above mean sea level
Mbgl	meters below ground level
IGS	Institute for Groundwater Studies
TLC	Temperature Level Conductivity *Meter*

1 INTRODUCTION

1.1 Purpose of the study

The general purpose of this study is to determine an initial set of aquifer parameters that shall be used for future groundwater surface water interaction studies at the Modder River study site.

Most of South Africa is underlain by the Karoo Supergroup which is characterized by low permeability formations; hence most of the boreholes drilled in the Karoo have low yields (<1 l/s). Because of the fore mentioned Karoo characteristics, in South Africa, groundwater is said to be an unreliable source of water. Woodford and Chevallier (2002) stated that Groundwater contributes only 10 % to the national water budget.

Studies show that the Modder River catchment like many other South African catchments is being exploited beyond its limits with a great percent of water being used for irrigation agricultural purposes. According to Kinyua *et al* (2008), the limited availability of water resources in the catchments means that only a portion of the irrigation demand estimated at 55.5 %, can be met by the existing water supply within the catchment, whereas 97.7 % of the urban water requirement seems to be met. It is also estimated that 74 % of the total water requirement is for irrigation purposes compared with 26 % for urban water need. This means that the water requirement for irrigation places a large demand and pressure on water resources within the catchment.

For the purposes of water conservation and groundwater surface water interaction, there is a need to study the near river aquifer systems. This is done so that the guidelines may be set as to how much should be abstracted in a catchment for a particular use, and how far from the river should a borehole be drilled. Thus there is a need to quantify groundwater usage and availability in the Modder River catchment through determining the aquifer parameters that dictate the amount of groundwater that can be accessed from the catchment aquifers. Hence the aim of this study is to determine the hydraulic parameters of the near river aquifers of the Modder River system as a first step in this process.

1.2 Scope of the study

1.2.1 Aim

- This study aims to characterize the hydrogeology of the site along the banks of the Modder River downstream of Krugersdrift Dam. Characterization of aquifer hydrogeology

entails the study of the aquifer formation, groundwater flow behaviour, the physical hydrogeological parameters of the aquifer, and the biological and chemical hydrological parameters in the aquifer system.

1.2.2 Specific objectives

- Geological characterization and soil analysis. Use of site investigation (desktop study), surface inspection and borehole geological logs in order to construct a geological conceptual model.
- Chemical characterization including isotope analysis. Analysis of groundwater chemical data from boreholes, seepage (spring) and surface water bodies. Chemical characterization is made based on the macro elements, trace elements, and isotopes (^{18}O, ^{2}H, ^{3}H). Chemical characterization was done in order to give an understanding of the suitability of groundwater for different uses.
- An investigation of groundwater flow characteristics and hydraulic parameters by use of aquifer tests (pumping tests and tracer tests).
- Investigation of groundwater level behaviour by use of water level time series, natural discharge and recharge.

1.3 Thesis structure

Chapter 1 introduces the study site by focussing on the natural features locally and regionally.

Chapter 2 highlights the investigation approach and research methodology that was followed in this study. This chapter discusses every tool that was used to characterize the aquifer system.

Chapter 3 discusses the geology of the study area, including all the methodology that was applied for geological characterization. The methodology includes steps such as desktop study, surface inspection and analysis of geological cuttings from the air percussion drilling.

Chapter 4 illustrates the design of the borehole network including their orientation in the study area, their location and altitude and the processes that were undertaken to develop and construct the boreholes. It also looks at the groundwater behaviour in terms of flow direction in the study area, water level fluctuation over time and recharge calculations.

Chapter 5 discusses the pumping and tracer test procedure that was followed for hydraulic characterization.

Chapter 6 discusses the hydrochemistry (macro elements and trace elements) including isotope analysis for previous water flow path and its source.

Chapter 7 looks at the conceptual model which includes all parameters that were obtained in the study. It also shows the graphical view of the conceptual model and the conclusions reached in the study.

1.4 Site description

1.4.1 Location of site

The study area is in the Free State province, Krugersdrift about 35 km north-west of Bloemfontein city, South Africa. The area is in the South Western part of the Free State province. The site is 790 meters downstream of the Krugersdrift Dam (approximately 25.9505° E, 28.8887° S). The site is located 250 m from the Modder River which runs generally south-west of the Krugersdrift Dam.

This area falls within the *Kalkveld* (Afrikaans word for calcrete field) which is characterised by calcrete surface outcrops and calcite rich top soil. Figure 1-1 shows part of the map-sheet *2528AB* where the study site is located.

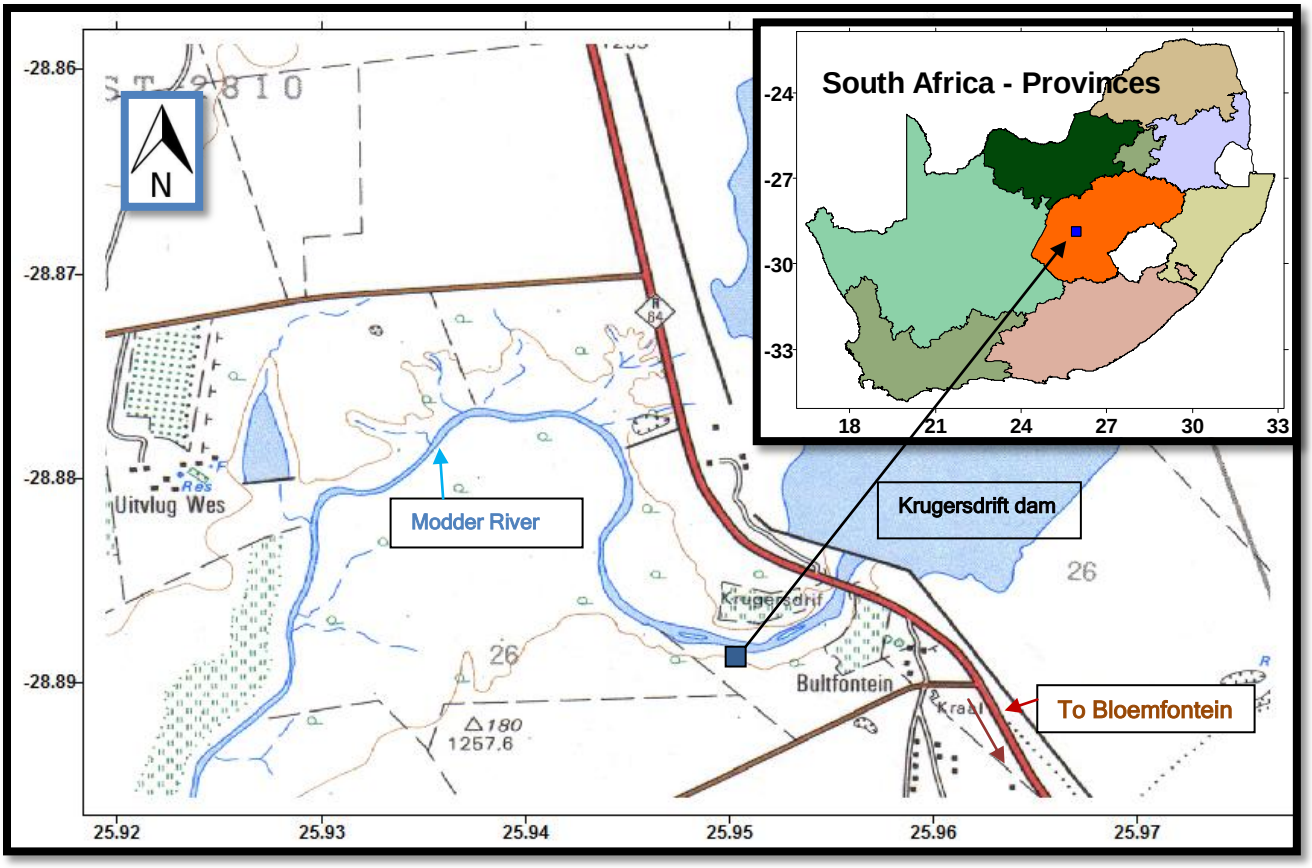

Figure 1-1: Location of the Krugersdrift study site in Free State, South Africa

1.4.2 Climate

The Modder River basin is characterized by low and unpredictable seasonal rainfall with annual average precipitation of 550 mm (Kinyua *et al.*, 2008). Studies show that the highest rainfall in the Modder River catchment is experienced starting January to March and the lowest from June to August. For the year 2010, rain fall followed almost a similar trend by decreasing from 133.3 mm in January to 0 mm in July and then increased in October as shown on Figure 1-2. The area is therefore characterized as a summer rainfall area. The total annual rainfall was 588 mm for the year 2010.

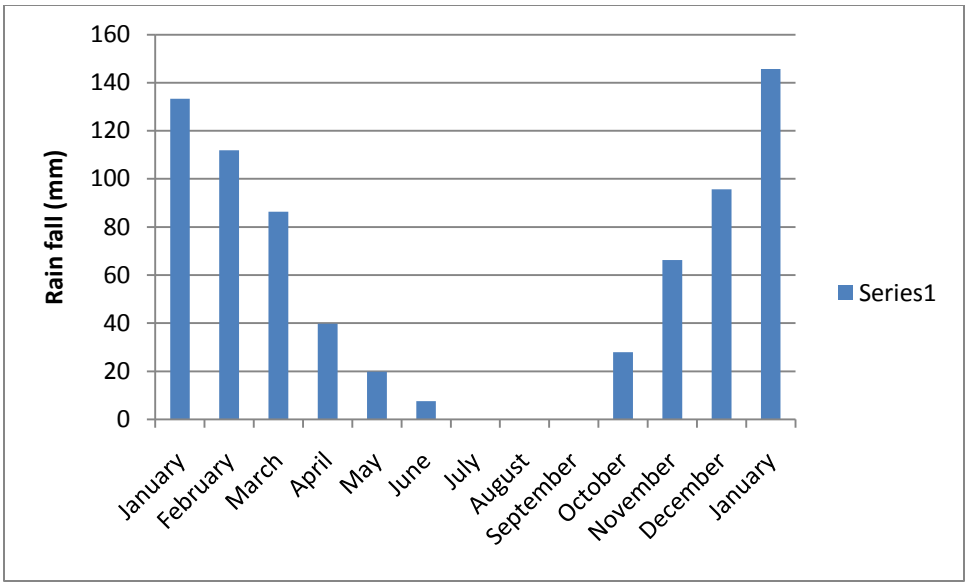

Figure 1-2: Change in rain fall in year 2010 to Jan 2011

Usher (2005) states that a study was done on the Kalkveld to further understand the climate of the area. In this study, the average yearly rainfall from a Bloemfontein weather station was recorded as 559 mm. Rainfall data was obtained from three other weather stations namely, Petrusburg, Dealesville, and Krugersdrift Dam. To further understand rainfall patterns of the area, three more rainfall data loggers were installed in the proximity of the town.

After Usher (2005) compiled all rainfall data, it was observed that there is a great spatial variability in rainfall across the area. The highest average annual rainfall was recorded at Bloemfontein (560 mm/a) and the lowest annual rainfall at Petrusburg (390 mm/a).

The evaporation rate at Dewetsdorp where the Modder River originates is 1500 mm per year and where the Modder River converges with the Riet River the annual evaporation is 2100 mm per year (DEAT, 2001). There is therefore more rainfall in the lower reaches of the catchment than there is up the catchment.

1.4.3 Vegetation, land, and water uses

Much of the area within the Modder River catchment is used for cattle and game farming in the west and sheep farming towards the east (with up to 75 % of the land-use being natural grass land and Bossieveld). The irrigated agriculture in the basin is sustained by pumping out water from the river pools and weirs. Figure 1-3 shows the large pumps that are used for agricultural purposes on the Western side of the river. The domestic, agricultural and industrial water users of the Modder catchment are heavily reliant on the Modder River for water supply. According to

the estimates, these are already exploiting the Modder River catchment to the limits of sustainability (Kinyua *et al.*, 2008).

Figure 1-3: Large pumps drawing water from the Modder River on the opposite side of the river

Figure 1-4 compares water use in upper, middle and lower Modder River. Irrigation farming in the catchment is mainly practiced in the lower reaches (middle and lower Modder River) of the river and it takes much more water than any other water use activity within the catchment. Due to the low rainfall and soil type which is prone to crusting, farmers frequently encounter scarcity of soil water which results in low crop yields. Crop farmers are therefore forced to go for a costly approach of drawing large amounts of water from the groundwater and surface water bodies. These climatic and environmental situations are believed to be discouraging small scale farmers to produce their own food (Kinyua *et al.*, July 2008).

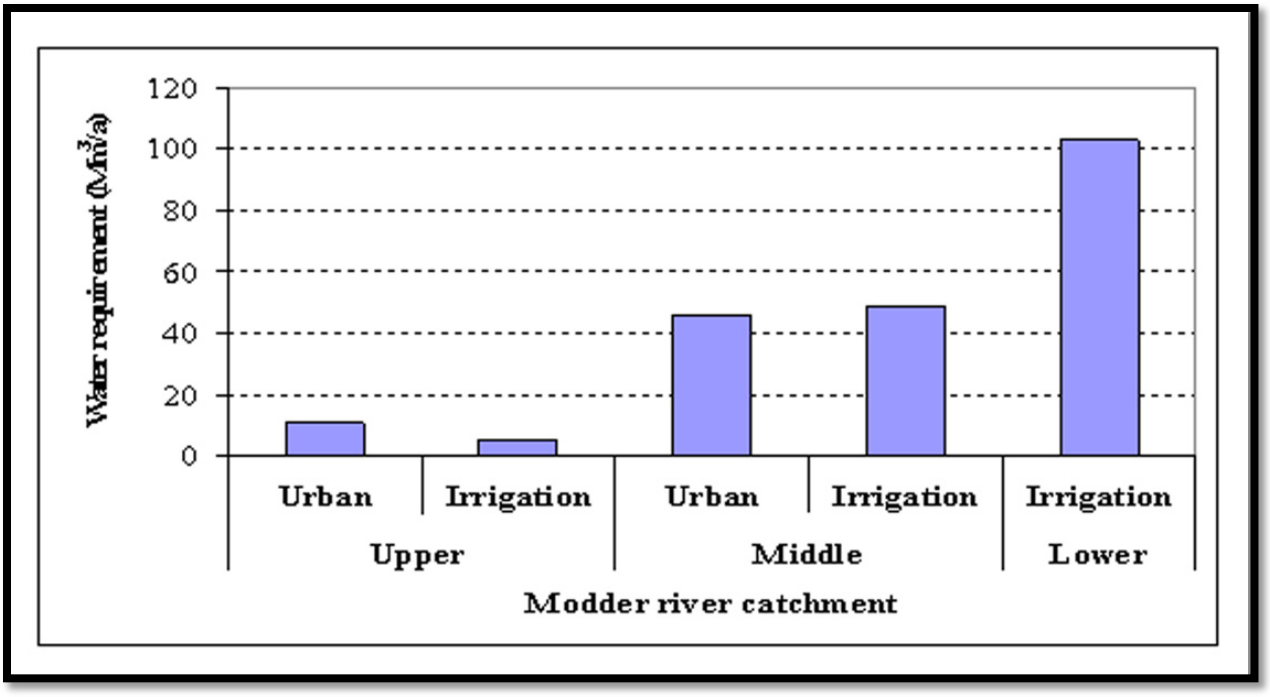

Figure 1-4: Water requirement for irrigation and urban use in the Modder River catchment (Kinyua *et al.*, 2008).

The immediate area (on the western side of the river) is a wild animal nature reserve a home for animals like impala, monkeys, springboks, ostriches, tortoises and many other herbivores as seen on Figure 1-5.

Figure 1-5: The oryx that live on the western side.

Figure 1-6 presents a collective summary of the land use of the area and some features of hydro-geological interest which shall be discussed in the forthcoming chapters (Chapter 3: Geology).

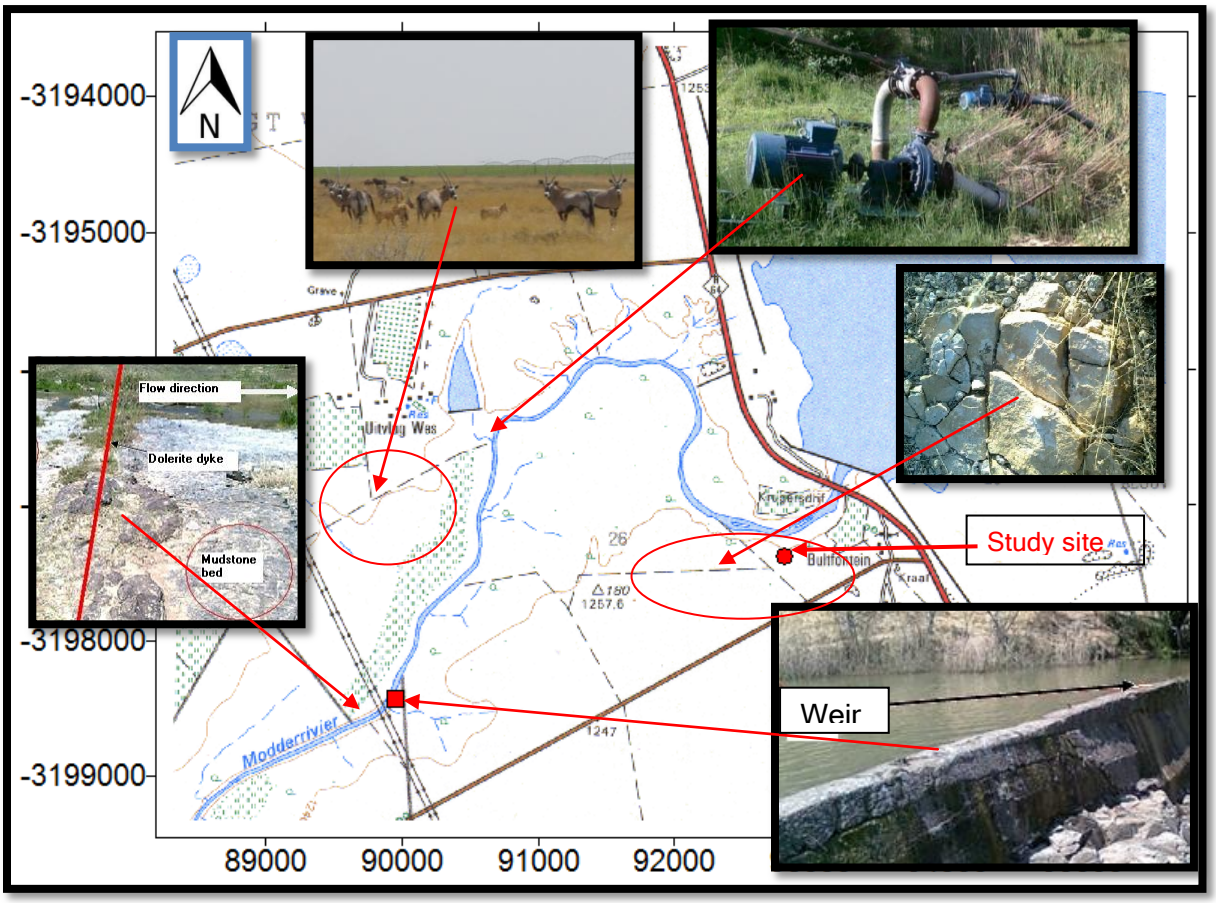

Figure 1-6: Land use summary and geological features.

1.4.4 Topography and hydrology

1.4.4.1 Introduction

The water table in an unconfined aquifer usually follows the shape of topography by flowing towards the direction in which topography is sloping. This therefore means that in an unconfined aquifer, there is a high correlation between topography and water levels. In this case then, topography may give a picture of the direction in which groundwater flows. When water reaches the water table, it no longer flows vertically but rather horizontally to the direction of slope at the rate that depends on the permeability of the formation. The water table slope depends on the formation permeability and on the rate at which water is added to the system. Topography also has a huge impact on the amount of recharge that occurs in an area, the more steep the topography the more run-off and the less recharge.

1.4.4.2 Hydrology

The study site falls within the Modder River catchment which has a surface area of approximately 17 400 km^2. The Modder River Basin is the main drainage feature in the Free State Province.

The Modder River was initially a seasonal river like many other traditional inland rivers in South Africa but due to the construction of the three significant dams, i.e. Rustfontein, Mockes and Krugersdrift dam the river now resembles a permanent river (Raboroko, 2005). But the characteristics of the seasonality of the Modder River are still witnessed in the catchment whereby the dams can go up to full in rainy seasons while the water in the lower reaches is basically stagnant in winter during dry season. The Modder River catchment comprises the Modder River and the Riet River whose sources are in the hills near Devertsdorp at an altitude of 1600 mamsl. The Modder River has a number of tributaries. Most of the main tributaries are clustered north of Botshabelo near Rustfontein dam. This cluster includes the Kaal, Os, Doring, Renoster, Koranna, Sepane, Klein Modder, Krom River, and the Gonnaspruit as shown on Figure 1-7.

The Modder River catchment has two major dams namely Rustfontein and Krugersdrift dam. Flow from Rustfontein goes generally north-west into Krugersdrift dam. The water from Krugersdrift dam flows westwards past Kimberly and later joins the Riet River. Below Krugersdrift Dam, the river flows through a very low gradient terrain where numerous pans are found. These pans are filled at the end of good summer rain fall but they seldom overflow (Raboroko, 2005).

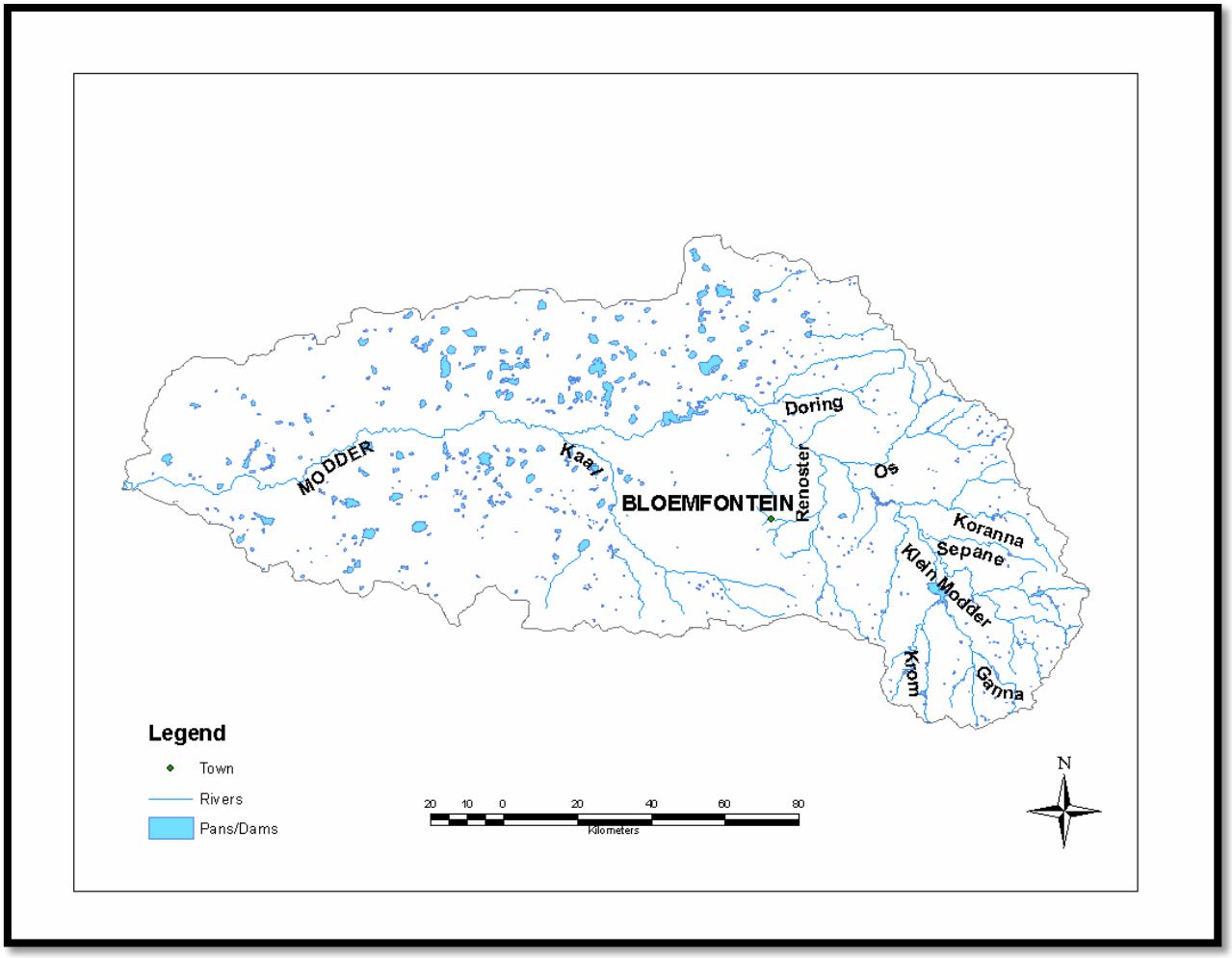

Figure 1-7: Modder River catchment drainage showing the pans and tributaries that constitute the catchment. (DEAT, 2001)

1.4.4.3 Topography

The Kalkveld has a generally flat topography broken only by drainage lines and the occasional flat topped hills. Figure 1-8 shows the map of the Modder River catchment showing the elevation of the catchment and the three sub-catchments of the Modder River catchment. Most of the Modder River catchment is relatively flat with limited high elevation surfaces. There are a number of pans within the low-gradient western half of the Modder River catchment. These pans are filled in summer after the rainfall but they hardly overflow (Usher, 2005). This therefore means that there is little runoff and possible recharge positions since:

Precipitation - Evapotranspiration = Recharge

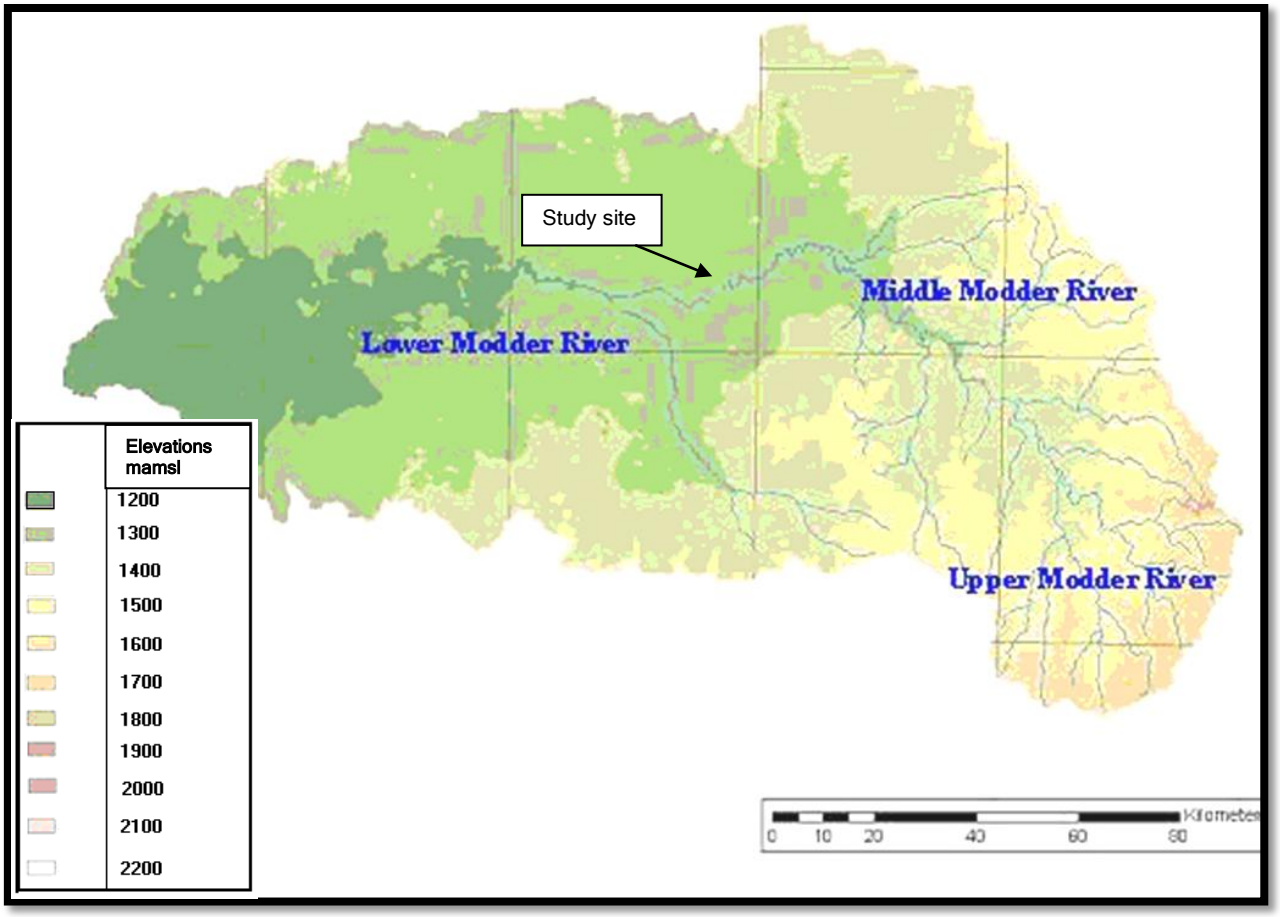

Figure 1-8 : Topography of the Modder River catchment (adapted from Kinyua et al. 2008).

Figure 1-9 presents the position of the study site on the sloping topography. This area is positioned along the slope between the points 1243 mamsl (low) and 1249 mamsl (high) which are 240 m apart. This makes a general slope of 0.03.

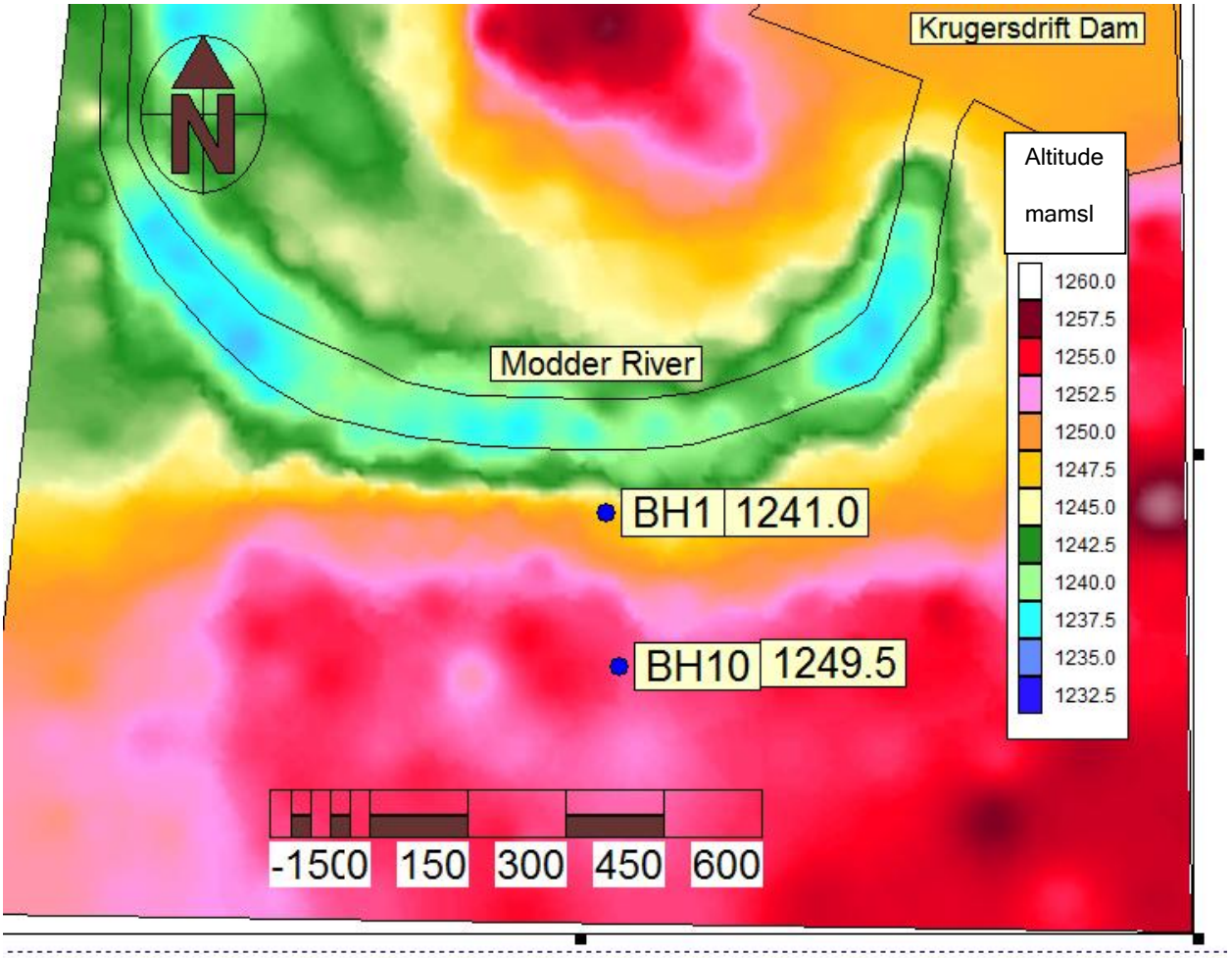

Figure 1-9: The elevation contour map of the study area showing two points and their elevations.

1.4.5 Geology

The geology of the area is mainly sedimentary rocks of the Karoo supergroup that is dominated by the mudstones and shale at varying depths. The surface of the area is covered by calcite rich soil and consolidated outcrops which were observed during land surface inspection. The geological cuttings from all the boreholes showed the presence of alluvium sand with rounded highly oxidized mudstone pebbles and rough gravel at an average depth of 12 mbgl where the water strike was observed. Figure 1-10 shows the pebbles and gravel as obtained from the boreholes; the in-depth description of the site geology is given on Section 3.3.

Figure 1-10: Typical rounded pebbles and gravel obtained during drilling in all boreholes at varying depths.

1.5 Conclusion

This chapter introduces the thesis objectives and the study area. It looks into the study area location, climate, vegetation, topography, hydrology and geology. The study area is characterized as a summer rainfall area within an average annual rainfall of 550 mm. The geology of the area is characterized by surface calcrete formation and a spread of gravel water bearing formation at the average depth of 12 mbgl where the water strike occurred. Now that the study site has been defined, the next chapter looks at the methodology that was undertaken to meet the project objectives.

2 INVESTIGATION APPROACH AND RESEARCH METHODOLOGY

2.1 Introduction

Depending on the objective of the study, different techniques are applied in order to meet the study objectives. This chapter aims to present the methodologies that were applied on the study to characterizing the alluvial aquifer on the Modder River bank downstream of Krugersdrift dam. Figure 2-1 summarises the research approach that was followed. The study incorporates the following main steps in the research approach (see Figure 2-1).

- Desk study
- Field work
- Data interpretation

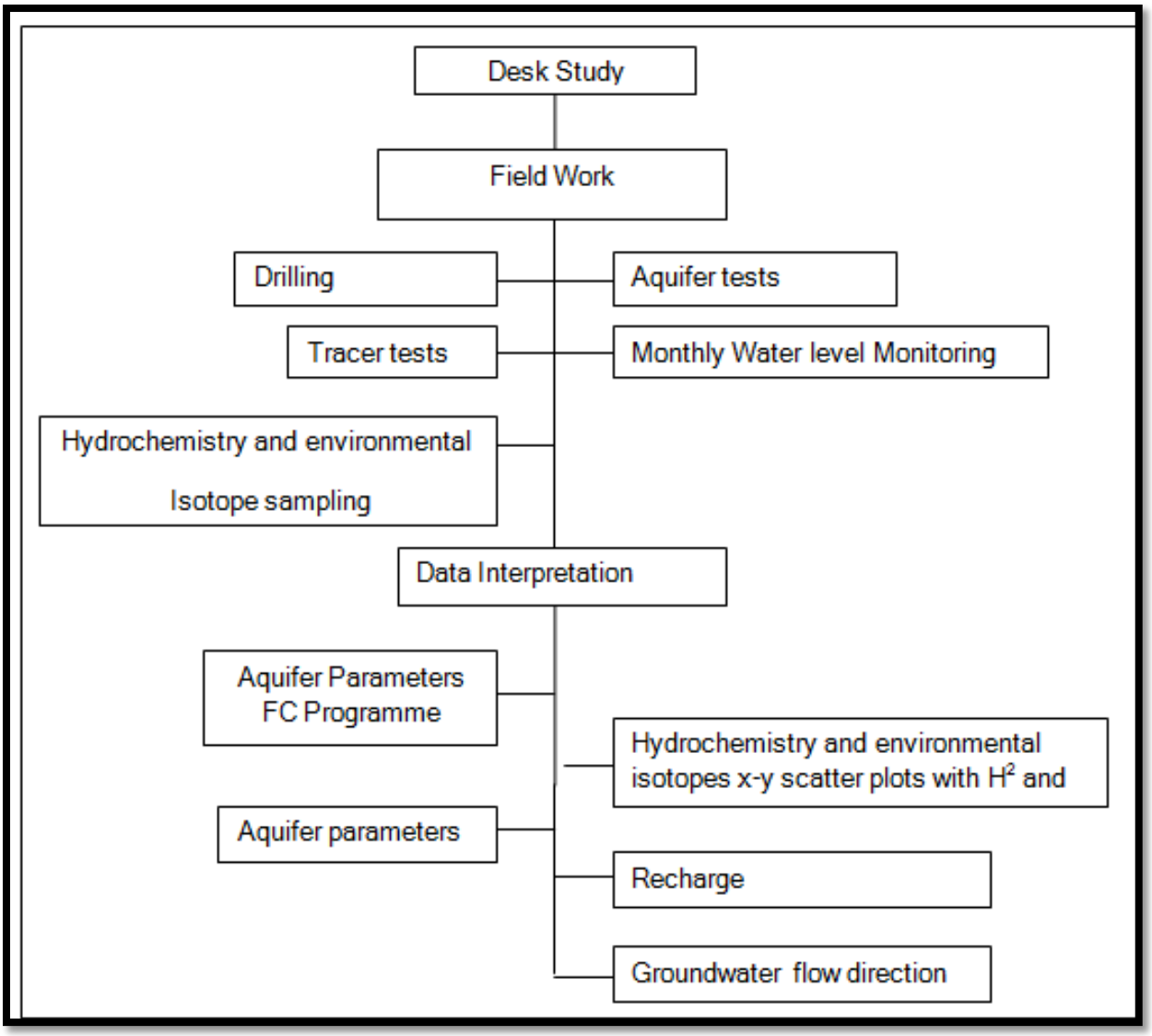

Figure 2-1: Flow Diagram-Research Approach

2.2 Desk study

A Desktop study was done to get a general hydrogeology understanding of the Kalkveld and its surroundings. It involved a review of all available information including climate data obtained from South African Weather Services, geology of the area from geological maps, and land and water use information from various documents and publications on the study area.

The desktop study was also done on the project itself in consultation with the project leaders to find out what the project is all about, its objectives and the anticipated direction of research. After a clear picture was obtained, a further desktop study was done to obtain more information on the following:

- Types of interactions between groundwater and surface water (river water).
- Parameter estimation for the alluvial aquifer in the riparian zone.
- Management and characteristics of alluvial aquifers in the riparian zone.
- Applications of hydrochemistry and environmental isotopes in the conceptualization of the aquifer.

2.3 Fieldwork

This section was more site specific than the previous section (desktop study). Fieldwork was carried out during the course of the project with a primary intention to meet the project specific objectives. Fieldwork done included the following as illustrated in Figure 2-1.

- Site inspection study and drilling
- Water level monitoring
- Aquifer testing
- Hydrochemical and environmental isotope sampling
- Tracer testing

2.3.1 Site inspection study and drilling

Prior to the commencement of the drilling operation, the stakeholders in this project, including the project leaders and students involved visited the site to share knowledge on proposed activities. It was from this tour that the surface geology and other hydrogeological features were identified:

- The rich vegetation, terrain of the area and its drainage. These features are more important in the recharge/infiltration versus runoff estimations.

- The calcrete outcrops that blanket the area and the gradual change in lithology as one approaches the river banks from inland. This was to be used in the construction of the geological conceptual model.
- The seepage zone at the edges of the river banks where water continually seeps into the river. This was to be used in the determination of groundwater flow, its anticipated fate, and through isotope analysis to determine whether the water from seepage has the same source as groundwater from the boreholes.

Fifteen boreholes of different depths (6 m to 42 m) were drilled on site using the air percussion drilling technique. Nine boreholes were drilled next to the river, while six were drilled further from the river. The geological samples were collected and further analysed at the IGS (Institute for Groundwater Studies) noting the colour texture and geological class of the formations. The information of the geological cuttings was intended to be used during the construction of the geological conceptual model.

2.3.2 Water level monitoring

Water level time series data is very important in hydrogeology since it gives an understanding of whether the aquifer is gaining or losing in a given time period. In this study, water levels were monitored once every month in the study site boreholes.

2.3.3 Hydraulic tests

Since these were the newly drilled boreholes, no previous pumping test data could be obtained. Aquifer tests were performed with an intention of determining the following:

- The maximum yield below which pumping must be done during constant discharge test by slug test.
- The strengths of the boreholes by determining their transmissivity values by using constant discharge methods and recovery methods.

2.3.3.1 Slug test

Slug tests analysis methods were first developed during the 1950's (Weight, 2008). They are an important tool in obtaining a cost effective quick estimate of the hydraulic properties of an aquifer.

In addition to being cost effective, slug tests are also advantageous in that they can be used to obtain hydraulic property estimates at waste and pollution sites where pumping in the aquifer could further disperse the pollution (Vivier *et al*, 1995).

Slug tests involve disturbing the static water level in a borehole and monitoring the time it takes for the water level to recover back to the initial level. If the water table is shallow, the water level can be disturbed using a bailer or a bucket. A small volume of water is removed from the borehole after which the rise of the water level in the borehole is measured. Alternatively, a closed cylinder can be submerged to raise the water level and monitor the time it takes for the water level to lower back to the static water level. In some instances a small slug of water is poured into the borehole and the subsequent fall of the water level is measured (Kruseman and De Ridder, 1994). This can be very useful to determine the transmissivity of the upper soil layers at the irrigation site where no water levels occur (Vermeulen, 2006).

Enough water must be removed or displaced to raise or lower the water level by about 10 cm to 50 cm (Kruseman and de Rider, 1994). From the slug test measurements, aquifer transmissivity and hydraulic conductivity can be determined. If aquifer transmissivity is higher than 250 m^2/d, recovery will be so quick that manual measurements cannot be used but rather automatic recording devices will be needed (Kruseman and de Rider, 1994).

In South Africa, slug tests are conducted for the following reasons:

- To estimate the hydraulic conductivity (K) and Transmissivity T of the aquifer in the vicinity of the borehole (Van Tonder and Vermeulen, 2005).
- To obtain a first estimate of the yield of a borehole (Vivier *et al*, 1995).

In this study, slug tests were performed by inserting a slug to raise the water level and measuring with a water level meter the time it takes for the water to lower back to static level.

2.3.3.2 Constant discharge tests

This test is very important for the aquifer parameter determination, especially in high yielding boreholes. Here the borehole is pumped at a constant rate that is enough to cause a drawdown in the borehole and not too much to cause the drawdown to reach the pump inlet or main water strike (Kotze, 2001). The yield is determined in the preceding tests (slug and step-draw down test). The choice of how long the test should be conducted depends on the required precision in sustainable yield, also on the intended use of the borehole water. Most pumping tests in South Africa are conducted within 48 hours, often because of the expenses affiliated with long pumping hours (Kotze, 2001).

In spite of the given advantages for the slug test, constant discharge tests are a better method of analysing the physical properties of aquifers since their influence goes beyond the immediate vicinity of the borehole due to the fact that they can cause a wider cone of depression.

In this study, the boreholes were tested using the constant rate test and different pumping hours from 1 hour to 4 hours.

2.3.3.3 Recovery tests

Evaluation of the recovery data can be used to confirm the aquifer parameters determined from the main test. The recovery of the water level should be measured from the time the pump is switched off, at the same interval as during constant discharge for a period equal to the duration of the main test or until the water level has fully recovered, whichever occurs first. In cases where the automatic level loggers are used, the loggers should be removed at the end of the recovery period.

2.3.3.4 Which test to conduct?

Conducting and analysing pumping tests depends on the objectives of the study. The choice of which test to conduct depends on the number of factors which include:

- What is your time budget?

Slug tests can be conducted relatively quickly, so that several point estimates of the hydraulic conductivity can be collected within a day's work. So when one wants to obtain a quick estimate of the hydraulic conductivity, it becomes essential to do a slug test.

- What is it that you want to determine?

The determination of sustainable yield does not require slug test. A slug test gives the transmissivity of the near formation (aquifer) but not how sustainable the water in the aquifer is.

If the objective of the pumping test is to estimate aquifer parameters that are to be used in a numerical management model, the constant rate test is the most important test and is set as **minimum requirement** for parameter estimation (Van Tonder *et al.,* 2002). Although a slug test and step drawdown test can also be conducted, they are not of much practical value (Van Tonder *et al.*, 2002).

- What is the intended use of the borehole?

For the large community or any project that has a large water budget, it would not be enough to perform a slug test alone, but a constant rate test in order to stress the aquifer so as to get its sustainable yield. If the single boreholes are used for private purposes then it is important to

determine the sustainable yield of the borehole in order to prevent drying up of the borehole. In most private boreholes, due to the high cost of drilling, there would not be any observation boreholes, therefore only the abstraction borehole is pumped and measured.

- What is the economic budget of the project?

For a cost effective hydraulic test, slug tests are used since they do not require costly pumping machinery. The constant rate test may still be performed where the budget is *tight* but factors such as pumping periods would have to be minimal.

The type of pumping test to be conducted; whether it is slug test, step draw down, or constant rate test depends upon the objective of the test.

2.3.4 Tracer tests

Tracer test is a field method used in hydrogeology to quantify selected hydraulic parameters (mainly mass transport parameters) and to finally perform site-characterization. A tracer test is usually conducted by placing an amount of traceable substance (or a heat source in some cases) into the aquifer and tracking it down the hydraulic gradient where at certain points of space and/or time, its quantity is measured (Weight, 2008).

The final result or objective of the tracer test interpretation is usually to determine the rate of flow of groundwater (Darcy velocity) and its flow direction, aquifer porosity and anisotropy, dispersivity, retardation factor and any other physico-chemical characteristics of groundwater.

The type of tracer test to be conducted whether it be Single well, Point source/one sampling well, Point source/two sampling wells, Point source/multiple sampling wells depends upon the objective of the test as stipulated above.

Single well tracer tests monitor tracer decay in time while multiple well tests measure tracer decay in space and time. Multiple well tracer tests make use of one pumping borehole and one or more tracer injection boreholes and the tracer decay is measured in the tracer injection borehole with time while the other observation boreholes are used to monitor how tracer plume migrates in space.

The Single well point dilution test was performed in this study. This method aims to relate the observed rate of tracer dilution in a borehole (Cherry and Freeze, 1979), or in a segment isolated in a borehole to the average velocity of the aquifer (Riemann, 2002). For this study, salt was used as a tracer with the objective of determining the Darcy velocity. The procedure for the analysis of data to calculate the Darcy velocity is given in Section 2.4.3.3 (Darcy velocity). Darcy

velocity is a transport parameter and it gives a measure of how much a contaminant would travel in a particular aquifer in time.

2.3.5 Hydrochemistry and environmental isotope sampling and analysis

2.3.5.1 Sampling procedure

This section presents the methodology that was followed in the hydrochemistry sampling and analysis. Figure 2-2 shows the location of the study area and the positions along the river RV1 and RV2 where sampling was done.

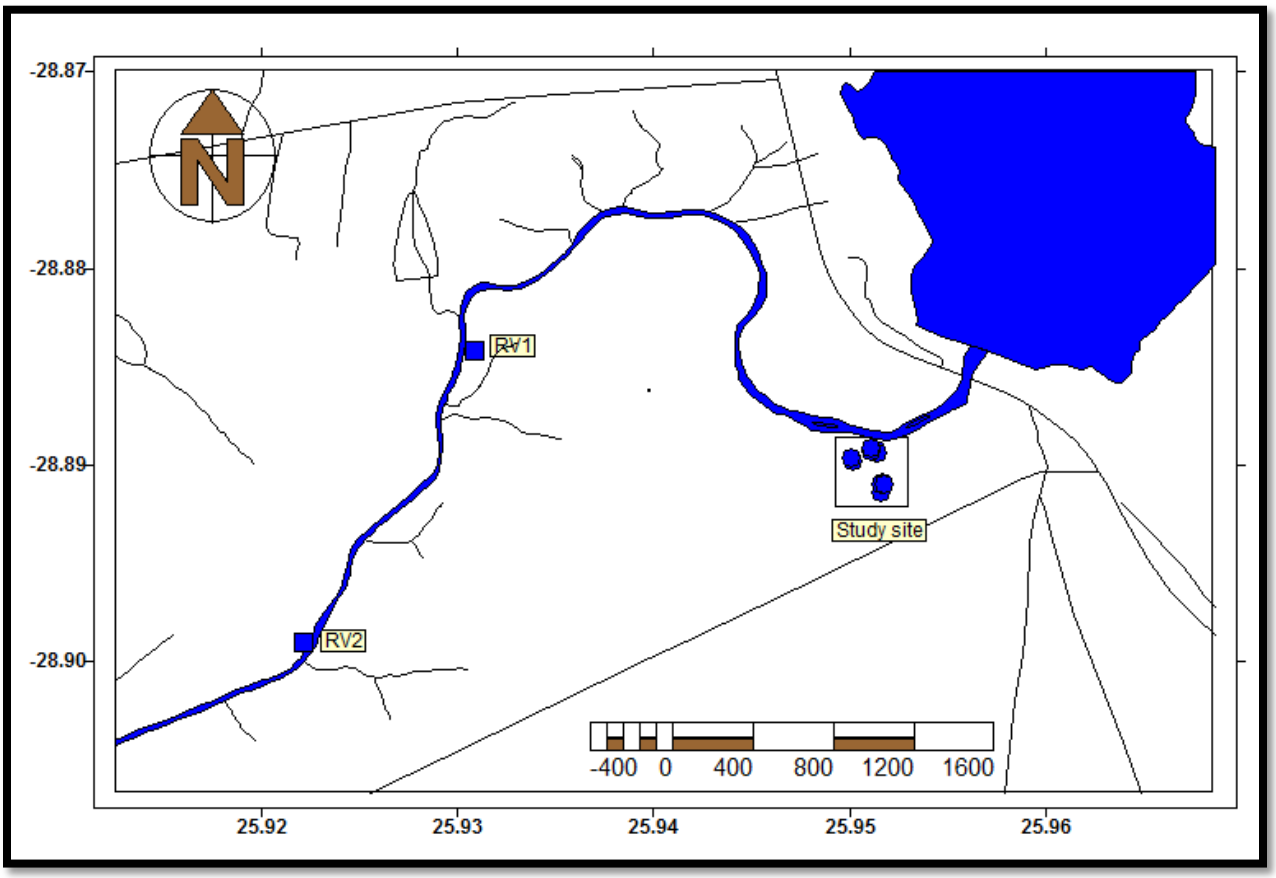

Figure 2-2: Spatial distribution of sites that were sampled.

The 15 boreholes, including the study boreholes and background boreholes were purged for a minimum of 30 minutes with a 0.5 l/s pump. Two 1 l plastic sampling bottles were then filled to the top with water samples. The same procedure was followed in all sites taking two samples per site. The bottles were then carefully labeled. Between the two bottles, one bottle was taken for isotope analysis while the other was taken for macro and trace element analysis.

2.3.5.2 Sample analysis

Macro and trace element analysis was performed by the IGS lab and the samples analyzed for included the following:

- Macro element analysis

pH, Electric Conductivity (EC), MAlk (that which produces a pH above Methyl Orange endpoint of approximately 4.2-4.4), PAlk (produces the pH above the Phenolphthalein endpoint of 8.2-8.4), Calcium (Ca), Magnesium (Mg), Sodium (Na), Potassium (K), Fluoride (F), Chloride (Cl), Sulfate (SO_4), Nitrate (NO_3), Nitrite (NO_2), Phosphate (PO_4) and Bromide (Br).

- Trace elements analysis

Iron (Fe), Manganese (Mn), and Aluminum (Al).

- Isotope analysis

^{18}O, ^{2}H and ^{3}H

2.4 Data interpretation

2.4.1 Hydrochemistry analysis

Water, because of its high capability to dissolve various solutes is termed a universal solvent. It easily takes the chemical characteristics of the environment that it interacts with. Groundwater generally originates as precipitation that infiltrates through the soil and later occupies the pores and fractures of the underlying geologic material. The soil usually acts as a sink for pollution or any other fluids that penetrate through it. In addition to that, the soil and the consolidated material itself have their specific chemistry that is due to their mineralogical composition.

Since water is a universal solvent, when it flows through the geological material, its chemistry is altered by the effects of a variety of geochemical processes and the pollution that may have sunk into the formation. By investigating the chemistry of groundwater in an area one can construct a conceptual model of the geology in which water was stored.

In order to understand the chemistry of groundwater, it is important to look at the chemistry of precipitation since it has an input in the subsurface hydrochemical system.

2.4.1.1 Chemistry of precipitation

Chemistry of precipitation varies a lot depending on the industrial or any other activities that influence the chemical composition of the atmosphere. Since water is a good solvent, as it comes in the form of rain it tends to dissolve chemical constituents in the atmosphere and its chemistry is therefore altered.

Rainwater and melted snow in the non-urban, non-industrialized area have pH values normally between 5 and 6. In the industrial areas the pH of precipitation is much lower than 6 and frequently as low as 3 to 4 (Cherry & Freeze, 1979). The unpolluted earth's atmosphere contains other gases such as O_2, N_2, and Ar. The most important of these gases is O_2 since it imparts an oxidizing capability to the water (Cherry & Freeze, 1979).

2.4.1.2 Soil water chemistry

The soil zone exerts a strong influence on the chemistry of water that infiltrates through it. Almost all the water that joins groundwater has to go through the soil material, during that process, mineral leaching happens where the minerals (or any chemical or biological constituents of the soil) are dissolved and alter the chemistry of water.

The chemistry of water changes as soon as it joins the soil system. As the water first infiltrates the land surface, the microorganisms in the soil tend to dictate the whole water chemistry evolution. The organic matter in the soil is degraded by microbes, and this process produces high concentrations of dissolved carbon dioxide (CO_2). Excess CO_2 in water produces carbonic acid (H_2CO_3) which causes a reduction in pH of soil water. Due to the corrosive nature of acid, carbonic acid causes a number of mineral-weathering reactions which result in the Bicarbonate ion (HCO_3^-) which becomes the most abundant anion in the water. Contact times between water and minerals in shallow groundwater paths are usually short and therefore the dissolved solids concentration becomes generally low. In such cases, limited chemical changes take place before groundwater is discharged to the surface water (Thomas *et al.*, 1998).

2.4.1.3 Groundwater chemistry

The chemistry of deeper water is usually different due to longer contact times and different geological material. Due to the long contact time, the initial reactions that occur in the soil zone that give rise to bicarbonate ions are replaced over time by the chemical reactions between water and minerals (geochemical weathering).

As weathering progresses, the concentration of dissolved solids increases. Depending on the chemical composition of the minerals that are weathered, the relative abundance of the major inorganic chemical species dissolved in water changes. Surface water in streams, lakes and wetlands can repeatedly interchange with nearby groundwater. Thus, the length of time water is in contact with mineral surfaces in its drainage basin can continue after the water first enters a stream, lake, or wetland (Thomas *et al.*, 1998).

2.4.1.4 Groundwater chemistry presentation tools used

The presentation tools that were used for hydrochemistry are Piper diagram, Stiff diagrams, Durov diagram and bar charts. Below is a brief description of how different these tools are used for hydrochemical analysis.

2.4.1.4.1 Piper diagram

This tool involves plotting the cations (Ca, Mg, Na+K) on one triangle while the ions (Cl, SO4 and HCO_3+CO_3) are plotted on the other triangle. This is achieved by working the percentages that are representative of the fraction of a specific ion to the total ions. The two positions from anions and cations are projected onto the main diamond shaped field of the piper diagram to plot as one point. The water is classified depending on the position of that point as illustrated on Figure 2-3. Figure 2-3 shows the projection facies of the cation and anion triangles onto a diamond shape of a Piper diagram.

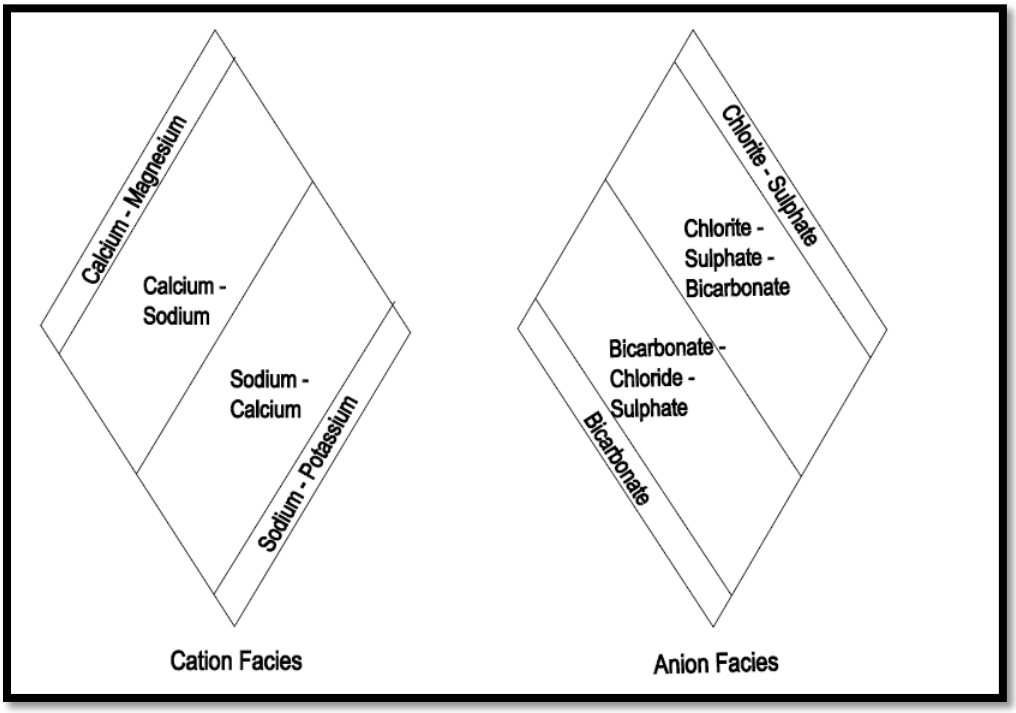

Figure 2-3: Cation and anion facies in a diamond shape of a piper diagram

2.4.1.4.2 Durov diagram

This tool was used in addition to the Piper diagram to plot EC (electric conductivity) and pH so as to see the distribution of EC and pH of different sites.

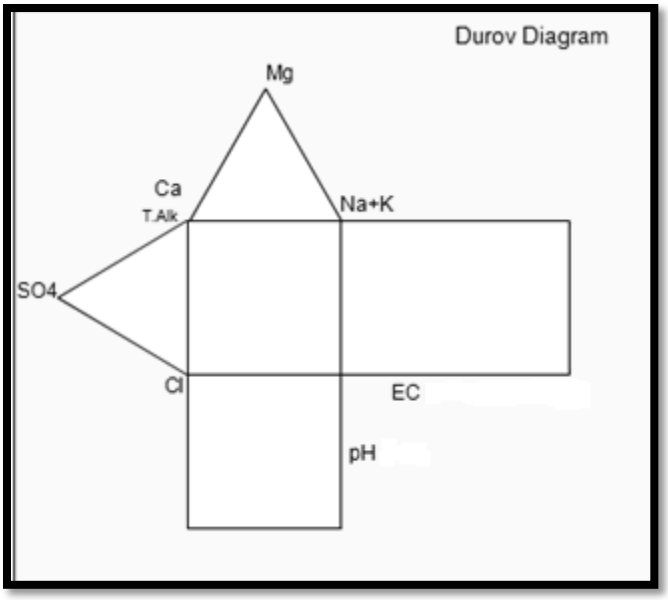

Figure 2-4: Durov diagram

2.4.1.4.3 Stiff diagrams

These tools give a visual impact of the water type so that water samples that have similar shapes can be visually identified as having the same chemistry. It plots major anions on one side and major cations on the other side with projected points depending on the abundance of the ion in milliequivalents per liter (meq/l).

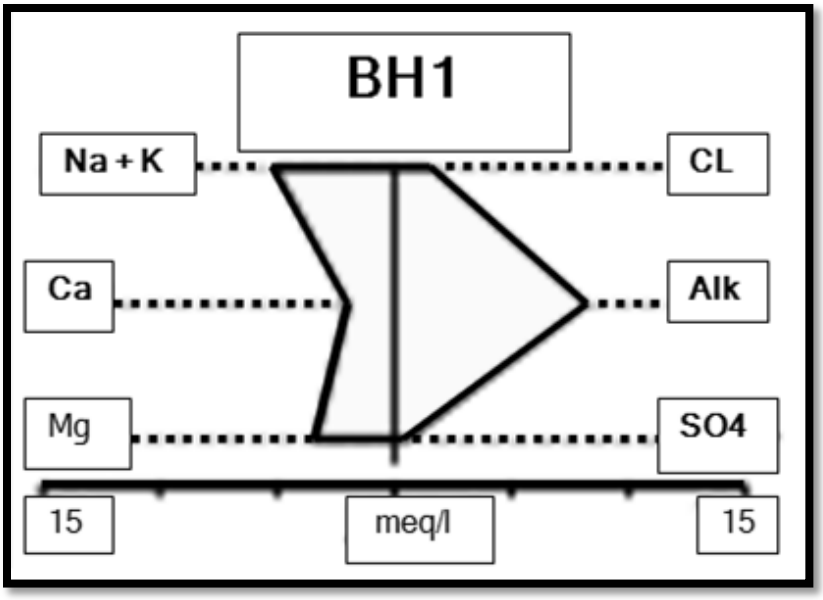

Figure 2-5: Stiff diagram

2.4.2 Environmental isotope analysis

2.4.2.1 General applications of environmental isotopes in hydrogeology

Many elements including hydrogen and oxygen exist in nature as atoms of different mass numbers which are called isotopes. Hydrogen occurs in nature as a mixture of the isotope ^{1}H (Proteum) and ^{2}H (Deuterium) while oxygen is found as isotopes of atomic masses ^{18}O, ^{17}O, and ^{16}O. The ratios of the least abundant isotope to the most abundant differ with locations and water bodies. For example, ocean water contains two ^{18}O atoms for every thousand ^{16}O atoms while the situation is different in fresh water (Appelo *et al.*, 2005).

Isotopes can be classified into two based on their radioactivity; stable isotopes (non-radioactive) and radioactive isotopes. Stable isotopes commonly used in the field of hydrogeology include ^{1}H, ^{2}H, ^{18}O, and ^{16}O. These isotopes do not engage in nuclear transformation, meaning that in a closed system, their abundance would remain constant with time. On the other hand, radioactive isotopes which include tritium (^{3}H) or radiocarbon (^{14}C) will decay over time and can therefore be used for groundwater dating (Appelo *et al.*, 2005). Radioactive isotopes unlike stable isotopes would have their abundance altered even if they are in a closed system.

The concentration of stable isotopes is normally given as the ratio of the least abundant isotope over the most abundant isotope and expressed relative to a standard. In cases of water as a molecule with isotopes, the internationally agreed standard that is used is the Vienna Standard Mean Ocean Water (VSMOW). The isotopic abundances, and the changes in these abundances are generally small, they are therefore studied more easily using the δ notation. This notation expresses the deviation of the isotopic ratio R in the sample with respect to the ratio in the standard:

Equation 2-1: Calculation of δ notation on isotope concentrations.

$$\delta\text{sample} = \frac{\text{Rsample} - \text{Rstandard}}{\text{Rsample}} \times 1000$$

where the measured ratios from the heavy to the light isotopes are R_{sample} for each sample and $R_{standard}$ for the ratio in the standard (i.e. VSMOW for H and O isotopes). The ratio in rain for $^{18}O/^{16}O$ can be described as $\delta^{18}O_{rain}$. It is possible for δ to be negative or positive depending on whether the water sampled contains less than, or more than the isotopic concentration of the standard.

^{18}O and ^{2}H are present in water in isotopic abundances (or ratios) of about $^{18}O/^{16}O$=0.2 % and $^{2}H/^{1}H$=0.015 % (Kotze, 2001). There is a wide range of possible combinations that make up the

water molecule and their molecular masses range from 18 ($^{1}H_2{}^{16}O$) to 24 ($^{3}H_2{}^{18}O$). Table 2-1 shows the known isotopes of hydrogen and oxygen. Eighteen combinations of the water molecule are possible using these nuclides.

Table 2-1: Some Environmental isotopes used in hydrogeological studies (Appelo *et al.*, 2005)

Isotope	Relative abundance (%)	Type
^{1}H Proteum	99.98	Stable
^{2}H Deuterium	$1.6x10^{-3}$	Stable
^{3}H Tritium	$0\text{-}10^{-15}$	Radioactive with half life 12.3 years by β^- emissions.
^{16}O Oxygen	99.76	Stable
^{17}O Oxygen	0.04	Stable
^{18}O Oxygen	0.20	Stable

Due to differing masses, stable isotopes behave slightly differently during physical, chemical and biological processes. During evaporation and condensation, the stable isotopes of $^{1}H/^{2}H$ and $^{18}O/^{16}O$ become fractionated (Apello *et al.*, 2005). The resulting small variations in isotopic concentrations may yield information on the climate at the point of infiltration or the origin of the water.

2.3.1.2 Applications of stable isotopes ^{18}O and ^{2}H

The concentrations of the environmental isotopes differ with locations and water bodies. Because of their differing mass numbers, isotopes tend to behave differently when exposed to different chemical, biological, and physical environments. In that regard, the changes in ^{18}O and ^{2}H concentrations along groundwater flow paths is an effective tool to determine the altitude of groundwater recharge, estimations of mixing proportions of different sources or component flows and the relationships between ground and surface water (Gat, 1996).

When water is in an open water body such as a dam, the lighter isotopes (^{16}O) will more easily be evaporated into the vapour phase while the heavier isotopes likely remain in the liquid phase. The opposite occurs during condensation, the heavier isotopes (^{18}O) will condense with ease into the liquid phase. The basic principle is that enrichment of the lighter isotopes ^{16}O occurs in the vapour during evaporation, as opposed to the loss of the heavy isotopes ^{18}O from the vapour first during condensation. This is a natural distillation or fractionation process which continues

with rainfall; therefore, precipitation in a certain area will have a distinctive stable isotope concentration.

As a result of these evaporation condensation processes, a plot of isotopes of $\delta^{18}O$ versus $\delta^{2}H$ gives a straight line for the meteoric water called the Global Meteoric Water Line (GMWL). Most rain water will plot close or parallel to this line. Vapour masses moving inland are subject to equilibrium isotopic exchange processes with the continued depletion in heavy isotopes in vapour travelling inland as a result of rainout. Condensation readily washes out heavy isotopes than lighter isotopes, so as a cloud moves inland, the heavy isotopes remain closer to the coast while the lighter ones are carried more inland. As a result of this, the stable isotopic content of meteoric water lies on a GMW regression line represented by the equation below:

Equation 2-2: Global Meteoric Water Line

$$\delta^{2}H = s\delta^{18}O + d$$

The GMWL is characteristic of a line with s=8 and d=+10. The slope "s" is controlled by the rainfall and seasonal variations in precipitation while the ^{2}H-excess (d) is controlled by the deuterium in the vapour source region.

After the alteration of the isotopic concentrations in the atmosphere during evaporation and condensation, there remains the resultant surface layer that is rich in the heavy isotopes. This layer is then readily mixed into the bulk of the water body through convective processes. The isotopic pair $\delta^{2}H$ and $\delta^{18}O$ will plot to the right of the meteoric water line and make an evaporation line of a lesser slope s and lower d than the GMWL. The slope of the evaporation line is usually between 4 and 5 (Kotze, 2001).

Generally, the isotopic concentration in groundwater becomes fixed from the surface because of the end to atmospheric effects such as evaporation and condensation. i.e., recharge starts when evaporation ends. The evaporation losses from groundwater generally occur under isotopic equilibrium, i.e. without fractionation (Kotze, 2001). This causes the isotopic concentrations of groundwater to be closely equivalent to the isotopic concentration state of the water just before infiltration. As a result of this, it becomes possible to identify groundwater that has recharged from precipitation from groundwater that has recharged from a surface water body on condition that sufficient evaporation took place in a water body. Water that has recharged from precipitation either through piston recharge or preferred pathway shall have a high concentration of the lighter isotopes hence a low concentration of the heavier isotopes that plot on the GMWL.

While the water that has recharged from the water body (after a significant evaporation has occurred), will have a high concentration of the heavier isotopes and shall therefore plot on the Evaporation Water Line.

2.4.3 Aquifer parameters

Characterization of aquifer parameters involves the determination of aquifer behaviour that is define by its transmissivity, hydraulic conductivity, storativity, Darcy velocity, groundwater flow direction, porosity and other physico-chemical characteristics.

2.4.3.1 Transmissivity

This is the rate at which water is transmitted through a unit width of an aquifer under a unit hydraulic gradient (Driscoll, 1986). Transmissivity is a product of the hydraulic conductivity *K* (m/d) and the thickness of the saturated aquifer *b* (m) as shown on Equation 2-3 below:

Equation 2-3: Transmissivity as product of hydraulic conductivity and aquifer thickness.

$$\mathbf{T = Kb}$$

Transmissivity can be obtained from pumping test data, preferably from constant rate test. For the first estimate of the T-Value of the formation, the Logan equation can be used (FC Program, Van Tonder *et al.*, 2001):

Equation 2-4: Logan equation for determination transmissivity.

$$T = \frac{1.22Q}{s}$$

where Q is the abstraction rate in m^3/d and "s" is the drawdown at the end of the test. A qualified guess of the T value can also be obtained if the maximum yield of the borehole is known:

Equation 2-5: A qualified guess estimate of transmissivity.

$$T = 10Q$$

Where Q (maximum yield) is measured in l/s

In this study the transmissivity of the aquifer was determined using the Cooper Jacob method from FC Programme by Van Tonder *et al.* (2001).

2.4.3.2 Hydraulic conductivity

The hydraulic conductivity indicates the quantity of water that will flow through a cross-sectional area of a porous media per unit time under a hydraulic gradient of one at a specified temperature.

Hydraulic conductivity depends on the size and arrangement of the particles (in an unconsolidated formation), the size, and character of the crevices, fractures and solution openings in a consolidated formation and the viscosity of the fluid as determined by the temperature. The hydraulic conductivity may change with any of these parameters (Driscoll, 1986).

For a short time-budget, slug tests are a cheaper way of determining the hydraulic conductivity of the aquifer in the vicinity of the borehole (van Tonder and Vermeulen, 2005). For the mathematical models, the aquifers are usually assumed to be homogeneous. In the real situation, there is a lot of heterogeneity, so the K value that is obtained in a slug test is site specific; it is only valid for that borehole only.

The Hydraulic conductivity of the unconsolidated matter can be obtained using infiltration tests. Table 2-2 shows the hydraulic conductivities of different geological materials.

Table 2-2: Hydraulic conductivities of some rock types and unconsolidated matter (Brassington, 1998)

Rock Type	Grain size (mm)	Hydraulic Conductivity K (m/d)
Loose unconsolidated matter		
Clay	$5x10^{-4}$-$2x10^{-3}$	10^{-8}-10^{-2}
Silt	$2x10^{-3}$-$6x10^{-2}$	10^{-2} - 1
Fine Sand	$6x^{-2}$ -$25x^{-2}$	1-5
Medium Sand	0.25-0.50	5-20
Coarse Sand	0.50-2	20-100
Gravel	2-64	$1x10^{-2}$-$1x10^{3}$
Sedimentary rocks		
Shale	small	$5x10^{-8}$ - $5x10^{-6}$
Sandstone	medium	10^{-3}-1
Limestone	variable	10^{-5}-1
Igneous rocks		
Basalt	small	$3x10^{-4}$-3
Granite	large	$3x10^{-4}$-0.03
Slate	small	10^{-8}-10^{-5}
Schist	medium	10^{-7}-10^{-4}

2.4.3.3 Darcy velocity

The Darcy velocity is in some cases called specific discharge and written as “q” in the Darcy velocity equation. Darcy velocity has the dimensions of length/time (*L/T)*. Specific discharge

(Darcy velocity), q, is the volume of water flowing per unit time through a unit cross-sectional area normal to the direction of flow (Bear, 1979). This is mathematically expressed as shown in Equation 2-6.

Equation 2-6: Specific discharge (Darcian velocity)

$$q = -K\frac{dh}{dl}$$

Darcy velocity can be obtained by tracer tests. In this study, point dilution tracer tests were performed on four boreholes. Equation 2-7 was used to calculate Darcy velocity in each borehole using the standardized concentrations.

Equation 2-7: Darcy velocity equation.

$$q = \frac{w}{\alpha At}\ln\left(\frac{Co}{C}\right)$$

where:

w= Volume of fluid contained in the test section (m^3)

A = Cross sectional area normal to the direction of flow (evaluated from ∏rL, assuming a radial flow model with fractal dimension "n" = 2) (m^2),

C_0 = tracer concentration at t = 0

C = tracer concentration at time = t

α = borehole distortion factor (between 0.5 and 4; = 2 for an open well).

Note that $q\alpha = v^*$, where v^* = apparent velocity inside well.

t = time when concentration is equal to C (days)

L = test section length (m)

2.4.4 Recharge

Recharge is a natural mechanism in which groundwater that has been abstracted is replenished in the aquifer to keep up the regional static water levels. In the Karoo, recharge estimation mechanisms are not different from other geological formations. The only drawback is that since the Karoo formation has a thin layer of top soil, the Karoo formation disqualifies other recharge estimation methods that relate to the unsaturated zone (Woodford and Chevallier, 2002).

The rocks and dolerite outcrops are regarded as the preferential areas of recharge. Therefore the most reliable and most practical methods entail a mass balance approach such as a water quality balance using the chloride method (Woodford and Chevallier, 2002).

The exploitation of groundwater must incorporate the prior estimation of sustainable yield of the aquifer. The sustainable yield is dependant on the rate of recharge from rainfall, storativity, and the subsurface in- and outflows to and from the aquifer system. Most of the rivers in the Karoo are gaining rivers not loosing, therefore recharge from surface bodies is negligible.

Woodford and Chevallier (2002) state that there are two mechanism of recharge into the porous matrix formation:

- Direct, vertical infiltration via the soil layer, and
- Via vertical fractures (preferential pathway) exposed at the surface.

Recharge via the vertical fractures initially enters the fractures and then flows into the matrix formation due to the pressure gradient between the fracture and the matrix. This most feasible recharge mechanism for rainfall to the Karoo fractured formations is via vertical fractures.

As stipulated earlier by Woodford and Chevallier (2002), mass balance method of determining recharge such as chloride method is the most reliable method. Chloride method was performed in this study to determine recharge using chloride values from the four boreholes.

Chloride method

This is an effective method of determining recharge in the unsaturated zone, as a first approximation (Kotze, 2001). The method makes use of a relationship between chloride concentrations in rainfall and chloride concentrations in groundwater. This method assumes that the increase of chloride concentrations has resulted from evapotranspiration losses and that no additional chloride has been added by contamination from or leaching of rocks or from the overburden (Woodford and Chevallier, 2002). Chloride is a conservative tracer and enters the soil or the rock formation as part of infiltrating rainfall, where after it is concentrated in the soil by transpiration from plants and direct evaporation from the soil.

The chloride method is represented by the equation as follows:

$$\mathrm{REav} = \mathrm{a} \times \mathrm{Rfav}$$

where:

RE_{av} =average recharge

$$a = \frac{Cl.rainfall(\frac{mg}{l})}{Cl.groundwater(\frac{mg}{l})}$$

Symbol "α" represents a unit-less recharge coefficient.
Cl=Chloride concentration
Rf_{av} =Average rainfall (=559 mm/a for Bloemfontein)

According to Section 1.4.2 (climate), the average annual rainfall in Bloemfontein is 559 mm/a. The chloride concentration in rainfall is approximated to 1 mg/l. This technique was used in this study to determine percent recharge. Literature states that recharge percent of 2.6 % was approximated for the Karoo aquifer using the measurements made in Dewetsdorp using chloride method (Woodford and Chevallier, 2002).

2.4.5 Groundwater flow direction

Groundwater usually flows towards and eventually drains into streams, rivers, lakes or any other water body. But groundwater flow does not always occur in the direction of topography and does not always mirror the direction of surface water. It is therefore inappropriate to always assume groundwater flow considering the topography alone. It therefore requires special measures to determine the groundwater flow direction.

The technique of using tri-wells has been used in the past to determine the direction in which groundwater flows. According to the Idaho Division of Environmental Quality (IDEQ, 2010), the direction of groundwater flow in an unconfined aquifer can be determined using the following steps:

Step one: The three boreholes are drilled into the **unconfined** aquifer forming a triangle. Once the surface elevation and the water-level have been determined, the depth to water level is subtracted from the surface elevation at each well in order to obtain the water table elevations.

Step two involves subtracting the water table elevation of a well which has a higher elevation from the water table elevation of a well which has a lower elevation on each of the three straight lines connecting the wells. These three elevation differences are divided up into equal increments. The water table elevation levels shown have been placed on the figure by adding the initial water level to each increment.

Step three involves determining the direction in which groundwater flows. The lines are drawn connecting the increments that have the same value and these lines represent the water table contours. Groundwater will flow from higher elevations to lower elevations in the direction of

maximum change in elevation. The line that is perpendicular to the straight line which connects the elevation increments indicates the direction that groundwater flows.

Step four: In order to determine the hydraulic gradient, the vertical change in groundwater elevation over horizontal distance in the direction of groundwater flow is the hydraulic gradient which tells how many meters does water elevation decrease for every meter that groundwater flows as illustrated by Equation 2-8.

Equation 2-8 : Hydraulic gradient determination.

$$\text{Hydraulic gradient} = \frac{\text{Water table change in direction of flow}}{\text{Horizontal distance between measured points.}}$$

The flow characteristics of groundwater systems have been determined in the past by use of various methods that include aquifer mechanics, geophysical methods, and tracer tests (natural gradient), etc.

In this study, a three point system was used to determine the direction of groundwater flow on site. A spreadsheet called Flow direction.xls (Dennis, 2006) was used to determine the direction of groundwater flow that was used in this study. It requires the following information about the three boreholes:

- Borehole identity
- Coordinates of the boreholes in meters.
- Borehole water level elevation in meters above mean sea level.

The mathematics involved in this spreadsheet is as follows:

A system with three boreholes *P1, P2*, and *P3* of coordinates *P1(X1, Y1), P2(X2, Y2), P3(X3, Y3)* and water level elevations in meters above mean sea level (mamsl) *Z1, Z2* and *Z3* respectively can be used as follows using gross product technique:

Gross Product1 $G1 = (Y2 - Y1)(Z3 - Z1) - (Z2 - Z1)(Y2 - Y1)$

Gross Product2 $G2 = (Z2 - Z1)(X3 - X1) - (Z3 - Z1)(X2 - X1)$

Gross Product $G3 = (X2 - X1)(Y3 - Y1) - (Y2 - Y1)(X3 - X1)$

IF G3<0, then δ=$-\sqrt{G1^2 + G2^2 + G3^2}$

But if not δ=$\sqrt{G1^2 + G2^2 + G3^2}$

δ is a parameter that is meant to maintain a positive angle from the normal vactor.

The technique involved the use of Tangent rule: if 90° - θ= angle from normal (North).

$$opposite = \frac{G2}{\delta}$$

$$adjacent = \frac{G1}{\delta}$$

$$Tan\theta = \frac{O}{A}$$

$$90° - (^{-}Tan\theta) = angle\ from\ normal$$

The worked spread sheets that were used to determine groundwater directions can be accessed in Appendix C on the provided Appendix disc.

2.5 Conclusion

This aim of this chapter was to introduce the project and methodology that was applied in characterizing that alluvium aquifer on the Eastern bank of the Modder River down stream of Krugersdrift dam. Aquifer characterization field techniques included borehole drilling/ geological classification, water level monitoring, aquifer testing, hydrochemical and isotopic sampling. Geological classification is aimed at developing a geological conceptual model of the area, water level monitoring for groundwater recharge, aquifer tests for aquifer parameters (transmissivity and Darcy velocity), and hydrochemistry for groundwater type, source, fate and age. Now that a study methodology has been established, the next chapter looks into the geological classification following the proposed methodology.

3 GEOLOGY

3.1 Introduction

It is of great importance to consider the geology of the site if one is going to study its hydrogeology. One of the misconceptions about groundwater is that groundwater occurs inside flowing underground rivers. On the other hand, studies show that groundwater occurs inside the pores of the *geological* material (Botha *et al.*, 1998). The geology of the aquifer material therefore has an impact on groundwater occurrence.

The more porous the material the more water it can contain in its pores. In addition to porosity, the transmissivity of a rock matrix plays a major role in groundwater exploration. The geological material may have a high porosity but that does not make it a good source of water, it is the interconnection of the pores that makes water to readily flow into the well during pumping; hence the formation with high transmissivity is the main focus in groundwater exploration.

Transmissivity is described as the measure of the ease with which groundwater flows in the subsurface. The more transmitting the material the more likely it is to get good pumping yields provided there is high storage and good recharge. The baked zone near a dolerite dyke is highly fractured and has a high transmissivity. Because of this transmissivity dependency, the fractured geological material becomes a target in groundwater exploration. This therefore confirms the importance of studying geology in groundwater exploration.

3.2 Regional Karoo geology and hydrogeology

The Main Karoo Basin encompasses an area of approximately 630 000 km^2 including the greater part of the central plateau region of South Africa and *the whole of Lesotho* (Woodford & Chevallier, 2002). The Karoo covers an area of about 2/3 of South Africa and consists mainly of sandstones, mudstones, shale and siltstones of low permeability which have been intruded by numerous dolerite dykes and sills.

The formation of the Karoo sequence happened about 300 million years ago when the sediments filled an intracratonic basin on Gondwanaland (Fourie, 2003). These sediments were deposited under varying environments such that some layers that show clearly distinguishable groups of sediments were formed. After the sedimentary deposition, the Drakensburg lava outpourings concluded the Karoo sequence by burying the Karoo sediments to the depths of

2500 m to 3500 m (Botha *et al.*, 1998). The Drakensburg formation (Lesotho formation) is clearly visible over the Lesotho Highlands and the Maluti-Drakensberg frontier.

The high pressure and temperature of the subsurface led to the lithification of the sediments which led to the formation of the sandstone, siltstone and mudstone layers. Lithification also brought about low porosities, low permeability and reduced elasticity of the Karoo rocks (Botha *et al.*, 1998). The low porosity was aggravated by the deposition of the secondary minerals containing carbonates and silica (Botha *et al.*, 1998). The Jurassic age brought about plenty of volcanic activities that included the eruption of dolerite laccoliths, sills and dykes. These eruptions increased the degree of fracturing of the sedimentary rocks.

Most of the Free State Province is underlain by sedimentary rocks belonging to the Beaufort group and Ecca groups of the Karoo Supergroup. These rocks are known to host major coal and clay deposits of South Africa (Geoscience, 2006). Figure 3-1 shows the geology of the Karoo and the location of the study site.

The Karoo basin, due to its uneven distribution of geological intrusions makes its aquifers to be very complex and to have an unpredictable behaviour. This unpredictable behaviour makes groundwater to be an unreliable source of water; hence the major characteristic of Karoo aquifers is low permeability and low yields (<1 l/s) (Woodford & Chevallier, 2002).

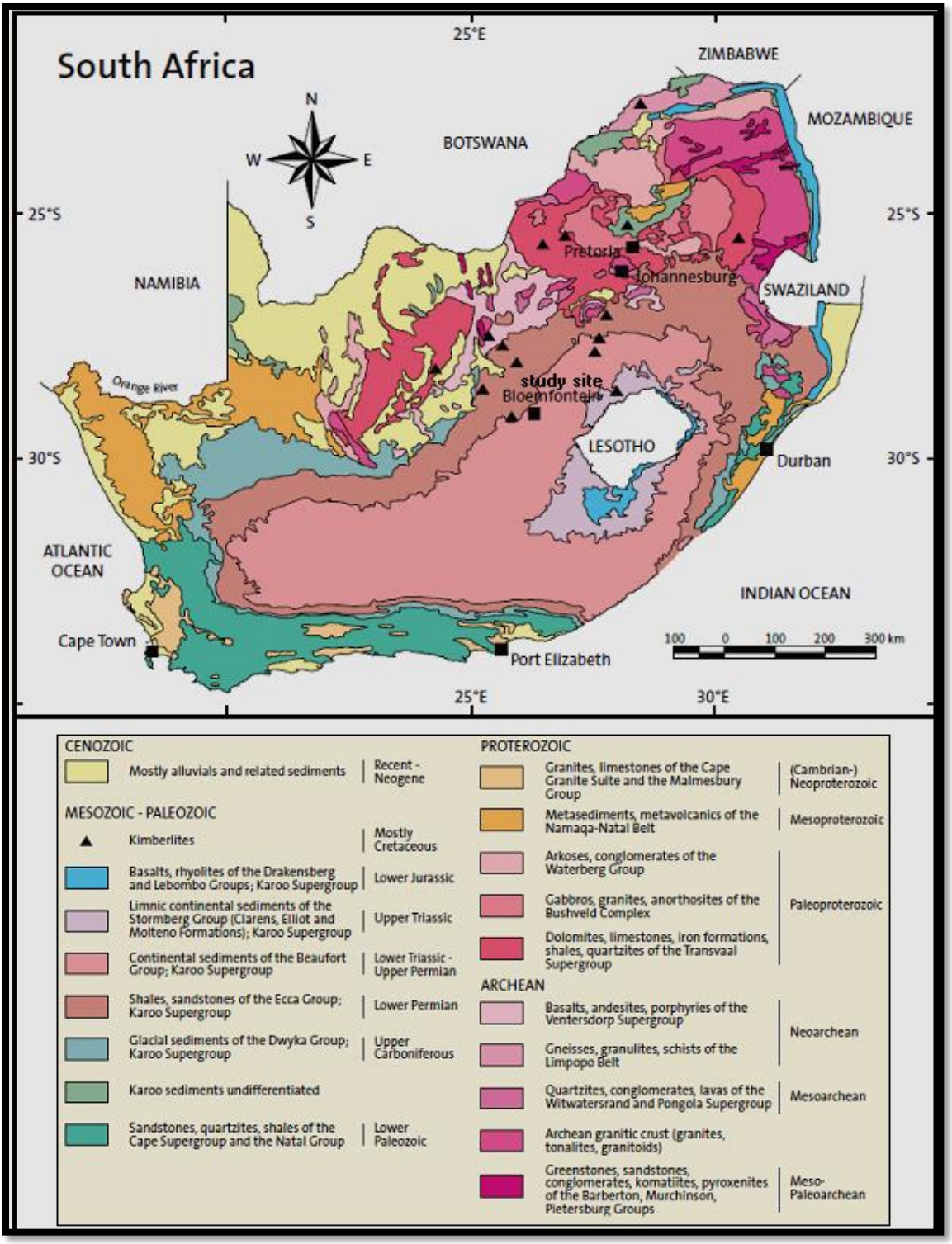

Figure 3-1: The simplified geological map of South Africa showing the approximate location of the study area. (www.geoscience.org.za)

Flow in the Karoo is characterized by two flow types which are matrix flow and fracture flow. For a borehole that intersects a fracture, flow in the matrix is predominantly vertical and linear and not radial and horizontal (Botha *et al.*, 1998). As for a borehole that does not intersect a fracture, matrix flow is radial and horizontal. The flow velocities in the fracture are higher than in the matrix. Figure 3-2 illustrates the situation between two different boreholes one intersecting the fracture and the other penetration strictly through the matrix.

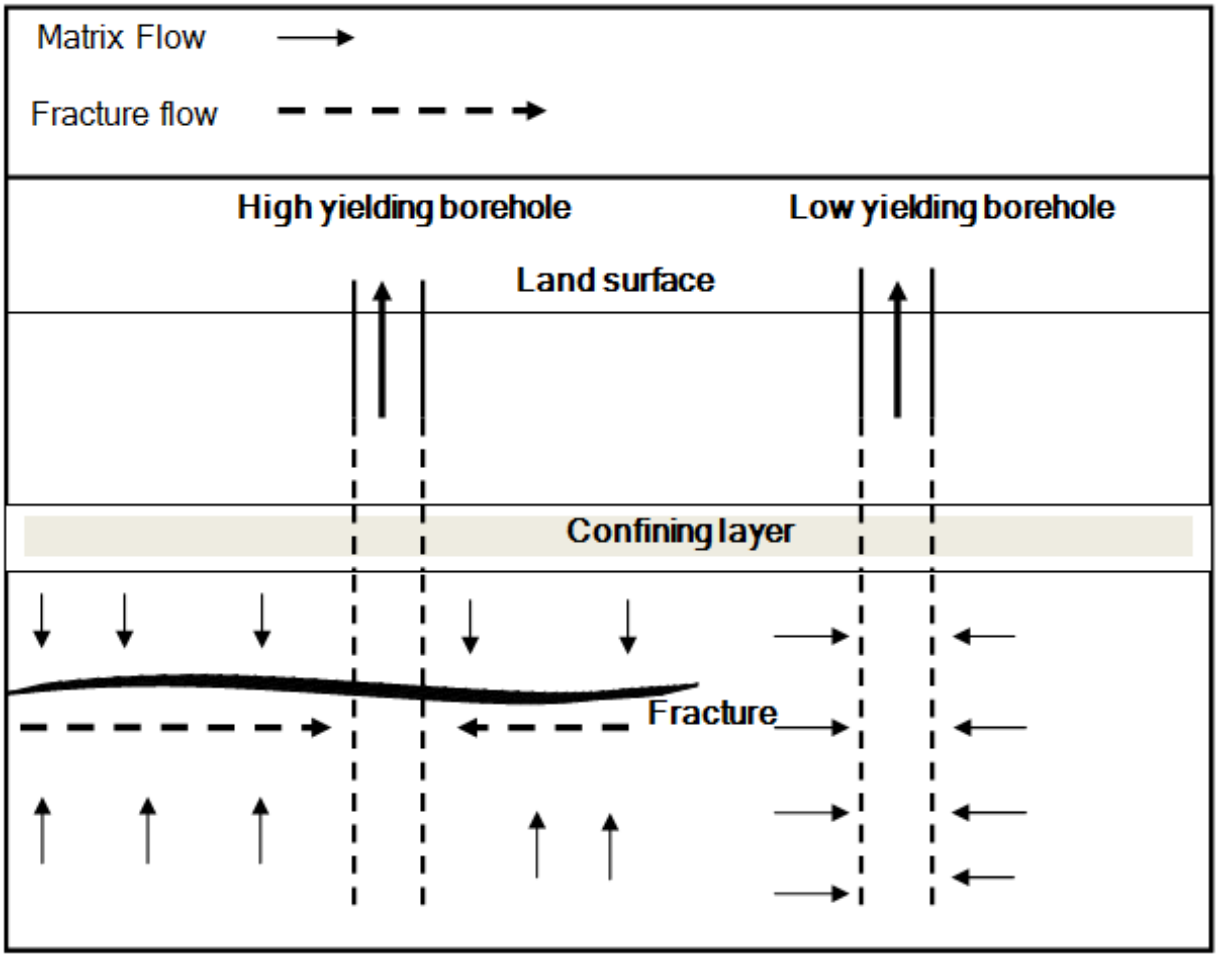

Figure 3-2: Matrix and fracture flow in Karoo aquifers (adapted from Fourie, 2003).

A borehole that intersects a fracture yields more water than one that depends entirely on matrix storage. This is because a fractured formation has higher transmissivity than a matrix formation.

The aperture and areal extent of water yielding fractures in the Karoo are limited and therefore unable to store large quantities of water (Botha *et al.*, 1998). This means that water in the Karoo aquifers is not stored in the fractures but in the micro-fractures of the rock matrix and therefore the formation acts as the main storage unit of water in Karoo aquifers. Figure 3-3 shows a

photograph of the *micro fractures* (called the matrix of the aquifer) in an aquifer sample (from Botha *et al.*, 1998).

The contact plane in between various strata of the Karoo rocks are favourable positions for the development of fractures (Fourie, 2003). This is because the relatively more inelastic sandstones in the Karoo formations are more likely to be fractured than the more elastic siltstone and mudstone layers (Botha *et al.*, 1998). These types of fractures become targets in groundwater exploration because of their high transmissivity values.

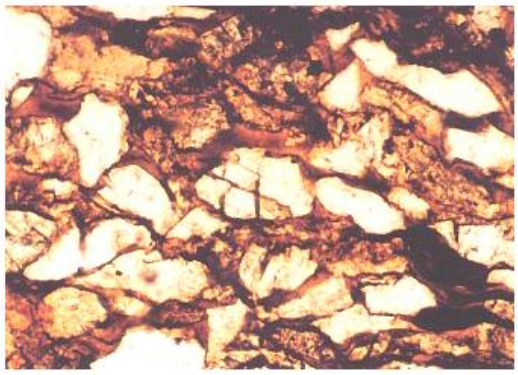

Figure 3-3: Photograph of micro fractures in 0.25mm quarts grains, from a core sample of the campus Test Site (Botha *et al.*, 1998).

In as much as the fractures are so important in Karoo formations, they are at the risk of deformation if the abstraction is not performed in the safe manner. One cause of deformation is the weight of the over-burden that is highly enhanced when groundwater is being over-exploited i.e. when the water level goes below the fracture position. A deformation of this nature will be disastrous for production boreholes that depend on horizontal fractures for their water supply. The yields can be greatly lowered by a minor deformation; for example, 20 % decrease in fracture aperture during pumping may decrease the yields by 50 % (Woodford and Chevallier, 2002). This therefore calls for a need to determine the safe and sustainable borehole yield and to understand the aquifer parameters for the specific aquifer.

3.3 Site geology

The site geology was investigated using a number of geological methods. The geological methods commonly used to determine the geology of an area are field surveys, geological maps, aerial photography and satellite imagery (Van der Voort, 1995). Unfortunately, these methods do not give an understanding of the subsurface geology, rather the properties of the earth's surface.

Two of the best methods of understanding the subsurface geology are the use of the drill chips from the air percussion drilling method; the other method is the use of the core samples from the core drilling method. Core drilling gives a better understanding of the subsurface geology than the chips since it provides an undisturbed geological profile that clearly shows the position of the fractures. Important as it is, core drilling is a very expensive technique.

The geology of the study area was investigated by use of geological maps, visual land surface inspection, and geological logs from air percussion drilling.

3.3.1 Desktop study

In order to understand the site geology prior to site visitation, the geological maps and other geology material were studied to bring a picture of what to expect from the field.

The study site falls under the Ecca group which consists of shale and mudstones within the Karoo Supergroup as shown on Figure 3-1. The area is located within the so called Kalkveld (Afrikaans for calcrete fields), which is characterized by high content of calcite rich surface material. The geology of the study area consists of sedimentary rocks of the Karoo covered with a blanket of calcite rocks and unconsolidated calcite.

3.3.2 Visual land surface inspection

As the name of the area states, Kalkveld (meaning calcrete fields), the result of the visual inspection that was performed in the area showed that some calcrete outcrops were seen on site as shown on Figure 3-4. The majority of the inland surface is overlain by calcrete rocks and calcrete derived soil formation except some minor portions towards the river that were covered by dark brown soil.

To further understand if the surface outcrop is really calcrete, an acid test was performed. A drop of dilute HCl gave rise to a chemical reaction that produced bubbles and a residue. This test is done in geology classifications to identify the content of calcium carbonate in a rock.

$$CaCO_{3(s)} + 2HCl_{(aq)} \longrightarrow CaCO_{3(s)} + H_2O_{(l)} + CO_{2(g)}$$

The production of a gas (CO_2) as shown on the chemical equation above is an indication of the carbonate content in a geological sample. Some rocks depending on the varying carbonate contest gave different amount of carbon dioxide. These results show the dominancy of calcareous material in a geological formation.

A geological profile on the river banks was observed to be in the order of top soil with highly decomposed organic matter, silt, dark/black clay, highly weathered soft shale, underlain by highly fractured shale with horizontal stratifications as shown on Figure 3-5.

Figure 3-4: Calcrete outcrops on the land surfaces.

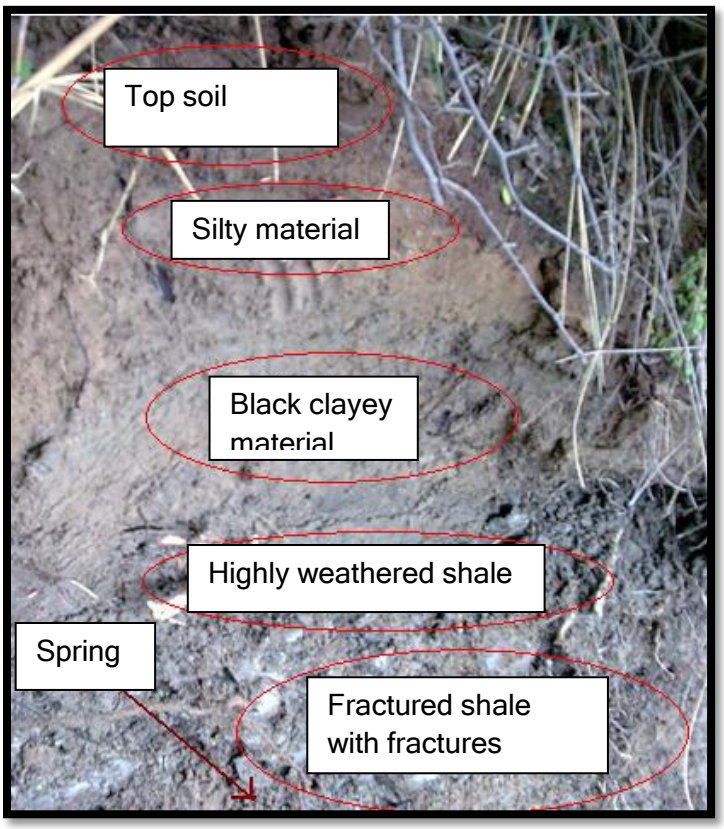

Figure 3-5: Geological profile on the river banks of the Modder River adjacent to the study site.

The highly fractured shale formation along the banks compared to inland may be due to exposure to weather elements; mainly changing temperature and exposure to air.

Figure 3-6 is a graphical illustration of Figure 3-5 which shows the side view of the river bank.

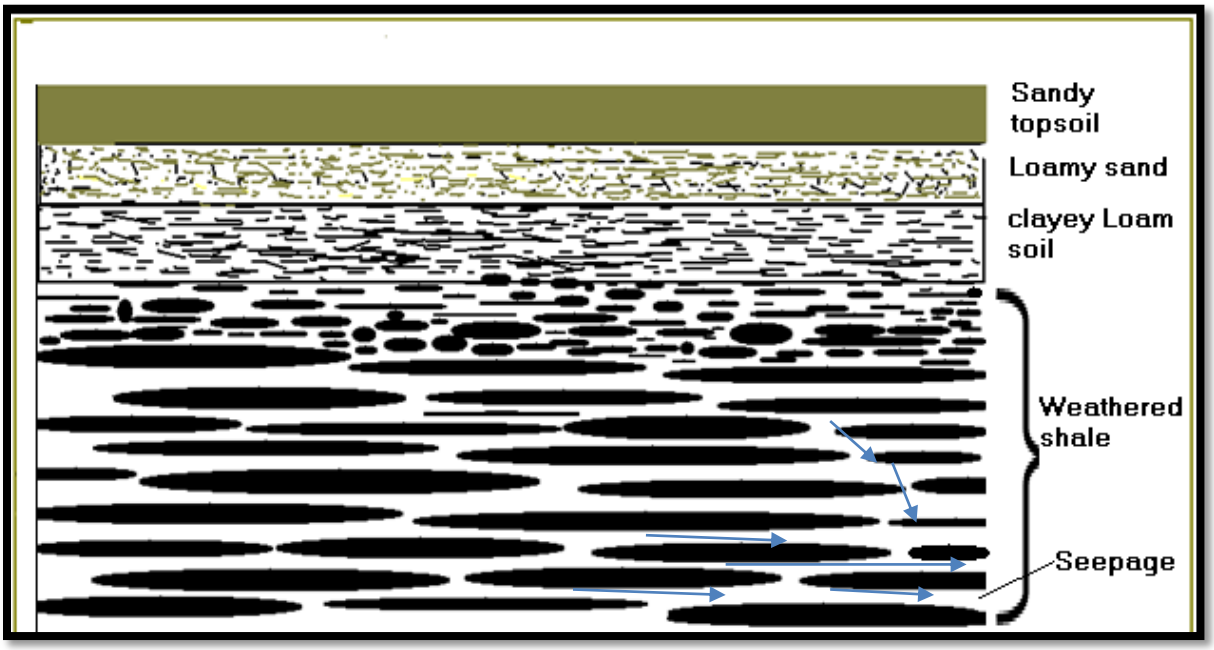

Figure 3-6: Vertical cross-section of the geology that makes the river bank.

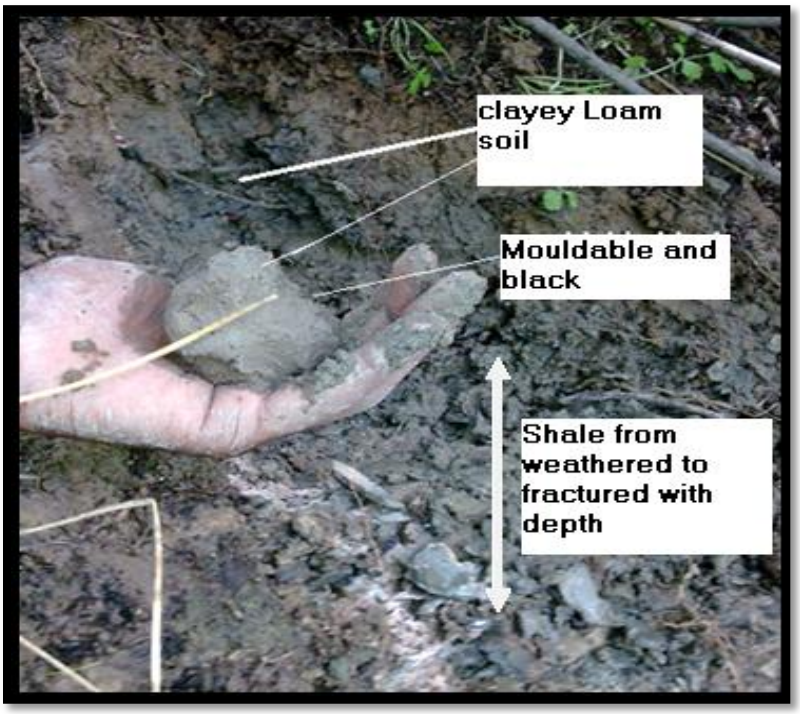

Figure 3-7: Clay caused as a result of excessive weathering of shale.

The weathering of shale resulted in soft and brittle horizontal layers. Excessive exposure to weathering causes shale to break down into black loam soil which is the same as that shown on Figure 3-7.

Figure 3-8 shows a spring that seeps through the shale formation along the river bank. Naturally, shale has horizontal layers due to deposition. When exposed to weathering, fractures are formed in between the layers and such fracturing gives rise to higher transmissivities, hence a spring is formed.

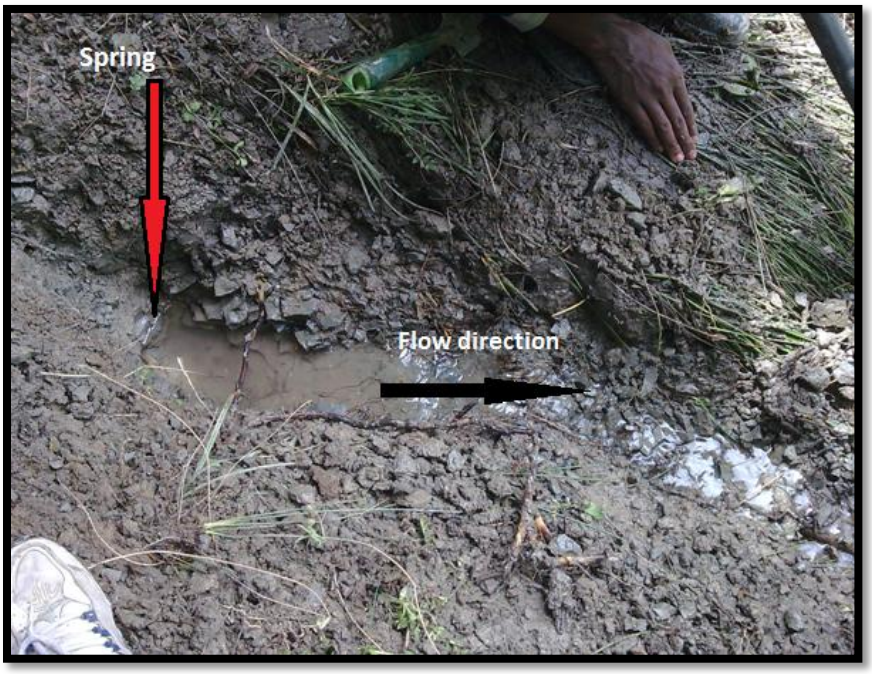

Figure 3-8: Spring water seeping through the shale layers

The geology of the area changes downstream. Below the weir about 5 km downstream of the site, there is a massive mudstone outcrop that forms a visible thickness of about 2 meters (Figure 3-9). Ten meters downstream of the weir runs a dolerite dyke that clearly outcrops the mudstone formation crossing the river (Figure 3-10).

Figure 3-9: The Mudstone river bed and the position of the weir relative to the mudstone mass.

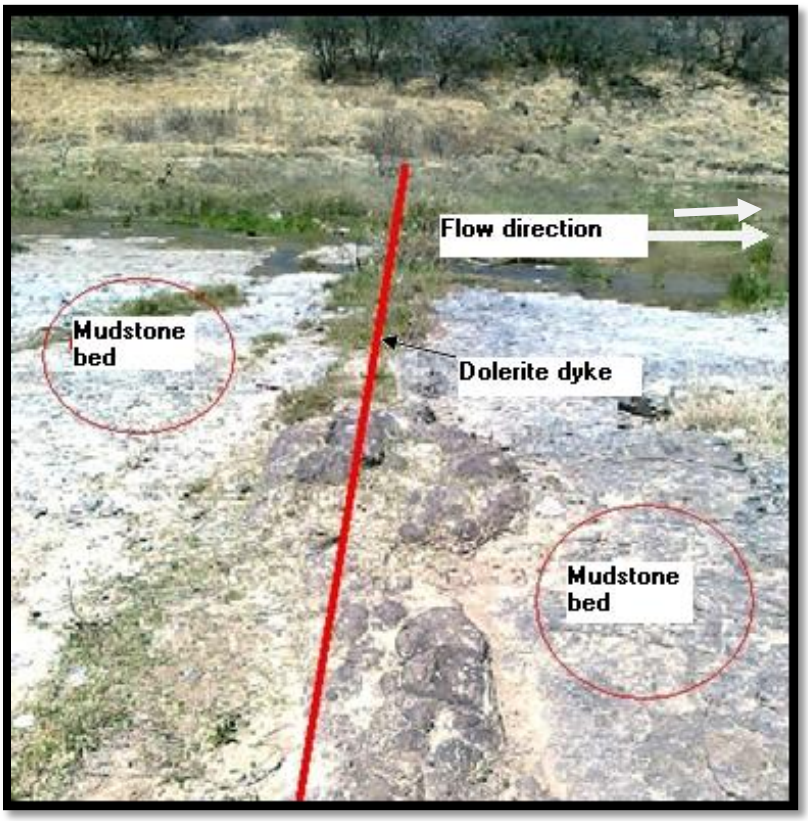

Figure 3-10: Dolerite dyke across the river bed.

Figure 1-6 shows the locations of the above described geological outcrops that were observed during land surface inspection.

3.3.3 Drilling

15 boreholes were drilled onsite with varying depths that were meant to hit different aquifers.

The drilling at the site was performed using the air percussion drilling method which is usually used for groundwater abstraction purposes (Figure 3-11). The drilling chips were sampled per meter and the water strikes recorded. Samples were taken to IGS where the consolidated matter was washed and carefully studied per meter noting the geological class, colour, and texture.

Most of the surface soils had calcrete traces of varying calcrete composition; therefore classification was performed based on the dominant geology within that meter depth.

For the purposes of this study BH10, BH11, BH12, BH13, BH14, and BH15 were used. The site is on average 200 m away from the river so for purposes of geological characterization, BH3, BH5, BH6, BH7, BH2 shall also be used in combination with the observed geology on the river banks in order to produce a clear and more accurate geological conceptual model that shows the transition of geology from the river to I nland.

Figure 3-11: Air percussion drilling machine in action on site

Table 3-1 shows the boreholes depths and their water strikes. The anticipated drilling network was a series of triangles of borehole which were intended to determine the groundwater flow

direction and the transport parameters of the aquifers. Figure 3-12 shows the positions of the boreholes and locations from which soil samples S1, S2, and S3 were obtained.

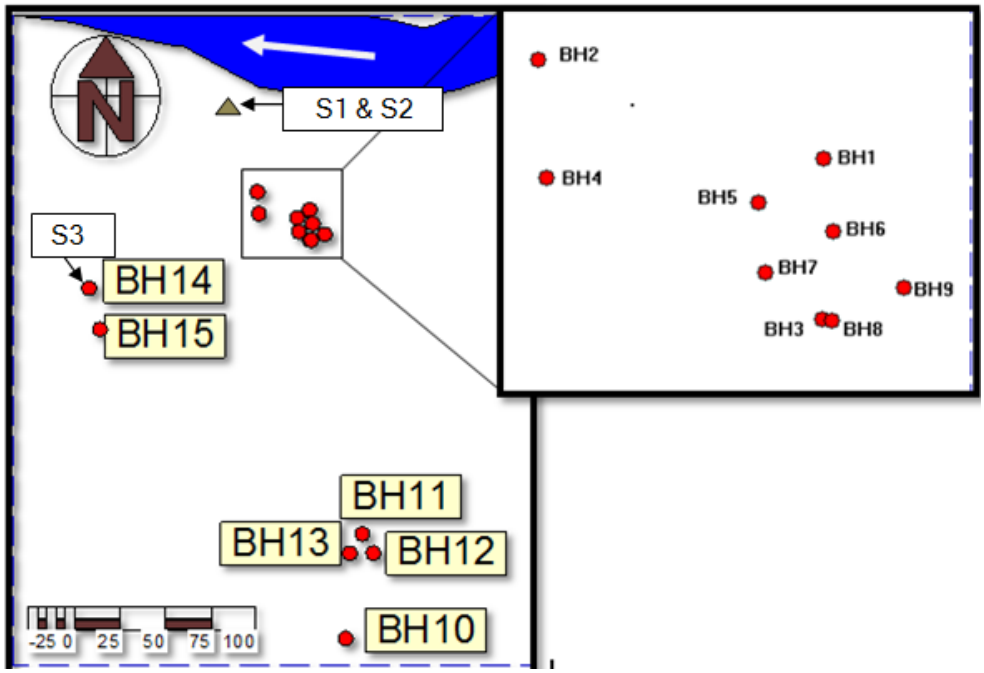

Figure 3-12: Boreholes and soil sampling positions

Figure 3-13 shows the geological cuttings of BH10 while that of BH11, BH12, BH13, BH14, and BH15 are in Section 9.1 Appendix A. The overall geology file of the area is provided in the appendix file as a WISH file.

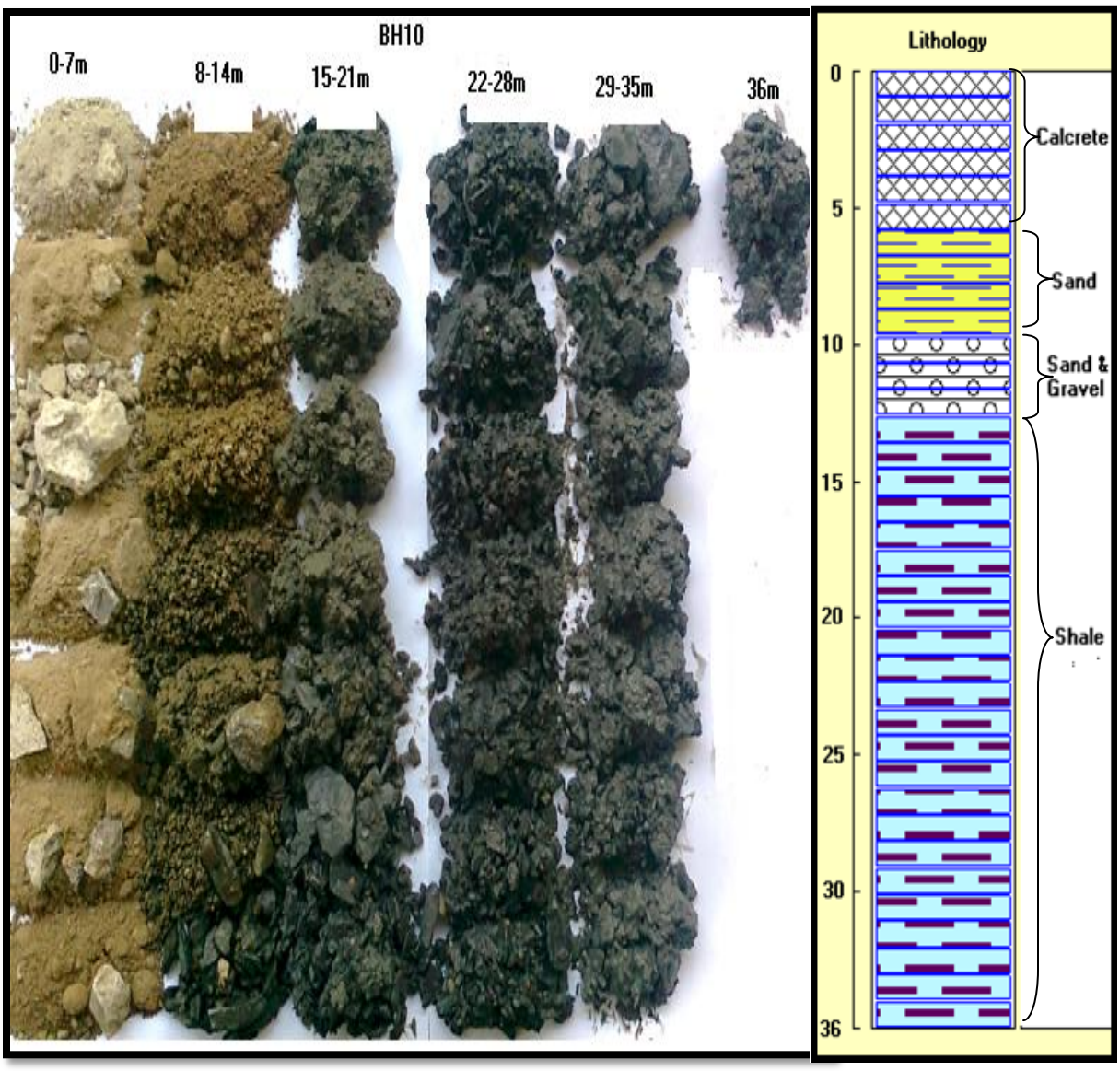

Figure 3-13: Geological samples and logging showing BH10 geology profile

Figure 3-14 shows the cross-sectional view of the boreholes that are used in this study. The figure shows the positioning of the boreholes relative to the others in terms of elevations, and depth. The figure also shows the construction of the boreholes, water strikes and the water level as obtained in February 2011. The figure also shows the river stage on 13 January 2011.

Because of the steepness at the river bank adjacent to the study site, the river stage could not be measured there. The nearest reachable site with a smooth slope was about 5 km downstream where this reading was made. A downstream weir keeps the river stage close to horizontal; therefore the river stage at the site may well be represented by the downstream value.

Table 3-1: Water strikes and depths of boreholes

BH Name	Water strike (maml)	BH depth
Triangle 1		
BH 5	1234.3	12
BH6	1235.3	12
BH7	1234.6	12
Triangle 2		
BH11	1236.7	18
BH12	1236.5	18
BH 13	1236.8	18
Other Boreholes		
BH10	1237.5	36
BH14	1236.1	12
BH15	1236.3	18

From the number of geological logs that were obtained, it was observed that the general geology is in the order; soil/calcrete, sandy gravel pack (which consists of well rounded cobbles and boulders of mostly mudstone), and the hard consolidated shale which acts as the lower aquiclude of the aquifer. The water strike in all boreholes was within the gravel formation which lies on top of the shale bed just above the consolidated shale (Figure 3-14). It can therefore be hypothesized that flow in this area occurs within the gravel material

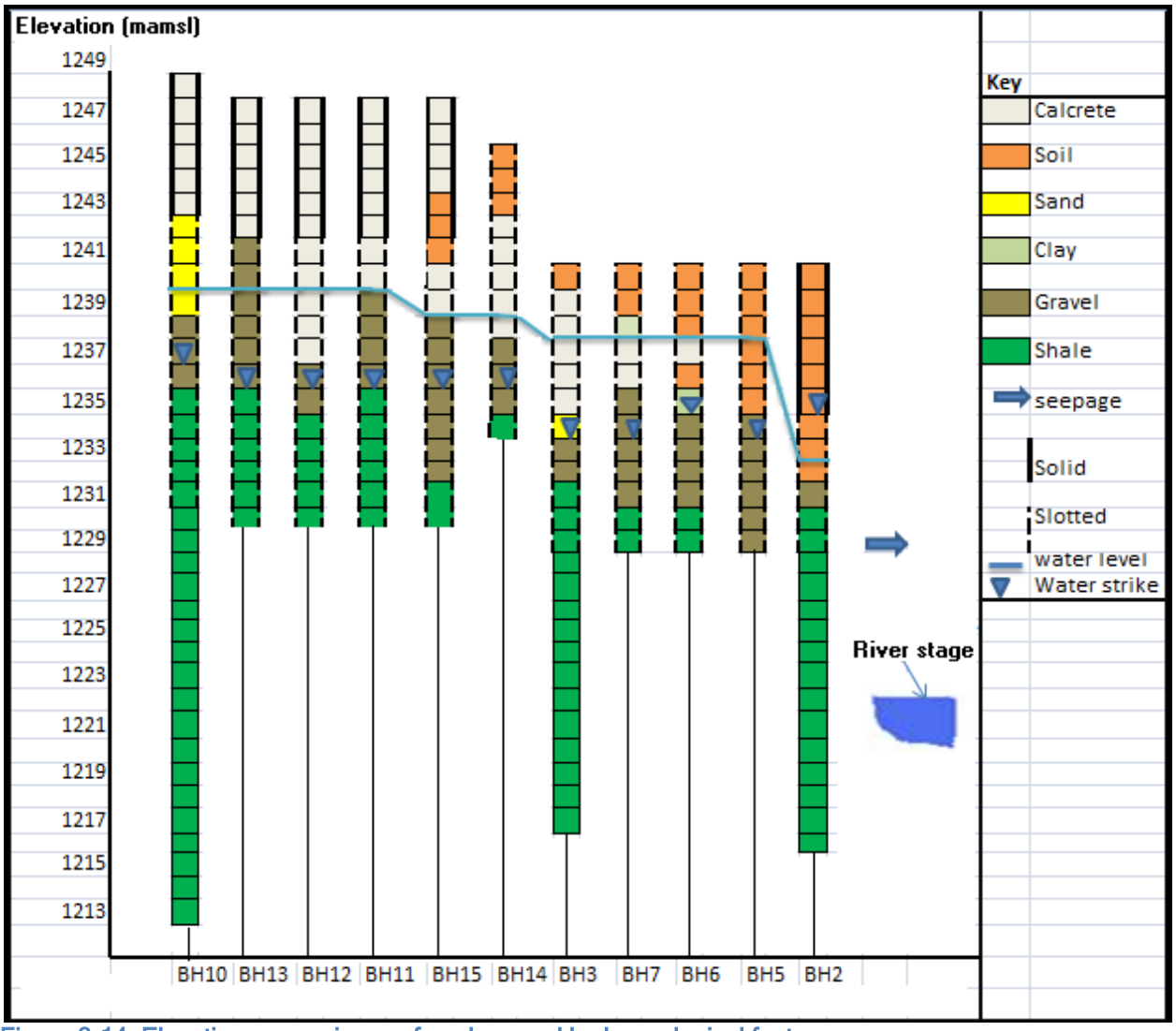

Figure 3-14: Elevation comparisons of geology and hydrogeological features.

3.3.4 Unconsolidated surface soil matter-Soil analysis

The study area is covered by a massive spread of calcareous rock that protrudes the calcrete rich soil at numerous locations. Some area is covered by a thin layer of top soil whose thickness is so minimal (about 30 cm) that the drill rig quickly reached the consolidated calcareous rock. The geological logs therefore show a surface that is more dominated by calcareous soil than top soil.

3.3.4.1 Soil analysis

Soil samples that were collected were: the weathered mouldable shale above the fractured shale (**S1**), the soil material on top of the shale formation (**S2**), and the inland soil cover in the vicinity of BH14 (**S3**). This was done with an objective of determining the sand and clay content in the soil cover on site. Figure 3-12 shows the positions on which soil sampling was done.

In preparation, the soil was crushed and sieved through a 2 mm sieve. Since soil is below 2 mm diameter (Laker *et al.*, 1982) and above 2 mm is gravel, the material that was bigger than 2 mm was thrown away. 25 g of each sample was weighed and 50 ml of a dispersing agent called calgon (sodium hexametaphosphate 10 g of Na_2CO_3) was poured into the sample. The dispersing agent is meant to separate clay from sand. Approximately 500 ml was added and the contents stirred for 10 minutes. The sample was then washed through a 0.5 mm sieve (into a 1000 ml cylinder) so that what goes through is clay, what remains is sand. The sieving was done until the filtrate from the sieve was clear as an indication that there is no more clay left in the sieve.

The soil content determination procedure involved two main sections which are the separation of the sand fractions and the separation of the clay/silt fractions.

Sand fractions

The sand sediments were put in the oven for drying. When completely dry, the sample was sieved through three tower sieves to separate coarse (2-0.5 mm), medium (0.5-0.025 mm) and fine sand (0.25-0.05 mm PAN). The separates were then weighed and their mass recorded.

Clay/silt fractions

This section was analysed using the Stokes Law theory by the pipette method for particle size analysis. This procedure makes use of the idea that when particles of different diameters are in a fluid and set to motion (shaking) such that the particles are spread evenly within the fluid, the rate at which the particles will settle will depend upon the diameters of the individual particles. If a sample is drawn immediately after shaking at t=0, and latter at t=1, and for the last time at t=2, the masses obtained at each sampling interval will decrease in the order M0>M1>M2. This is because, in M0 at t=0, the fluid is homogeneous (it contains coarse silt, fine silt, and clay), after some time the coarse silt particles settle first such that at t=1 M1 has no coarse silt but only fine silt and clay, finally at t=1 M1 has only clay. The extractions consist of the following masses; M0 consist of particles that are 0.05 mm (coarse silt), M1 0.02 mm (fine silt) while M2 has 0.002 mm (clay).

The 20 ml samples were drawn at 0 minutes, 5 minutes 10 seconds and 6 hours 10 seconds after shaking. Together with the soil samples a blank solution which contains tap water and 50 ml calgon was prepared and samples at equal intervals with the soil. The blank was prepared with the intention of clearing out the mass in the clay/silt component that is due to the weight of

calgon that was added in the soil. The drawn samples were dried in the oven and their masses measured and recorded.

3.3.4.2 Soil analysis results and discussions

The percentage compositions in respect of fractions of sand, silt and clay were calculated and recorded as shown on Table 3-2 and Table 3-3.

Table 3-2: Percentage composition of sampled soil showing six fractions

	Percentage composition (%)						
Sample ID	Coarse sand	Medium sand	Fine sand	Corse silt	Fine silt	Clay	Total
S1	4.12	17.36	61.92	3.20	4.40	7.04	98.04
S2	1.96	4.48	41.04	15.00	20.60	14.24	97.32
S3	16.32	10.88	50.92	7.00	9.00	4.84	98.96

From Figure 3-16 it can be concluded that the soil sample S2 is finer than all other samples because there is more weight in the fine section towards clay than there is in the other samples hence the soil is classified as a loam soil in the textural class.

Figure 3-15 and Figure 3-16 show the soil analysis results comparing the composition abundance of sand, silt and clay in the soils sample. From this, it is evident that the most abundant soil class is sand followed by silt and clay. The soil cover on the edges of the river bank (S1), is the most sandy, while the soil just above the fractured shale (S2) is the most silty. Figure 3-17 shows the textural triangle for the analysis of the soil. S1 is classified as loam soil; S2 and S3 are loamy-sand soils. According to the textural composition, S1 and S3 are the same but chemically, S3 has more calcrete traces than S1.

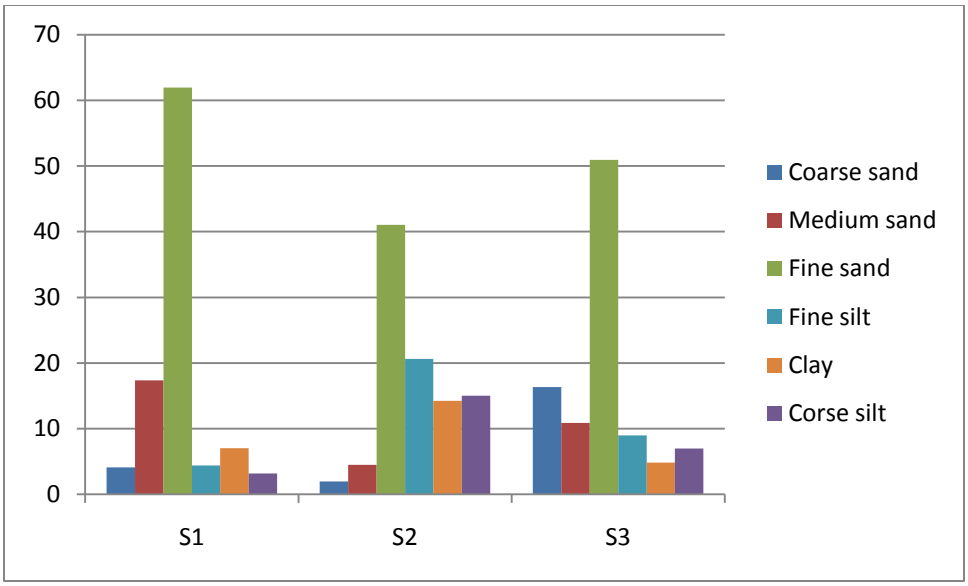

Figure 3-15: Percentage composition of soil in six soil classes.

Table 3-3: Percentage composition of soil in three soil classes

	Percentage composition (%)		
Site ID	Sand	Silt	Clay
S1	83.4	7.6	7.04
S2	47.48	35.6	14.24
S3	78.12	16	4.84

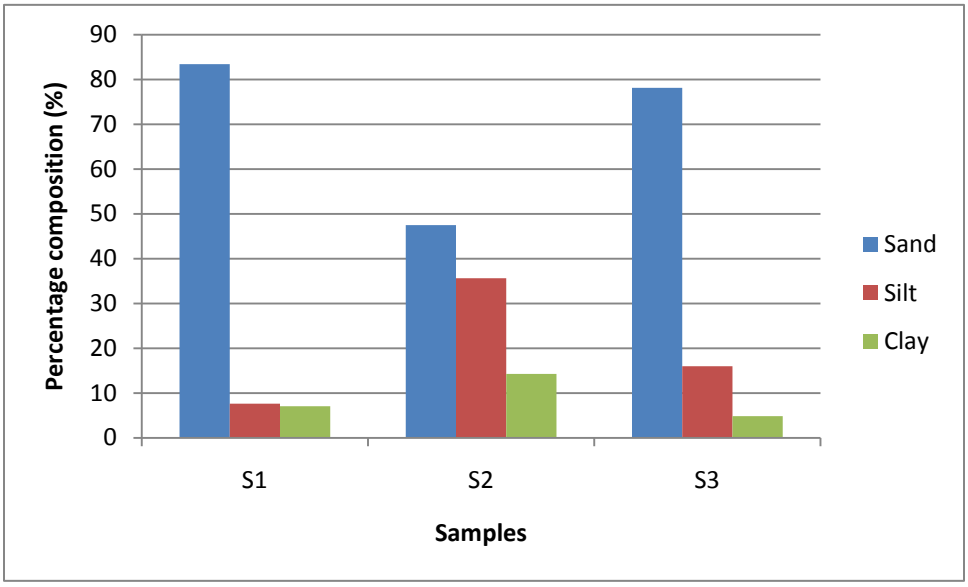

Figure 3-16: percentage composition of the soil samples in three class separations

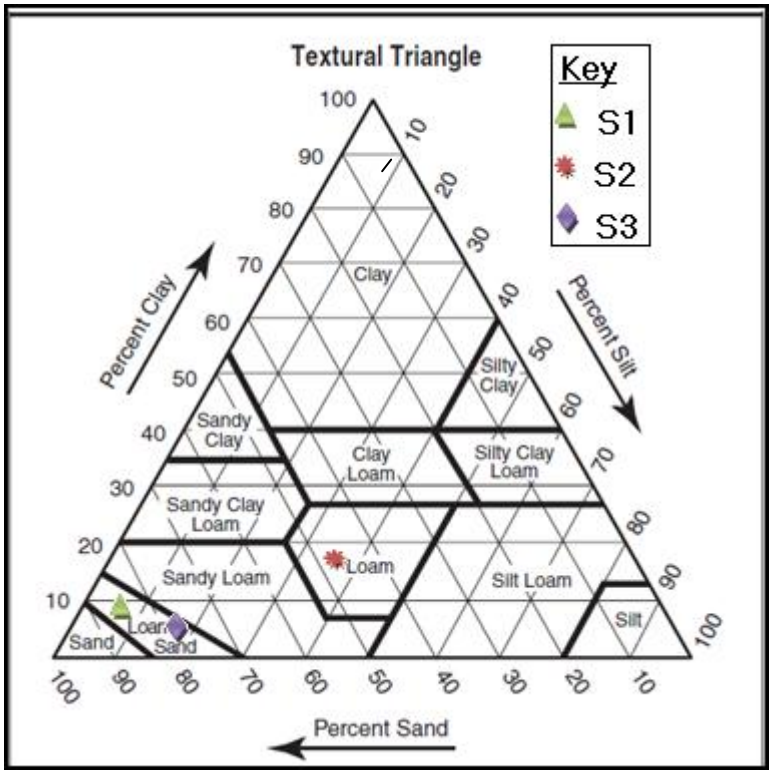

Figure 3-17: Soil textural triangle used for determination of soil type on site.

To establish the chemical difference between the two soil samples, acid test was performed on the soil and it was observed that the addition of dilute HCl on S3 soil sample gave rise to effervescence (CO_2) while just a little was produced in S1. Figure 3-18 illustrates the reaction that occurs between dilute hydrochloric acid and carbonates to produce carbon dioxide in S3. The reaction is explained by reaction (1).

$$CO^{2+}_{3(s)} + 2H^{+}_{(aq)} \longrightarrow H_2O_{(l)} + CO_{2\,(g)} \qquad (1)$$

Figure 3-18: The production of CO_2 from the reaction of dilute HCl and Carbonates in the soil.

In conclusion, the soil cover at the edge of the river bank (S1) is texturally similar to the soil inland (S3) and they differ from the soil from the weathered shale above the fractured shale formation (S1). S1 and S3 are loamy-sand soils while S2 is loam soil. Chemically, S1 and S3 are different by that S3 has more carbonates than S1. The soil cover can therefore be conceptualized to the changing from inland to the bank by having a decrease in calcrete formation as one approaches the river.

3.4 Conclusion and geological conceptual model

Land surface inspection reveals that there is a change of geology as one approaches the river. The gravel layer becomes less visible, the calcrete outcrops are replaced by a loamy-sand on the bank edges, and the shale becomes more weathered and fractured which may be due to exposure to the weathering elements such as air, water, and temperature variations.

The dominant geological overlying material for the entire area is consolidated calcrete that protrudes calcrete rich soil at numerous locations. According to the logs, BH14 and BH3 have an overlying loam-sand material. This material has some traces of calcrete pebbles and calcrete derived soil. Based on the geological content of the top log, it can be concluded that the whole area has its overlying material as calcrete.

Below the calcrete layer lays a thickness of about 3 meters of gravel and sand material. This layer comprises rounded mudstone pebbles and rough gravel which includes quartz particles (Figure 1-10) which have possibly been brought by river deposition.

The smoothness of the geological structure is an important tool in hydrogeology to determine a formation (from the drill cutting) where water usually flows. It is needless to say that the roundedness of the pebbles assures that there is a movement of water within the gravel packing. Also considering the fact that this layer has both the highest porosity and the highest effective porosity compared to the whole geological profile is an indication that the gravel formation is the zone of groundwater flow.

The hydraulic conductivity of gravel is in the range 100 to 1000 m/d (Table 2-2) while that of shale is $5x10^{-8}$ to $5x10^{-6}$ m/d. Relative to all the other formations in the aquifer, shale has the lowest hydraulic conductivity value while gravel has the greatest value. Since the topsoil, calcrete, and shale all have a low hydraulic conductivity, it can be concluded that the main flow channel between the boreholes is in the gravel material which is at the general depth of 8 mbgl.

It is therefore concluded that the hydrogeology of this area is dominated by flow in the alluvium material at the general depth of 8 mbgl just above the shale bed. This flow possibly happens in the direction of topography. Figure 3-19 shows the general geological conceptual model of the area.

Knowledge of how deep the shale formation goes is beyond the aim of this study but the average depth of the shale surface is 10m below ground level. Even though this may be beyond the scope of this study, it is possible that below the shale formation could be a mass of mudstone. Figure 1-6 and Figure 3-9 reveal that 5 km down the Modder River from study area is a mass of mudstone that forms the base of a river. This *could* be a formation just below shale.

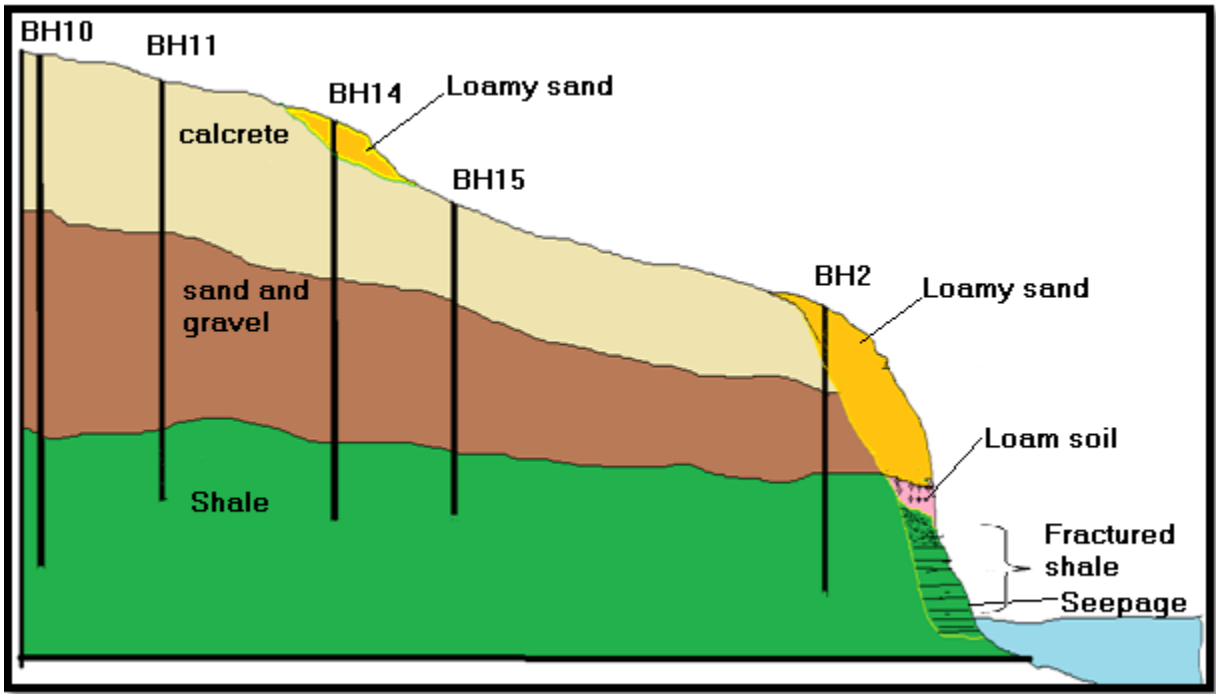

Figure 3-19: Geological conceptual model of the study area (Not drawn to scale).

4 BOREHOLE CONSTRUCTION, NETWORK DESIGN, AND FLOW BEHAVIOUR

4.1 Introduction

This chapter gives a brief on the borehole locations, construction techniques followed. It also explains the groundwater dynamics of the site being groundwater fluctuations, groundwater flow direction, natural groundwater discharge and recharge.

4.2 Network design and borehole construction

The monitoring network was installed on the banks of the Modder River with boreholes of different depths of which the idea was to target different aquifers systems. One of the objectives of this study is to determine the direction of groundwater in the study area. Therefore Figure 4-1 shows the aerial map of the area and the drilled borehole locations.

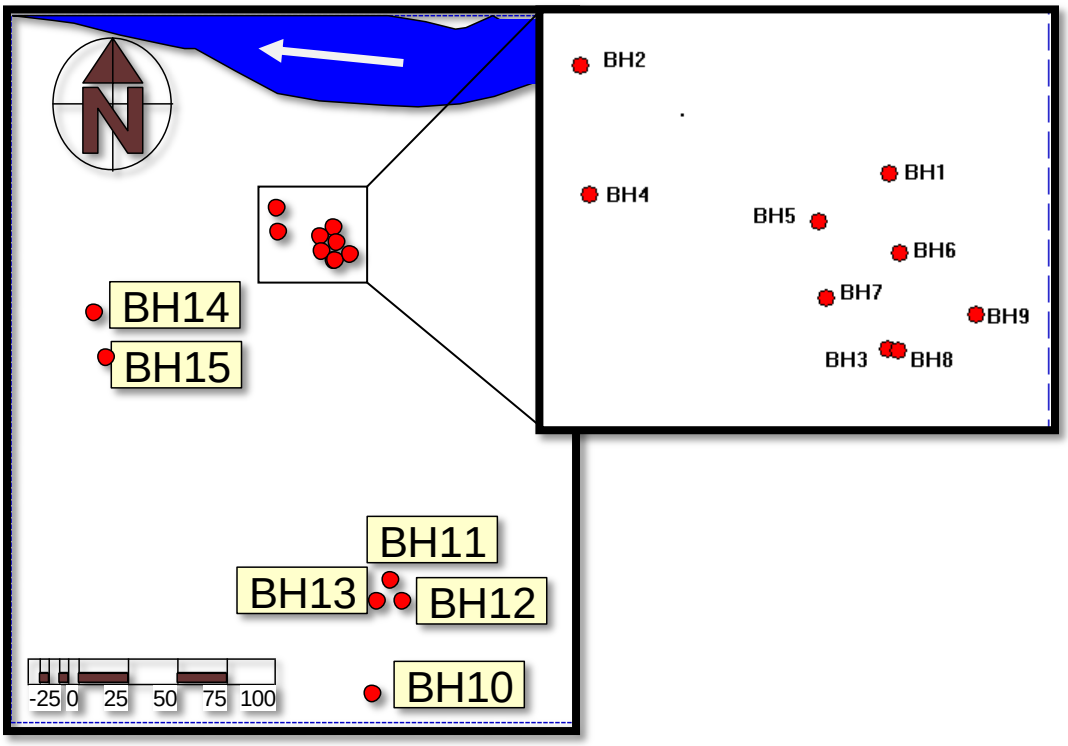

Figure 4-1: The aerial view of the boreholes that were drilled on site showing the river flow direction

The study area is at a rough topography hence it was important to do an elevation survey to obtain the proper surface elevations of the boreholes. The elevation information as well as the construction information is given on Table 4-1.

Table 4-1: The construction information of the boreholes including the positions of the water strikes.

Borehole names	Collar height (m)	Depth of casing (m)	Water strike (m)	Depth of Borehole (m)	Surface elevation (masl)
BH10	0.25	18	12	36	1249.48
BH11	0.25	18	12	18	1248.67
BH12	0.25	18	12	18	1248.47
BH13	0.25	18	12	18	1248.77
BH14	0.25	12	10	12	1246.10
BH15	0.25	18	12	18	1248.28

Figure 4-2: Sanitary seal of the boreholes.

A tri-pot theodolite and staff (Figure 4-3) were used to survey the elevations of the boreholes and other hydro-geological features given in this thesis as presented in Table 4-1.

Figure 4-3: Theodolite and staff used for surface elevation survey

Figure 4-4: Screening of PVC casings for borehole construction.

A 5.5 inch PVC casing was installed in all the boreholes and slotted based on the positions of the water strikes and the adjacent geology. Looking at the borehole logs, the consolidated geology starts between the depths of 11 m and 13 mbgl. The casings for 18 m boreholes were slotted from 13 m all the way while BH10 which is 32 m deep was cased for 18 m and slotted from 13 m to 18 m and the remaining depth left uncased. The boreholes were sealed and sanitized as shown in Figure 4-2, and the casings were screened as shown in Figure 4-4. Figure 4-5 shows the construction of BH10 and the positions where it was slotted

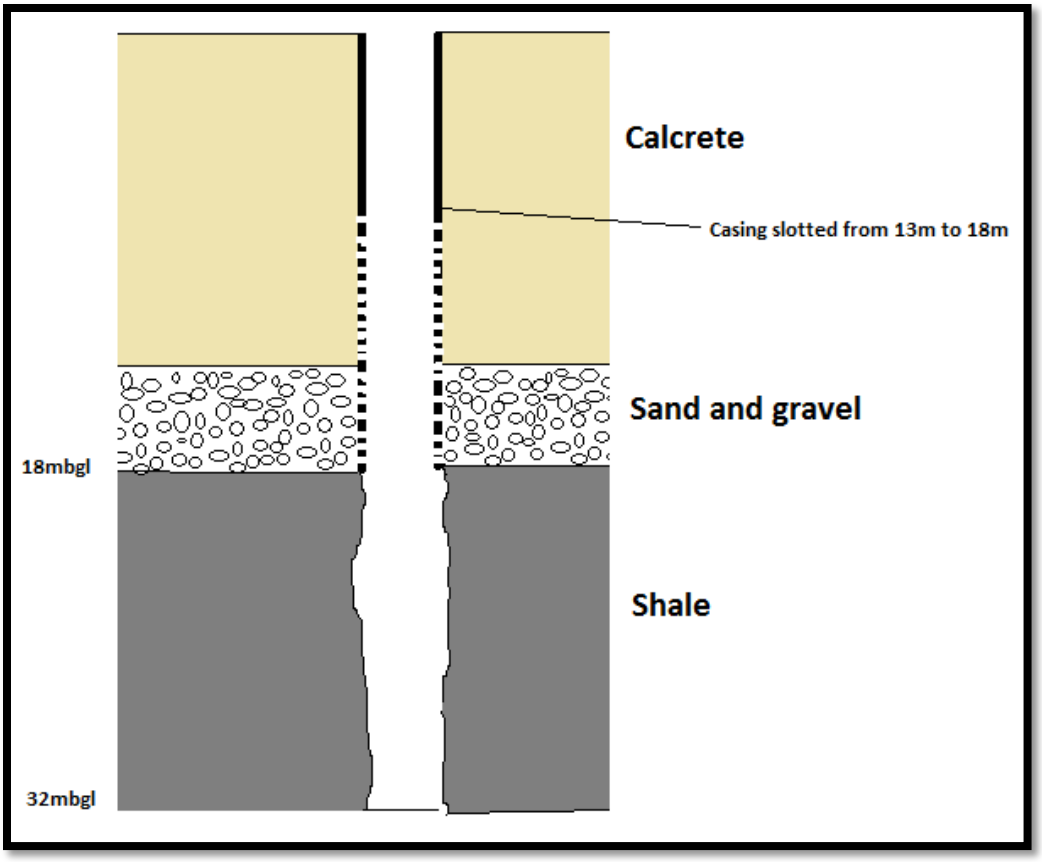

Figure 4-5: Diagram of the borehole casing as installed in BH10

4.3 Natural groundwater behaviour on site

4.3.1 Change of Water level with time

The direction and slope of the water table in an unconfined aquifer (or a potentiometric surface of a confined aquifer) are determined by measuring the water levels relative to a datum plane that is common to all wells. The datum plane most widely used and easy to use is the National Geodetic Vertical Datum of 1929 usually referred to as the sea level (Heath, 2004).

The unconfined aquifers have a high correlation between water levels in meters above mean sea level (mamsl) with surface elevations of boreholes in mamsl, meaning that, water levels in unconfined aquifers have a general behaviour of following topography hence the high correlation. Figure 4-6 shows a correlation of 91.3 % of surface topography and water levels from water level data of January 2011. A 100 % correlation would indicate the presence of an entirely unconfined aquifer system. Based on the correlation that is observed between surface elevations and groundwater levels on site, it can be concluded that groundwater on site is in an unconfined to semi-confined aquifer system.

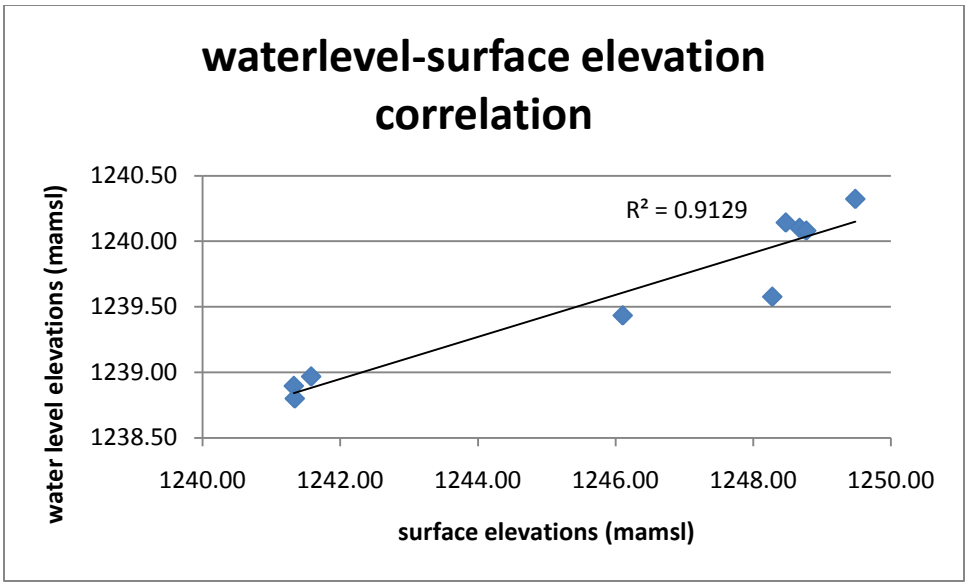

Figure 4-6: The correlation of water-levels with surface elevations

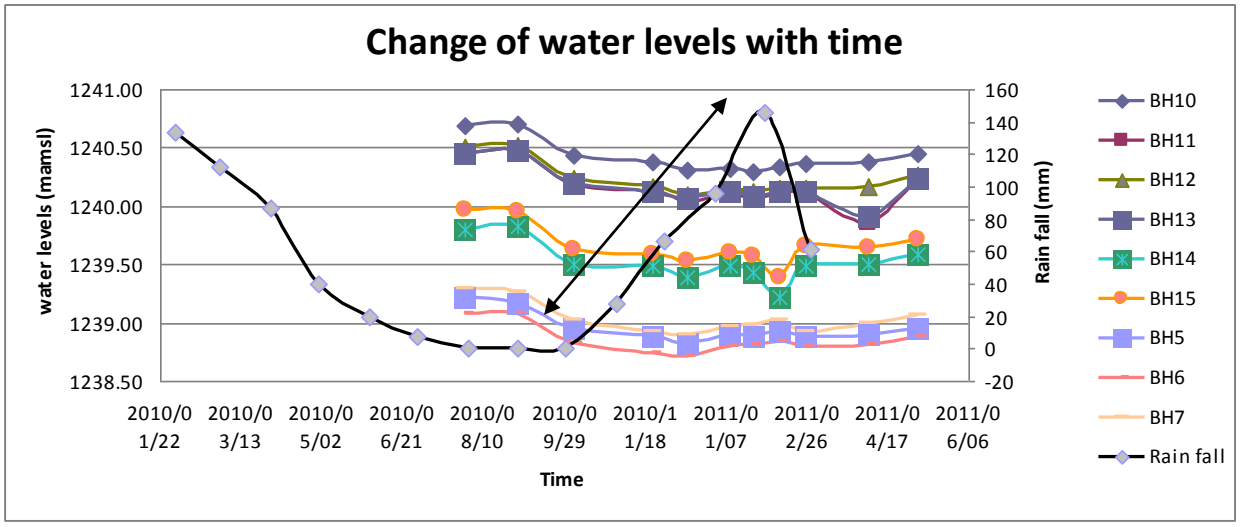

Figure 4-7: Change of groundwater water levels with time for the 6 months period

Figure 4-7 shows how the water levels in the area changed over a period of 11 months. The double arrow shows the period of increase in rainfall till it reached its peak. Based on the groundwater fluctuations, several conclusions can be established from Figure 4-7. Firstly, it can be concluded that groundwater on the study site is in the same aquifer system based on the similar fluctuation trend that is observed among the boreholes over the period of 11 months.

Secondly, the rate of recharge is low and runoff is high, this conclusion is made on the observation that rainwater increased from September 2010 and reached its climax in January 2011, but the groundwater level has remained relatively constant over the 4 months period.

4.3.2 Natural recharge and discharge

An aquifer can gain or lose water in a number of mechanisms. These activities may respectively raise or lower the water table/piezometric head. Aquifer recharge may occur in a number of mechanisms be it preferred pathway through horizontal fractures or vertically through the soil layers. Natural discharge occurs in various ways including evapo-transpiration and seepages from springs where the land surface makes a syncline that goes below the water table or where there is a preferential path through which water flows from the aquifer to the land surface. In this study, natural discharge was based on the natural seepages at the river banks.

4.3.2.1 Natural Recharge

The chloride method was used to determine recharge for the aquifer. The geometric mean of the recharge percentage for the aquifer is 1.7 %. The recharge percentage is low compared to the value of 2.6 % which was estimated for the Karoo (Woodford and Chevallier, 2002). The rest of the data for the estimation of recharge can be obtained form Section 9.3 in Appendix C.

4.3.2.2 Natural discharge calculation

Prior site inspection operation revealed that adjacent to the study site, there are numerous seepage zones that continuously discharge groundwater into the river. Figure 4-8 shows an approximate position of a belt of groundwater seepage from fractured shale formation into the river.

Figure 4-9 shows how the seepage yield was measured in this study. A plastic bag was put as a base on top of the hard shale so as to make an impermeable V notch weir that collects water to a common outflow. The discharge yield was found to be 0.05 l/s from a 20 cm section of the river bank. Considering a seepage zone of length 100 m along the river bank, the total amount of water estimated to be flowing out of the aquifer into the river is 25 l/s. This is the amount of water that the aquifer is losing to the river per second along a 100 m section.

Figure 4-8: Seepage zone along the river bank.

The seepage is located 7 m above the river stage (Figure 3-14). The stream does not lose water to the alluvial aquifer, but it gains water from the alluvial aquifer through the seepage zone. Therefore, relative to the alluvial aquifer, this section of the river that is adjacent to the study site can be classified as a gaining stream. As to whether there is another aquifer below the shale formation that gains from the river is beyond the scope of this study.

Figure 4-9: Yield measurement technique that was followed

4.3.3 Groundwater flow direction

There are graphical methods available to determine the direction that the water table or the *potentiometric surface* is sloping and the gradient within the area outlined by the wells (Fetter, 2001). The discovery of these graphical methods involve the input of Vacher (1989) who presented the analytical solution to the three-point problem with a computer code for convenient solution. The use of tri-point water level to determine the direction of groundwater flow has been used in the past and it is one of the very convenient and accurate ways to determine groundwater flow direction.

The direction of groundwater flow was determined using the water levels that were monitored over time. This type of a technique can only be applied on the boreholes that intercept the same aquifer system (usually whose depths are equal) (Van Tonder, 2011). This is because the idea is to determine the direction of flow in a specific aquifer system. If a deep borehole intercepts both the upper unconfined aquifer an a deeper confined aquifer, the confined aquifer has a high piezometric head such that the water level in that boreholes may rise above the other boreholes that did not intercept the confined aquifer. This will give the wrong calculations of groundwater flow direction if the tri-well technique is used.

In this study, the direction of groundwater flow was determined using BH5, BH6, BH7, BH10, BH11, BH12, BH14, and BH15. These boreholes show a correlation of 92 % as shown on Figure

4-6. They intercept the same geological formation except BH5 that did not go as deep as the shale. But since the main groundwater flow zone in this area is in the gravel not in the shale, it is ideal to consider the hydrogeology to be similar in all the boreholes including BH5.

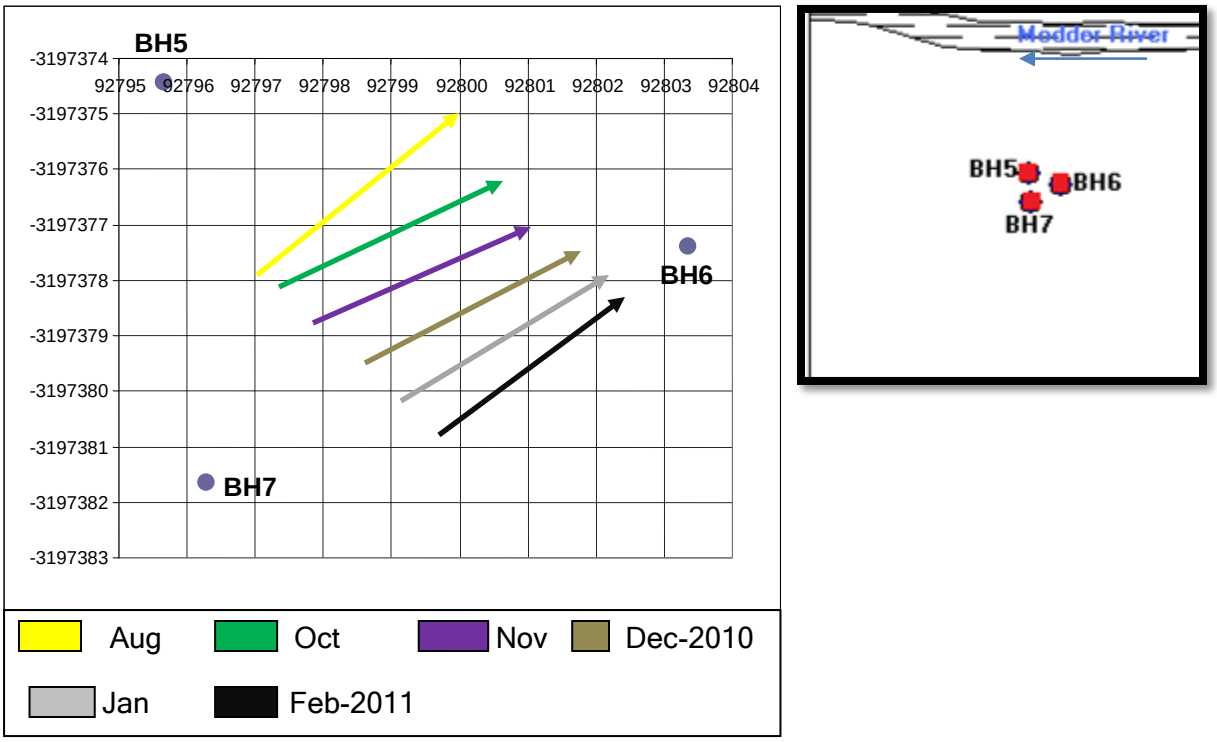

Figure 4-10: Groundwater flow direction as determined from BH5, BH6 and BH7.

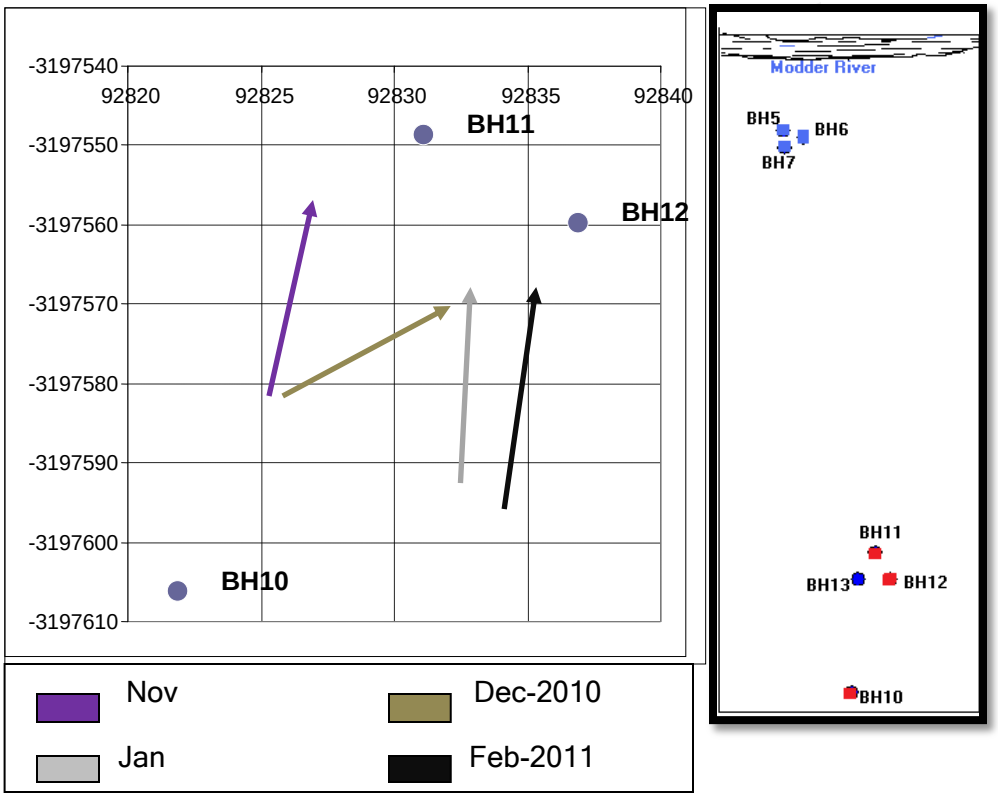

Figure 4-11: Groundwater flow direction as determined from boreholes BH10, BH11 and BH12.

Figure 4-10 to Figure 4-12 show the direction of groundwater as determined from different triangles of different sizes, locations and orientation. Small and large triangles were also used to determine the direction in which groundwater flows. Figure 4-11 and Figure 4-12 show how groundwater flow direction was determined from the bigger triangles while Figure 4-10 shows a smaller triangle closer to the river.

The choice of which boreholes to involve in a specific triangle was made based on the geology that the boreholes intersected; boreholes with similar geology were assumed to be in the same aquifer. The boreholes in each triangle have intersected similar geological formations and therefore qualify to be used in groundwater direction determination.

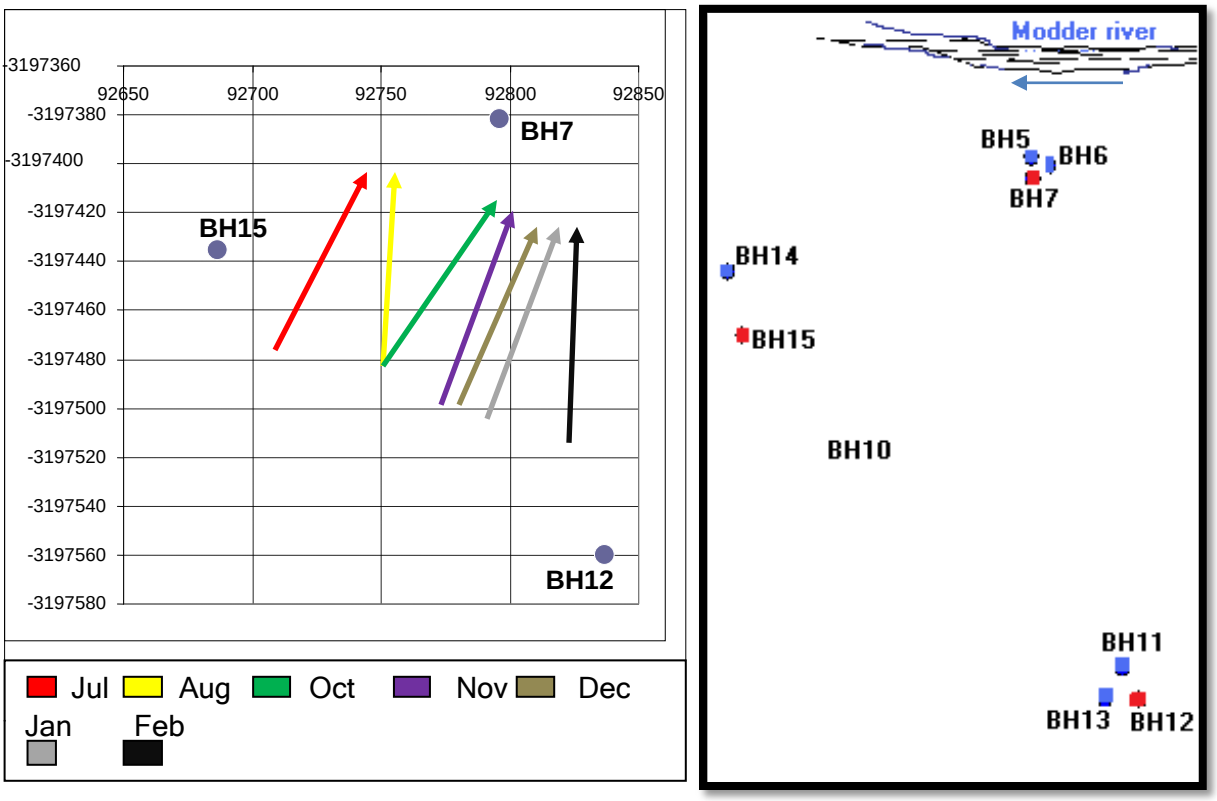

Figure 4-12: Groundwater flow direction determined from a bigger triangle 1

All triangles show that groundwater in this area flows in a north-easterly direction. Figure 4-13 shows the elevation contour map with vectors of surface slope showing the direction in which groundwater is flowing. The surface topography slopes between the directions north and north-east which is almost in the direction that groundwater is flowing. During land surface inspection a seepage zone was identified at the river bank located at the direction where groundwater is flowing. The seepage acts as a natural abstraction borehole, this maybe enhancing easy flow in the stipulated direction. A form of a semi-cone of depression is formed that creates a gradient towards the north-east such that groundwater tends to flow in that direction (Figure 4-14). The other reason for the direction of flow could be that there is a preferential flow path with a higher transmissivity in that direction such that groundwater moves with ease. Figure 4-13 illustrates the different directions of groundwater flow, surface slope, and river flow.

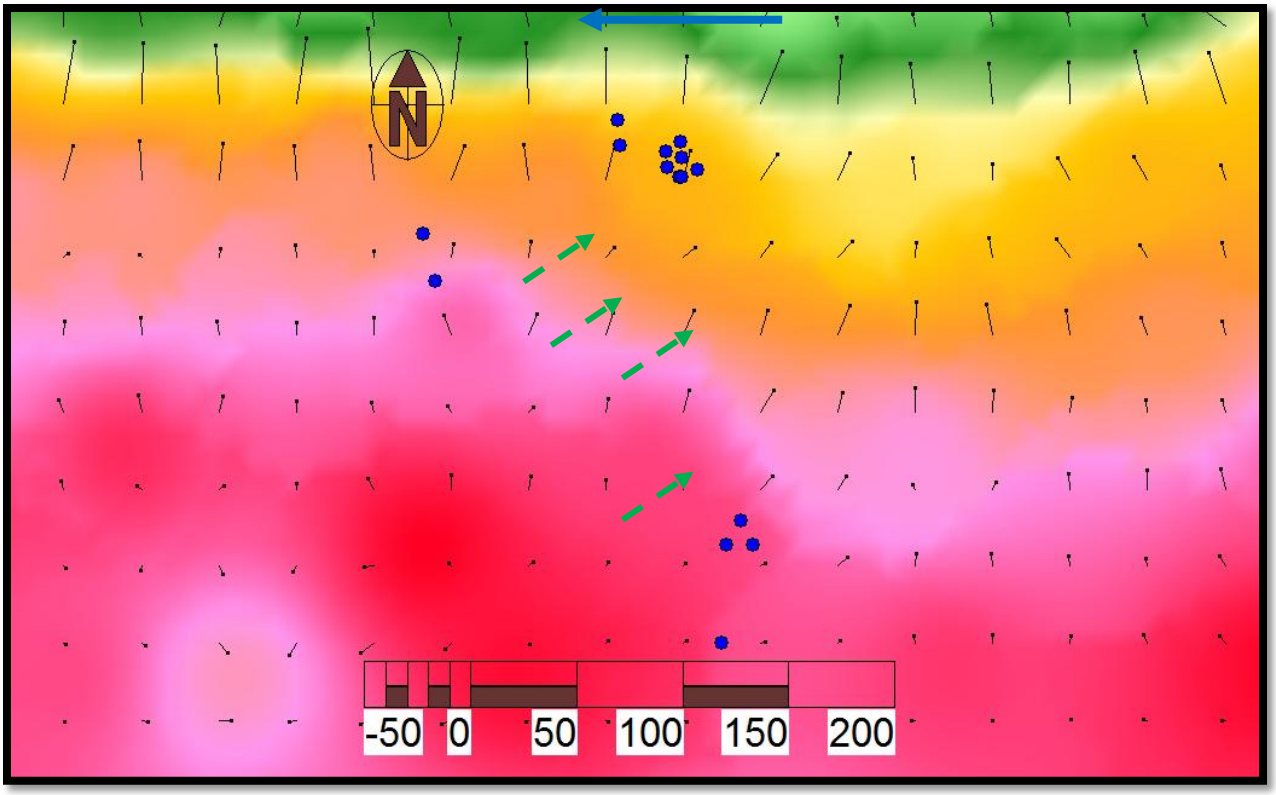

Figure 4-13: Groundwater flow direction versus change in topography (green dashed arrows are groundwater flow direction; black dotted arrows are topography slope direction).

4.4 Conclusions

Several conclusions have been established based on the observed groundwater dynamics on site. Because of the similar trend in increases and decreases of water levels among boreholes, it is concluded that all boreholes are drawing water from the same aquifer system regardless of their depth. Surface elevations versus groundwater levels have a correlation of 92 % and the aquifer is characterized as being between unconfined and semi-confined conditions. The alluvium aquifer releases water through a seepage zone into the river at an approximated rate of 25 l/s/100 m seepage length. The river section adjacent to the study site is therefore classified as a gaining stream. Groundwater naturally flows in the north-easterly direction which is in the direction of surface slope. Figure 4-14 shows a conceptualized groundwater flow direction on the entire study site.

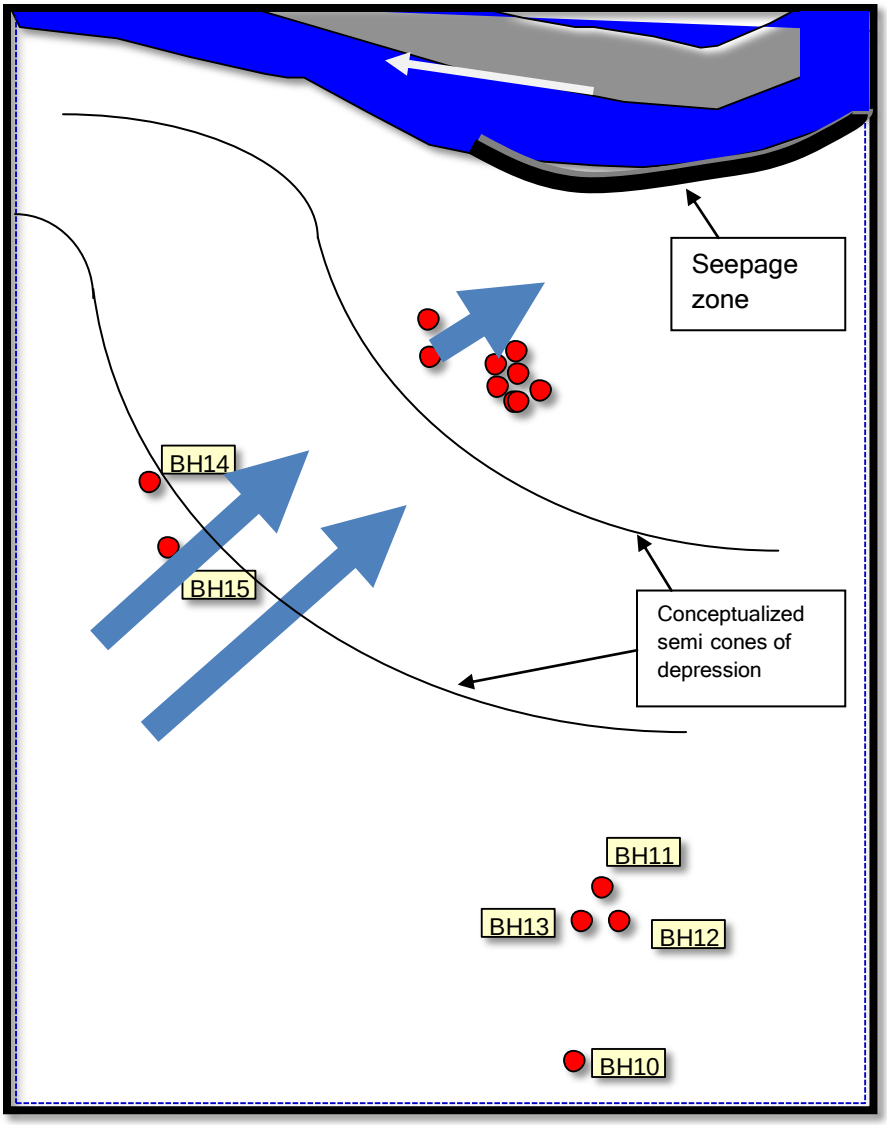

Figure 4-14: Summary of groundwater flow direction on site

Now that groundwater natural flow characteristics are understood, it is vital to explore the aquifer behaviour when exposed to pressure in hydraulic characterization which is followed by chemical characterization. Chemical characterization adds more information to the determination of the presence or absence of multiple aquifers in a system.

5 HYDRAULIC CHARACTERIZATION

5.1 Introduction

The hydraulic tests (aquifer tests) provide information on the type of flow that occurs in the aquifer and they are the simplest way to characterize the aquifer in terms of its parameters.

The two main reasons why hydraulic tests are conducted are, to obtain aquifer parameters, and to obtain the sustainable yield of the borehole. In some advanced cases where there is a multi-aquifer system, a number of observation wells and piezometers are drilled to reach different aquifers so as to obtain the characteristics of individual aquifer formations.

If a single private borehole is used for groundwater supply, a sustainable yield is determined in order to avoid the drying up of the well. In that case, there is no need for piezometers. The borehole is pumped and the hydraulic parameters for the intersected aquifer are determined (van Tonder *et al.*, 2001).

In this thesis, hydraulic tests have been divided into pumping tests and tracer tests. The types of hydraulic tests that meet these objectives include: (1) the slug test, (2) the calibration test, (3) the stepped discharge test, (4) the constant discharge test and (5) the recovery test (GHR 611 Lecture Notes, 2009). Tracer tests include (1) point dilution, (2) radial convergence, and (3) natural gradient tracer tests.

For the purposes of this study, only slug test, constant-rate test and recovery, and point dilution tracer test were performed.

5.2 Aquifer tests/pumping tests

5.2.1 Slug test

The slug tests were performed on all the boreholes to obtain the yield below which it can be deemed safe to conduct a constant rate test.

Rudolph *et al.* (1992) came up with the idea that there is a correlation between recession time of slug tests and the hydraulic conductivity of the borehole. Later, van Tonder *et al.* (1995) developed the technique that could be used to estimate the borehole yield from the slug test recession time. These researchers came up with Figure 5-1 which shows a correlation of 93 % between recession time and borehole yields. Table 5-1 shows data that was obtained from the slug test using Bouwer and Rice (1976) method. The borehole yield estimations in Table 5-1 were made using Figure 5-1.

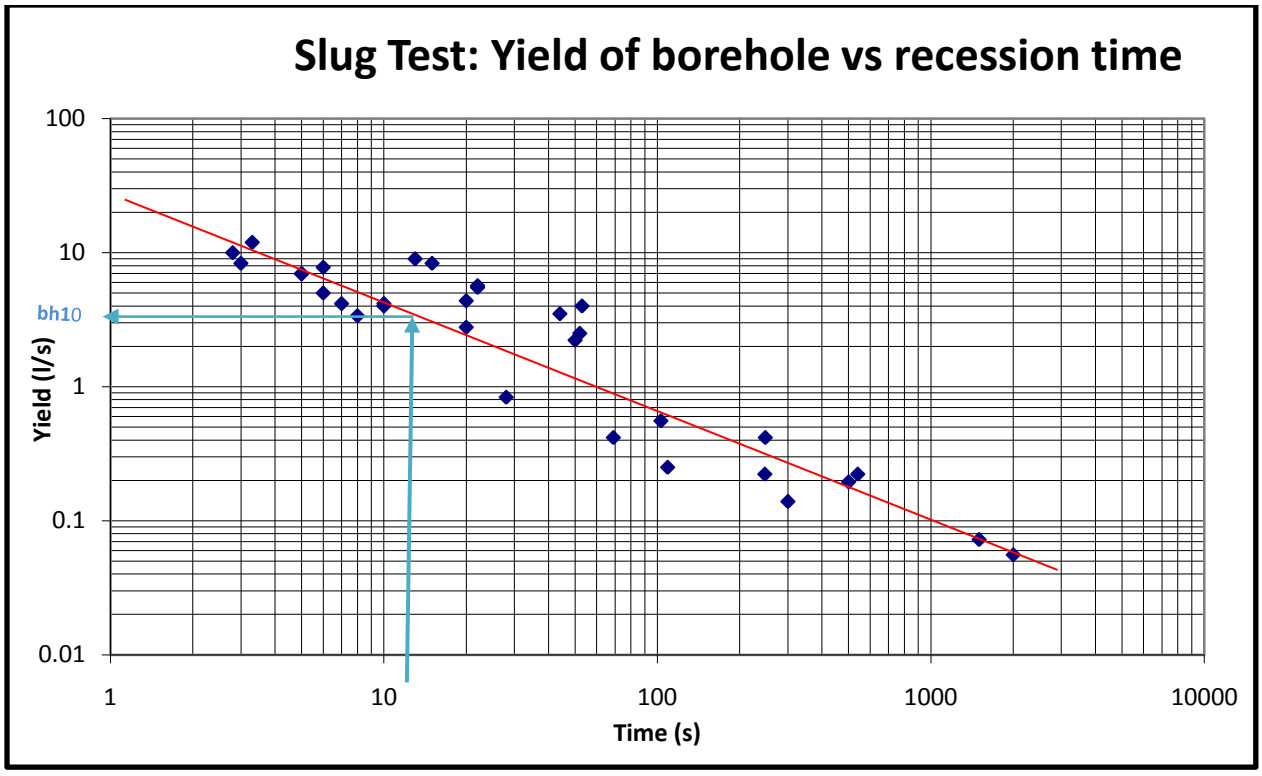

Figure 5-1: Correlation between recession time and borehole yields (representing BH10)

Table 5-1: Slug test results.

Borehole Name	Recession time (s)	Estimated yield (l/s)
BH10	13	3.3
BH11	52	1.1
BH12	25	2.0
BH13	28	1.8
BH14	8	4.0
BH15	43	1.3

Slug test recession time method shows that BH10 and BH14 are the strongest among the six boreholes (3.3 l/s and 4.0 l/s respectively).

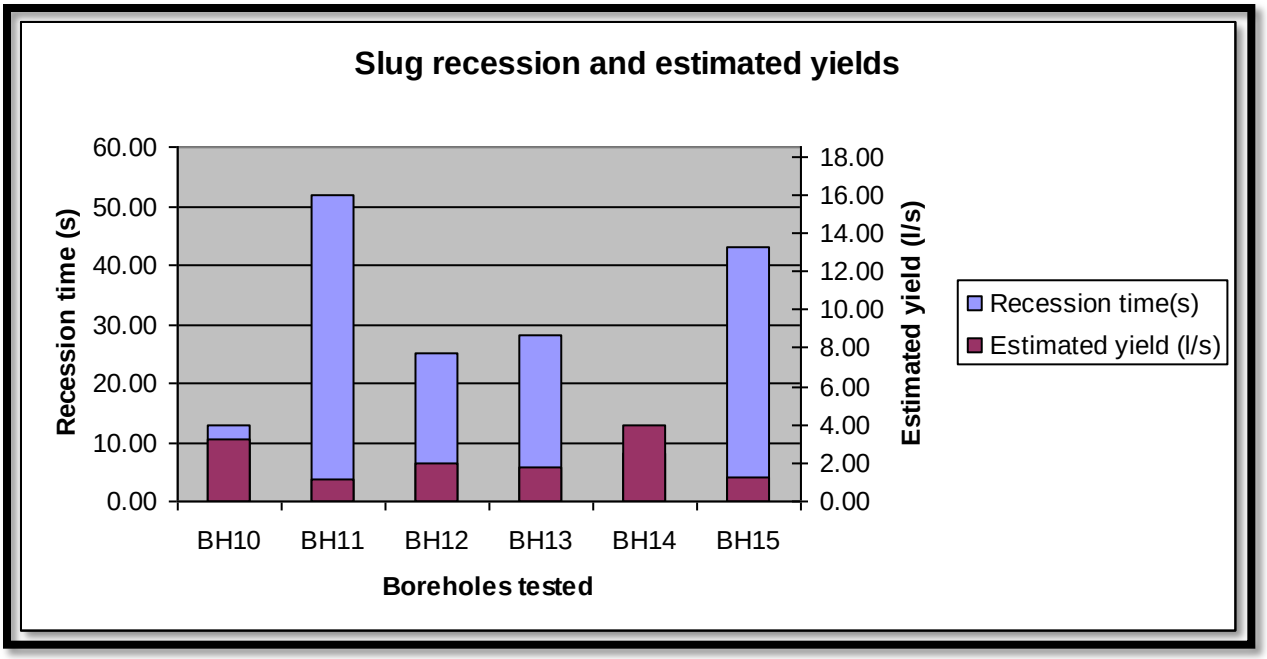

Figure 5-2: The comparison of estimated yields among slug tested boreholes.

5.2.2 Constant discharge test

Following the slug test predictions on borehole yields, the low yielding pump was used to pump the boreholes at the rate ranging from 0.5 l/s to 0.92 l/s with the intention to determine the aquifer transmissivity. The pumping yields were chosen with the idea of pumping at the rate that is not above the predicted yield from the slug test. Automatic water level loggers were used to record the water head in a borehole during pumping. The pump was eventually stopped and a period of average 30 minutes was allowed for the recovery. As soon as the pump stopped, residual water level was monitored against time using the level loggers.

The FC program by van Tonder *et al*. (2001) was used to determine the transmissivity of the aquifer formation and the best fit was obtained as in Figure 5-3 and Figure 5-4 for the Cooper-Jacob and diagnostic recovery methods respectively.

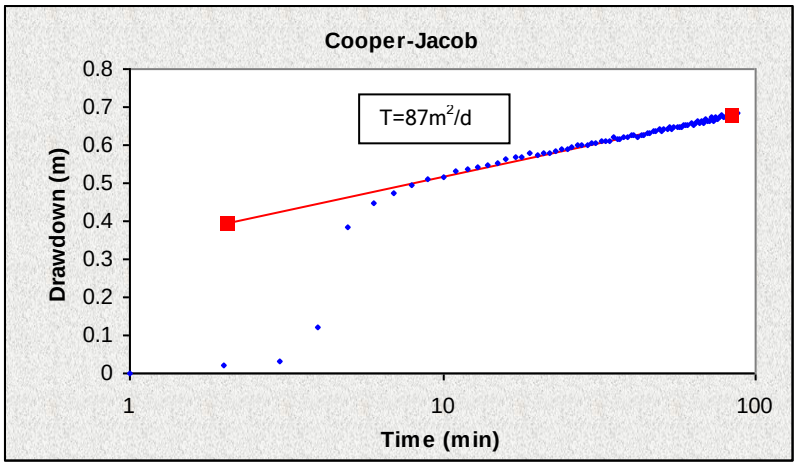

Figure 5-3: Cooper Jacob plot for pumping duration for determination of Transmissivity in BH10

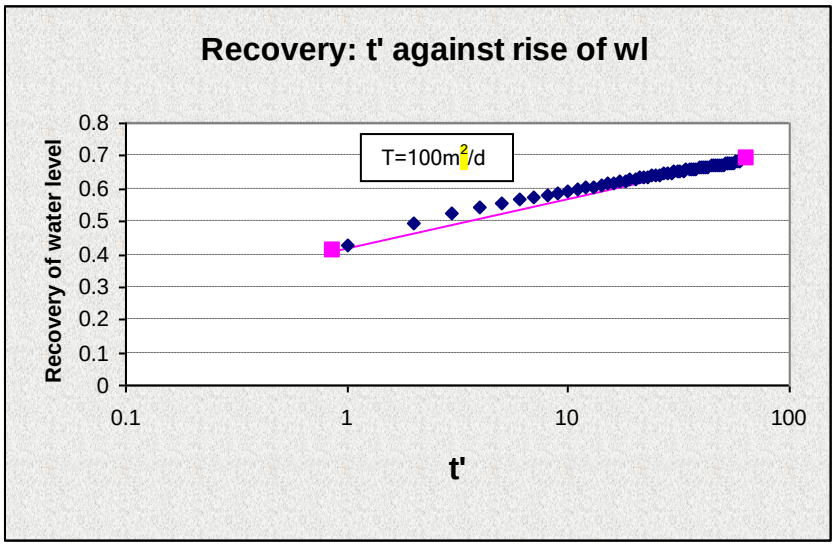

Figure 5-4: Recovery plot for BH10

Table 5-2 and Figure 5-5 show the transmissivity values of the boreholes as determined using the Copper Jacob method from the FC spreadsheet (van Tonder and Xu, 2001).

Table 5-2: Transmissivity values obtained from the constant rate tests.

BH NAME	Cooper Jacob estimated T (m^2/d)	Recovery estimated T (m^2/d)
BH10	87	100
BH11	44	19
BH12	49	20
BH13	2	4
BH14	269	139
BH15	58	54

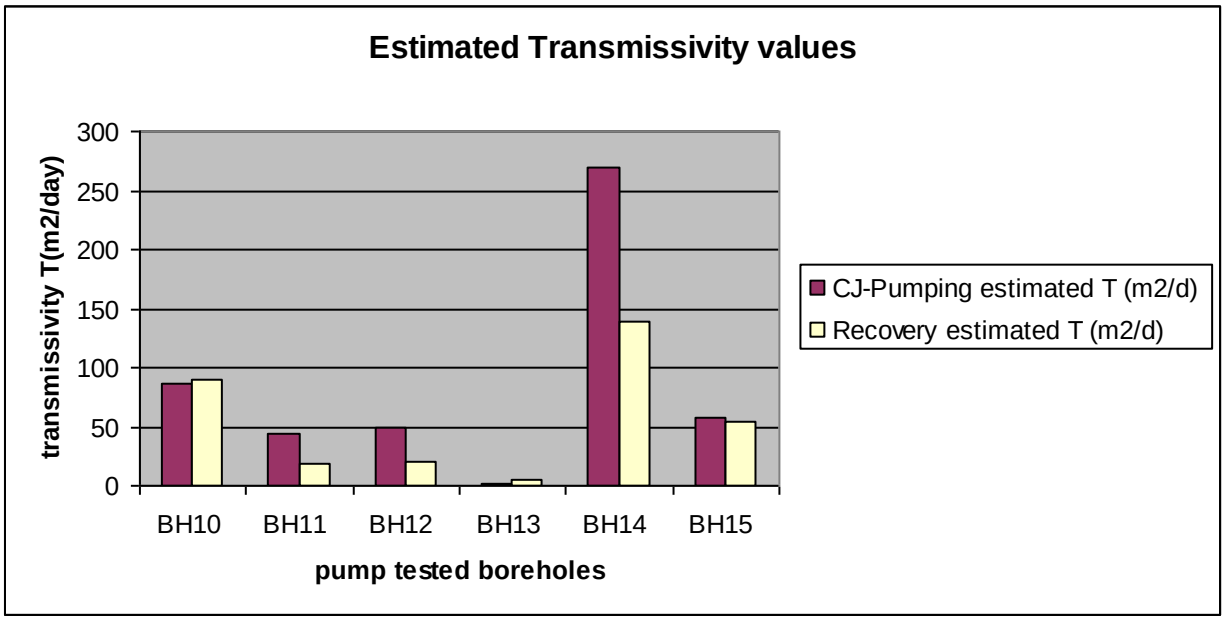

Figure 5-5: Estimated Transmissivity values from constant rate test.

On average, all boreholes intersect the same geological formations of gravel spreading over shale bed as shown on Figure 3-14. It therefore raises a concern to see BH13 behaving at an alarmingly low transmissivity from the others, the reason behind this is without doubt due to other reasons other than geological situation. It is therefore postulated that the reason behind the unusual behavior is due to faulty construction. BH13 runs dry from well bore storage, hence the need to exclude BH13 transmissivity in the harmonic mean calculations of the aquifer.

The harmonic mean calculations give the transmissivity range of the aquifer from 36 m^2/d (recovery) to 66 m^2/d (Cooper Jacob). It can be estimated that at any point on the study site

(provided that the geology is similar), the transmissivity shall be around or within the range of 36 m^2/d and 66 m^2/d.

5.3 Tracer tests

5.3.1 Point dilution test

For the purposes of this study, point dilution tests were done and the EC decay over time was measured at the tested section in order to determine the Darcy velocity (q).

Point dilution tracer tests were done on all the boreholes prior to the pumping tests. This was done before the pumping tests so that the pumping process can extract the tracer plume and leave the aquifer clean in its natural chemical state.

A natural gradient point dilution tracer test was done on the four boreholes BH10, BH11, BH12, and BH13. The background EC was measured before tracer injection. The test was then conducted whereby a 2 m section (except BH12 was 1 m) which was identified to be gravel was introduced with NaCl solution. For a good precision, the test section is the distance between the pump inlet and the tracer injection outlet in the borehole during pump circulation. The general procedure was done following Riemann (2002): *New developments in conducting tracer tests in fractured rock aquifer.* Except that this is not a fractured rock aquifer but an alluvial aquifer. After tracer injection, the EC decay was measured and recorded over time until 90 % EC decay to the background was reached.

The measured electric conductivity was first standardized before it could be applied on the Darcy velocity equation.

Equation 5-1 was used to standardize the measured EC. The standardized values were then imported into the Darcy velocity Equation 5-2 to determine the Darcy velocity. The Darcy velocity was calculated over varying time intervals and the geometric mean was determined for each borehole as shown on Table 5-3.

Equation 5-1: Electric conductivity-concentration standardizing equation.

$$C_t^* = \frac{C_t - C_b}{C_0 - C_b}$$

The standardization was done such that C = 1 at t_o and C = 0 when EC = EC of background.

Where: C_t^* = Standardized concentration

C_t = Equivalent concentration at any time after injection of a tracer

C_b = Background concentration in groundwater

C_o = Concentration in the at t_o just after injection

Equation 5-2: Darcy velocity equation by Drost et al (1968).

$$q = \frac{W}{\alpha\, At} \ln\left(\frac{C_0}{C}\right)$$

Where: W = Volume of fluid contained in the test section (m^3)

A = Cross sectional area normal to the direction of flow (evaluated from πrL, assuming a radial flow model with n = 2) (m^2)

C_0 = tracer concentration at t = 0

C = tracer concentration at time = t

α = borehole distortion factor (between 0.5 and 4; = 2 for an open well) (note that $q\alpha = v^*$, where v^* = apparent velocity inside well)

t = time when concentration is equal to C (days)

L = test section length (m)

Figure 5-6 shows the exponential decay of the standardized concentrations with respect to time.

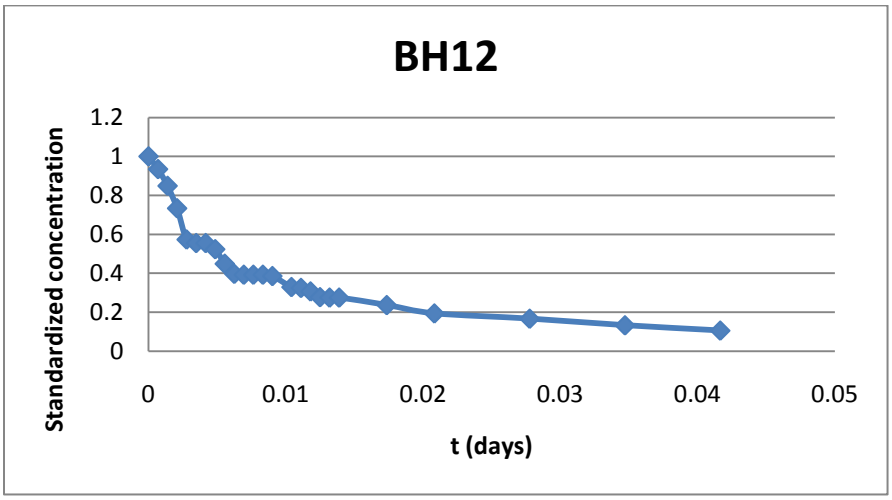

Figure 5-6: Standardized decay of EC concentrations for BH12 point dilution

Table 5-3: Geometric means of Darcy velocities obtained from point dilution test.

Borehole No.	q (m/d)
BH10	9.1
BH11	11.8
BH12	4.4
BH13	4.7
Geometric mean	6.9

Table 5-3 shows the geometric mean Darcy velocity values of the boreholes as determined from a point dilution tracer test. The geometric mean of the Darcy velocity is 6.9 m/d.

The rest of the data for tracer tests is in Section 9.2 (Appendix B).

5.4 Conclusions

Since blow yields were not recorded during drilling, slug tests were performed with the objective of determining an approximate pumping rate below which successive pumping tests should be performed. The estimated yield in all the boreholes was above 1 l/s. A 1 l/s pump was used for a constant rate test on all boreholes followed by a recovery test. The transmissivity harmonic means on all boreholes were 36 m^2/d (from Cooper Jacob) and 66 m^2/d (from recovery test). It can be estimated that the transmissivity of the aquifer at any point would be close to or within the range of 36 m^2/d to 66 m^2/d.

Point dilution tracer tests were performed on four boreholes with the objective of determining the Darcy velocity. The geometric mean Darcy velocity was found to be 6.9 m/d. The Darcy velocity is a function of the slope. This is the rate at which groundwater naturally flows in the aquifer system. It means that if contamination could be present in the aquifer, it would travel 6 m every day under natural conditions.

While the groundwater flow parameters have been established, the next chapter looks into the source and the fate and age of groundwater in the aquifer system.

6 CHEMICAL CHARACTERIZATION AND ISOTOPE ANALYSIS

6.1 Introduction

Hydro-chemical analysis is important in aquifer characterization since it gives a picture of the chemistry of the water in the area for purposes of comparison with the South African standards of water uses.

Water is a universal solvent; it dissolves many inorganic materials of all three states and partially dissolves some inorganic substances. Because of this unusual behaviour, water readily adopts the chemical behaviour of the environment which it interacts with. Water may react with the casing or components of the atmosphere. Suffice it to say that, water in a borehole (well bore storage) generally has a different chemistry from aquifer water hence purging the borehole before sampling remains key in groundwater sampling.

Chemical characterization involves a number of steps which include a proper sampling procedure. Once the sample has been obtained, it is put in a sealed non-reactive bottle and delivered to the laboratory for analysis. Depending on the objective of the study, different analyses may be made such as biological (or bacteriological), or chemical which may usually be the determination of the dominant ions (cations and anions), and the isotope analysis for groundwater dating.

Purging was performed on all the boreholes in the study area prior to sampling. Boreholes BH10, BH11, BH12, BH13, BH14, and BH15 were purged with a 0.6 l/s pump for an average period of 20 minutes to dispose off the well bore storage water.

6.2 Hydrochemistry characterization

In order to know if aquifer water has replaced borehole water, an initial EC value was obtained from the pump outlet using a TLC (temperature, level, conductivity *meter*) just after commencement of pumping. The EC value was monitored through pumping process until it stabilized. This was an indication that the pump is now obtaining water from the aquifer hence it is the right time to sample.

For each site, a sample was sent to the IGS laboratory for micro and macro analysis while the other sample for each site was sent to the Ithemba isotope analysis Laboratory in Gauteng.

6.2.1 Macro elements data analysis

This subsection deals with the ionic abundances in the water samples. Windows Interpretation Systems for Hydro-geologists (WISH) was used to plot the elements on the chemistry presentation tools such as Piper diagram, Stiff diagrams, Durov diagram and SAR diagram.

Groundwater in this area is characterized by pH between 7 and 8 and high Total Alkalinity (carbonates and bicarbonates) (5-10 meq/l). The major anion is carbonates (CO_3^{2-}) and bicarbonates (HCO_3^-) (Talk) while the major cation is sodium (Na^+) and calcium (Ca^{2+}). Figure 6-1 to Figure 6-4 present the diagrams that were used to characterize the chemistry of the Modder River bank aquifer.

From these diagrams, several observations were made regarding the chemistry of the aquifer. They are as follows:

Piper diagrams

Water is classified as a calcium-magnesium carbonate type of water. The major anion is the carbonate (T.Alk). The possible molecular combinations of calcium and magnesium with carbonates include Calcite-$CaCO_3$ magnesite-$MgCO_3$ or compounds of bicarbonates. This may be explained by the geology of the area that is dominated by white calcite rich material and top soil.

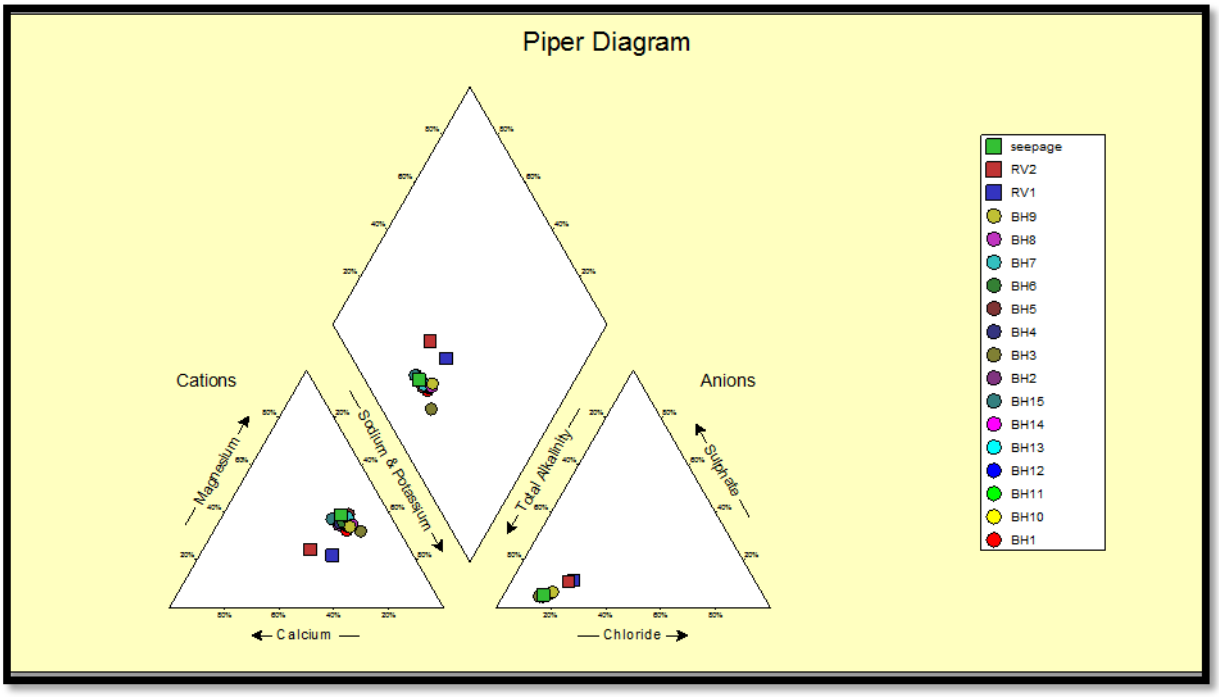

Figure 6-1: Piper diagram of all the sampled hydrochemistry data

Durov Diagram

Figure 6-2 shows the Durov Diagram of the data. It shows more separation and more parameters than the Piper diagram. From the Durov diagram, it can be observed that the abundant cation is sodium and potassium (Na+K) while the abundant anion is carbonates (Total Alkalinity).

Groundwater samples including the seepage have a higher electric conductivity and pH than river water. Groundwater has an EC and pH of 97.5 mS/m and 7.5, respectively, while river water has an EC and pH of 30 mS/m and 7.2 respectively. Compared to river water, groundwater has a higher EC. This may be due to effects of evapotranspiration from trees and vegetation that draws water from the aquifer and by so doing concentrating the salts in water.

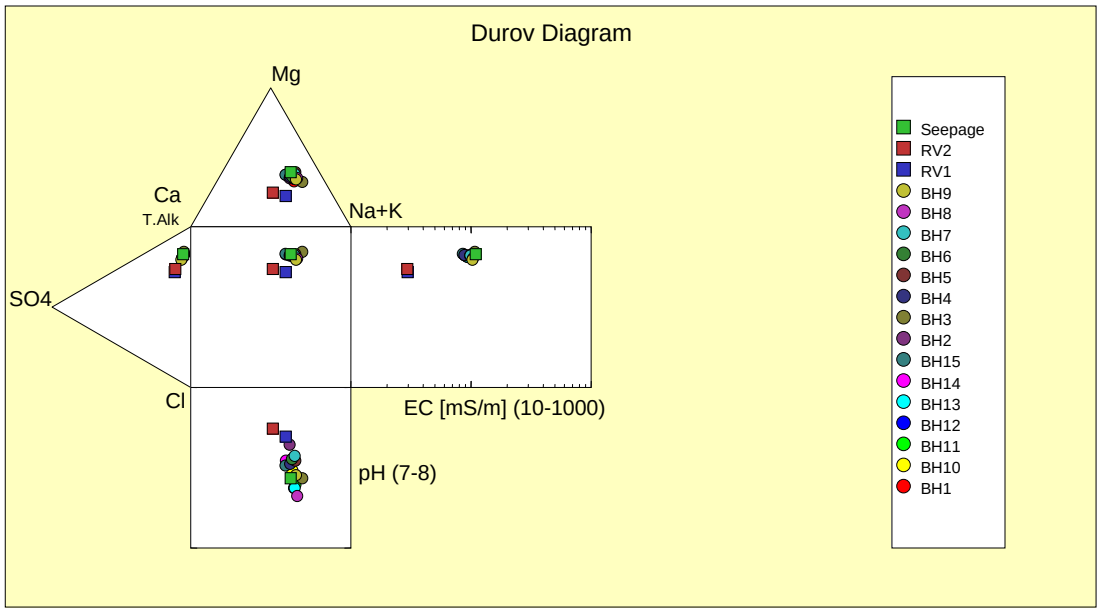

Figure 6-2: Durov diagram of all the sampled hydrochemical data

SAR Diagram

Table 6-1: Irrigation water type based on EC values (from IGS laboratory).

EC Range (mS/m)	Impact on irrigation agriculture
0-25	C1: Low salt content: No danger for brackishness on well drained soil
26-75	C2: Medium salt content. Provision must be made for leaching of salts and plants sensitive to brackishness must be avoided.
76-225	C3: High salt content. Can only be used on soils with a good drainage.

	Leaching is needed periodically and plants sensitive to brackish water must be avoided.
>225	C4: Very high salt content. Not fit for irrigation under normal conditions. Can be used in an emergency on sandy soils.

Table 6-2: Irrigation water type based on SAR values (from IGS Laboratory).

SAR Range	Impact on irrigation agriculture
0-10	S1: Low Sodium: can be used for irrigation. Contains low brackish danger.
10-18	S2: Medium Sodium: Mainly to be used in sandy soils with a very good drainage.
18-26	S3: High Sodium. Not to be used on soils with limited drainage.
26-34	S4: Very High Sodium: Not fit for irrigation because of the high Sodium content.

Table 6-1 and Table 6-2 give the standards used by the IGS laboratory to recommend the suitability of water for irrigation. These standards were used in this study to determine the suitability of the groundwater from the Modder River alluvium aquifer for agricultural irrigation purposes.

Figure 6-3 shows a plot of Sodium Adsorption Ratios (SAR) for all samples. The SAR of all the samples including groundwater and river samples are from zero to 10 which is S1 low level SAR. The salinity of groundwater is from 75 to 225mS/m which is identified as C3 high salinity level while that of river water is from 25 to 75mS/m which is identified as C2 medium level salinity. River water is of the type C2S1 while groundwater is of the type C3S1.

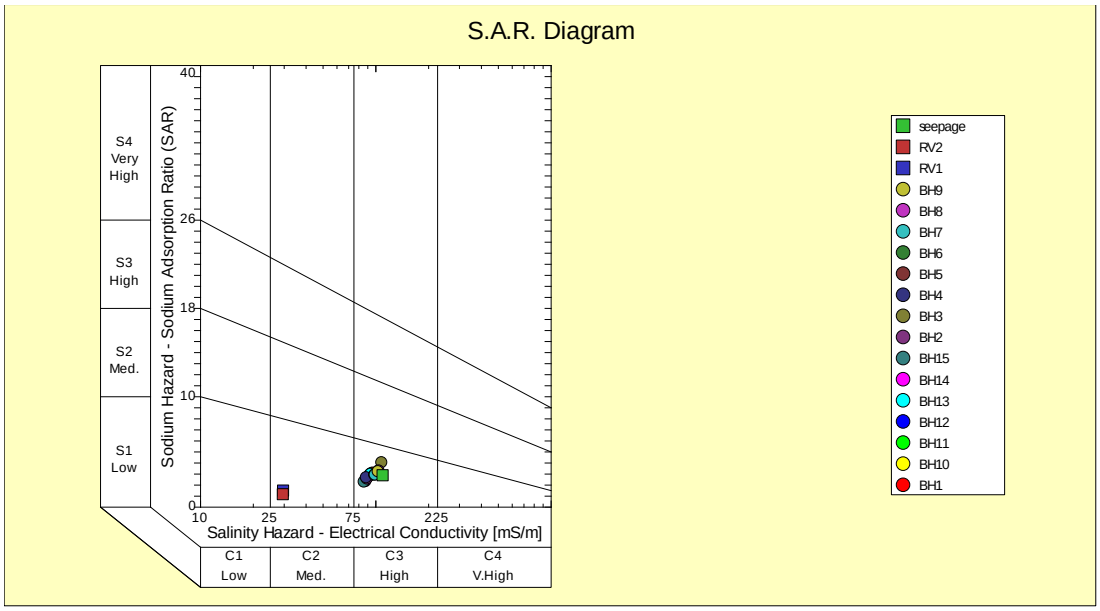

Figure 6-3: SAR diagram of all sampled hydrochemistry data

The SAR for groundwater and river samples is within the recommended range for irrigation and therefore it does not cause a danger to the plants. River water has a higher suitability than groundwater; it has low SAR and medium salt content.

Stiff diagram

Figure 6-4 shows the Stiff diagrams of the water samples. From the Stiff diagram data, the anion abundance relates and agrees well with the Piper diagram by that the dominant anion is carbonates (T.Alk) while the dominant cation in meq/l is sodium followed by magnesium and calcium. Water from boreholes and seepage is chemically similar based on the similar Stiff diagram plots. This water has the same source and is from the same aquifer system.

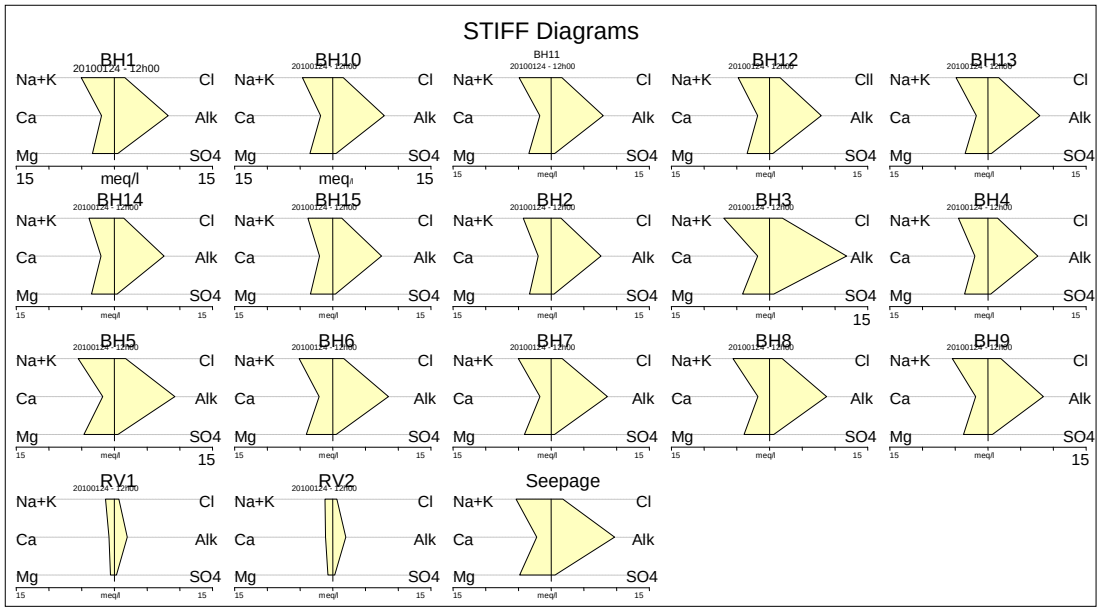

Figure 6-4: STIFF diagrams for all the sampled hydrochemistry data

6.2.2 Trace element data analysis

The trace elements that were analyzed for are Iron (Fe), Manganese (Mn), and Aluminium (Al) (see Figure 6-5). The trace elements data in the natural aquifer system that is not exposed to heavy industrialization is expected to be minimal. This is because dissolution of minerals from geological material is slower than that convectional movement of liquid effluents from industrial activities to groundwater.

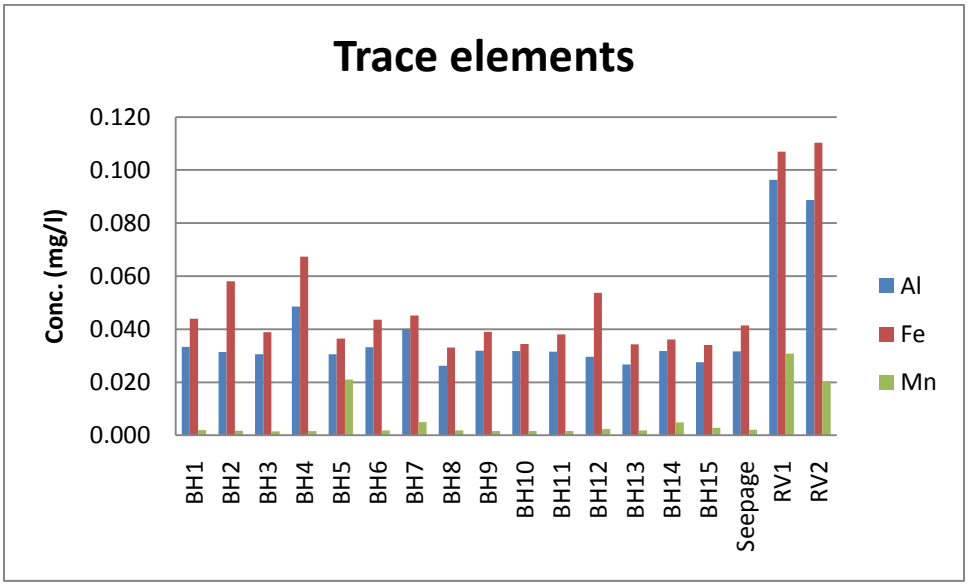

Figure 6-5: Bar graph of all the trace elements data

River water seems to have elevated amounts of trace elements compared to groundwater; this may be because of the following:

- Since the sampling period was during heavy rains, the trace elements could have been washed from the atmosphere directly into the river.
- The trace elements might have entered the river system at other locations upstream of the river from any surface water pollutants.

Surface water is more susceptible to be contaminated than groundwater hence surface water will mostly show elevated concentrations of dissolved elements than groundwater.

6.3 Environmental isotope analysis

6.3.1 Non-radioactive ^{18}O and ^{2}H

In this section what is termed **shallow** water is the water in the gravel material while **deeper** water is the water in the saturated crevices between the layers of shale formation.

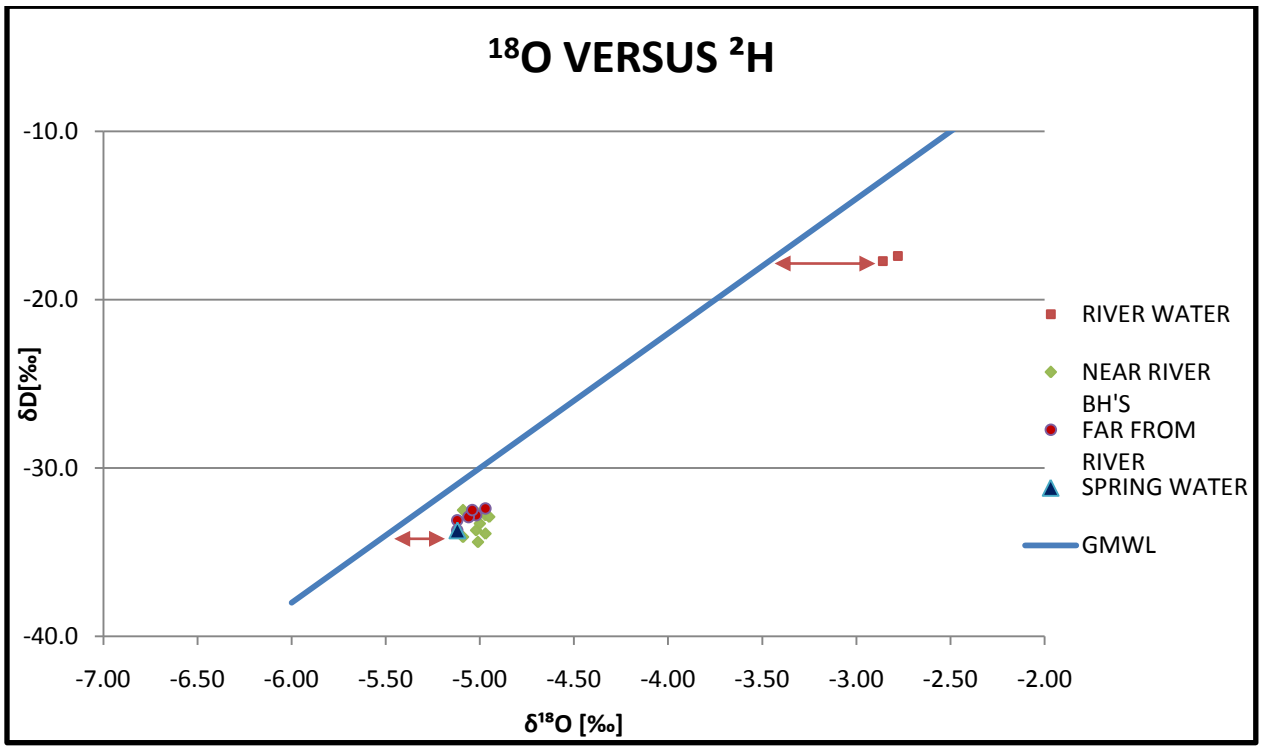

Figure 6-6: $\delta^{18}O$ versus $\delta^{2}H$ for groundwater in the alluvium aquifers.

Figure 6-6 shows the $\delta^{18}O$ and ^{2}H relationship for groundwater from study boreholes, spring water, and river water. Groundwater plots closer to the GMWL than river water. Groundwater may have recharged through a semi-preferred pathway not from a surface water body. This is

witnessed from its high content of lighter isotopes. River water experienced intense evaporation of light isotopes hence it plots further to the global meteoric water line. Since sampling was performed during rainy and flood season, expectation would be that water in the river is direct from the atmosphere and should have lower ^{18}O isotopes, but the opposite is observed in this particular case. This means that during sampling, fresh rainwater had not thoroughly replaced old evaporated river water hence the high ^{18}O content in the river.

Spring water plots at the same zone with groundwater while a different behaviour is observed for river water which plots more to the elevated values of ^{18}O. It is not surprising though that the signature of borehole groundwater agrees well with spring water, and that river water shows a different behaviour from groundwater. This is because the elevation of the spring is two meters into the shale formation (Figure 3-14) which is just at the base of the shallow boreholes. Hence the same signature is observed between shallow boreholes and the spring.

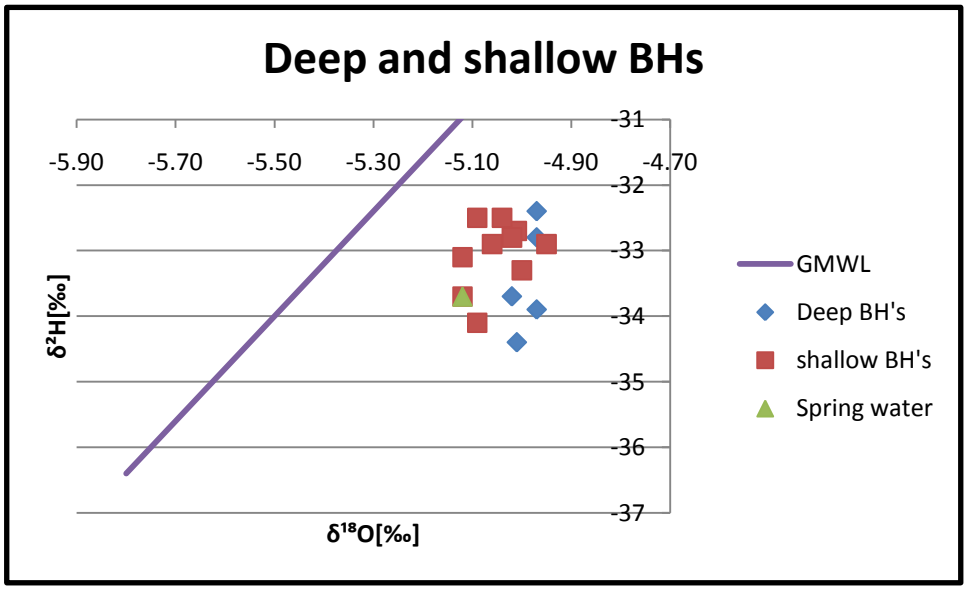

Figure 6-7: $\delta^{18}O$ versus $\delta^{2}H$ plot for shallow and deep boreholes

From the fact that seepage water is similar to groundwater, it was concluded from Figure 6-6 that they have the same source. Figure 6-7 further illustrates that the seepage water comes from the shallow groundwater. Spring water plots together with shallow borehole (BH14) water in Figure 6-7. This means that the seepage water flows from the shallow section of the aquifer not from the deeper section. And from the same figure, it is observed that shallow water plots closer to the Global Meteoric Water Line than the deeper groundwater. The deeper aquifer water is richer in the heavy oxygen isotopes. This may be because shallow water may have recently infiltrated and percolated from precipitation while deep water has been in the horizontal shale

crevices over a longer period. Despite the small difference that is observed in the isotopic finger sprints of the deep and shallow water, it may be inappropriate to conclude that shallow boreholes and deep boreholes are recharged at different sources since the variance is too small.

The vertical profile on the river bank shows that the top part of the shale formation is soft, brittle and highly fractured due to weathering. This may be the reason why seepage water plots with shallow water in that the highly fractured section of the shale formation provides a pathway for water to seep from the higher water table (of the shallow water) through to the spring where sampling was done.

6.3.2 Radioactive tritium

Tritium (T or ^{3}H) is a radioactive isotope of hydrogen that has two neutrons and one proton. T has a half life of 12.3 years (Apello *et al.*, 2005). Concentrations of Tritium are measured in Tritium Units whereby 1 TU is the occurrence of 1 tritium atom in 10^{18} atoms of hydrogen. Tritium can be used for age dating and to verify aquifer vulnerability to contamination because its concentration in groundwater provides a useful method for determining the degree of confinement of an aquifer. Tritium levels below 1 TU are obtained from an aquifer which is not vulnerable to contamination. On the other hand, groundwater that has a high value of TU is vulnerable to contamination. This is based on the idea that the natural TU levels in rainwater are 5 to 10 TU (Thatcher *et al.*, 1977). Provided there is no other source of Tritium on the surface and underground and assuming that rainwater fell at 5 to 10 TU, then for groundwater to have a high TU value it should have recharged just recently.

Before the advent of thermo nuclear testing in 1952, tritium natural average concentrations ranged from approximately 2 to 8 TU. But the atmospheric nuclear bombs era added about $1.13x10^{9}$TU in the northern hemisphere with the largest tritium concentrations peaking in 1963. Since the ending of nuclear testing, tritium levels have dropped to between 12 and 15 TU (William, 2011).

Groundwater systems with recharge occurring prior to the 1950's will have a tritium level decreased by radioactive decay to levels at or below 1 TU. Such a groundwater system is considered not vulnerable. On the other hand, groundwater systems which have been recharged after the early 1950's will contain tritium levels at or significantly above the natural background concentration and are considered vulnerable.

The usefulness of tritium concentrations for groundwater dating is decreasing since tritium concentrations are decreasing in the atmosphere and age dating groundwater recharge calculations are approaching an expiry date. Table 6-3 gives the indicators that are used to date groundwater.

Tritium analyses were performed by electrolytic enrichment and analysed with a liquid scintillation counting method. The results are reported in Table 6-4 as Tritium Units with an error range of ±0.2 to ±0.4 TU.

Table 6-3: Tritium concentrations and groundwater aging. (William, 2000)

Tritium range	Indication
<0.8 TU	indicates submodern water (prior to 1950s)
0.8 to 4 TU	indicates a mix of submodern and modern water
5 to 15 TU	indicates modern water (<5 to 10 years)
15 to 30 TU	indicates some bomb tritium
>30 TU	recharge occurred in the 1960s to 1970s

Table 6-4 shows the tritium concentrations for the 15 boreholes, two river samples and a seepage sample. Groundwater in this area is characterized as non-vulnerable to contamination. This is because it has a low Tritium concentration (<1 TU). Natural tritium concentrations in rainwater are from 5 to 10 TU. Assuming that a rain drop that falls on a land surface has 5 to 10 TU, then for groundwater to have >1 TU it must have recharged over 2 half lives ago. On the other hand, if groundwater had a high TU value, then it would mean the aquifer has recently been recharged.

According to Table 6-3, groundwater in this aquifer is the type sub-modern water since it has <1 TU, meaning it is influenced by a flux of groundwater that recharged late before the 1950s. It has decayed over time from the time it fell as rain from the range of 5-10 TU to <1 TU. BH9 shows a different behaviour, it is characterized as a mixture of sub-modern and modern water. BH9 plots in the same range with river water. River water is a mixture of Krugersdrift storage water and recent rain water so its tritium concentrations depend on the proportions between fresh rain water (5 to 10 TU) and storage water (of lower TU concentration) hence its plots in the range of sub-modern to modern water.

Knowing the aquifer to be an alluvial aquifer and the types of groundwater fluctuations that occurred over the past 11 months, it can be concluded that the estimated time at which recharge occurred in this system is more recent than stipulated by the tritium method. It is therefore

recommended that other follow-up methods be implemented or re-sampling for tritium be done so as to prove the age of water.

Pumping invokes groundwater movement and mixing from the observation boreholes to the pumping borehole. Since sampling for tritium was done after the pumping tests on boreholes which some are within 4 m from BH9, it is highly improbable to have tritium in BH9 5 times higher than in other borehole that are in the same vicinity of which some have 0 TU. This might have been due to an instrumental error or due to the fact that tritium determinations for groundwater dating have expired due to low compositions in the atmosphere hence it may as well be recommended to analyse tritium concentrations to more than two decimal places.

There is an inverse relationship between pH and concentration of hydronium ions (H_3O^+). Whether an aqueous solution is acidic, neutral or basic depends upon the hydronium ion concentration. The parameter pH is a convenient way of expressing the hydronium ion concentration in an aqueous solution and can be defined as the negative of the logarithm of the molar hydronium ion concentration which can as well be expressed as follows:

$pH=-\log [H^+]$

Table 6-4: Tritium concentrations in groundwater (from Ithemba laboratory)

Sampled boreholes	Tritium (TU)	Error range
BH1	0.1	±0.2
BH2	0.1	±0.2
BH3	0.0	±0.2
BH4	0.2	±0.2
BH5	0.0	±0.2
BH6	0.0	±0.2
BH7	0.3	±0.2
BH8	0.0	±0.2
BH9	2.3	±0.3
BH10	0.6	±0.3
BH11	0.0	±0.2
BH12	0.0	±0.2
BH13	0.5	±0.2
BH14	0.4	±0.2

BH15	0.1	±0.2
Seepage	0.0	±0.2
RV1	4.0	±0.4
RV2	3.0	±0.3

Because of this relationship, a T versus pH plot may have to follow a descending order. Figure 6-8 shows a poor 32 % correlation between tritium concentrations and pH. Nonetheless, river samples (RV) have a high tritium concentration and a lower pH compared to groundwater which generally has a higher pH but a very low tritium concentration.

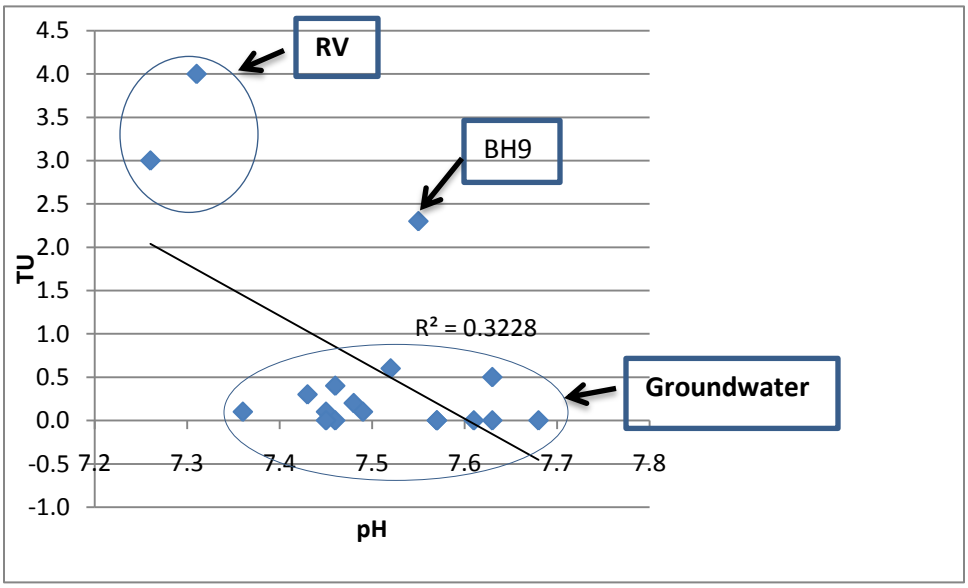

Figure 6-8: Correlation of tritium with pH of sampled sites

6.4 Conclusion

Chemical sampling and analysis were done on the boreholes, seepage, and the river. All the chemical presentation tools reveal that water from the boreholes and seepage has the same source. The major cations in groundwater are sodium, magnesium followed by calcium while the major anion is carbonate (T.Alk). Carbonates are usually found in sedimentary formations combined with alkali metals and alkali earth metals such as sodium, calcium and magnesium to form a whitish to pinkish rock depending on the level of maturity. Groundwater has an EC and pH of 97.5 mS/m and 7.5 respectively while river water has EC and pH of 30 mS/m and 7.2 respectively. SAR concentrations are within the recommended standards for irrigation agriculture use.

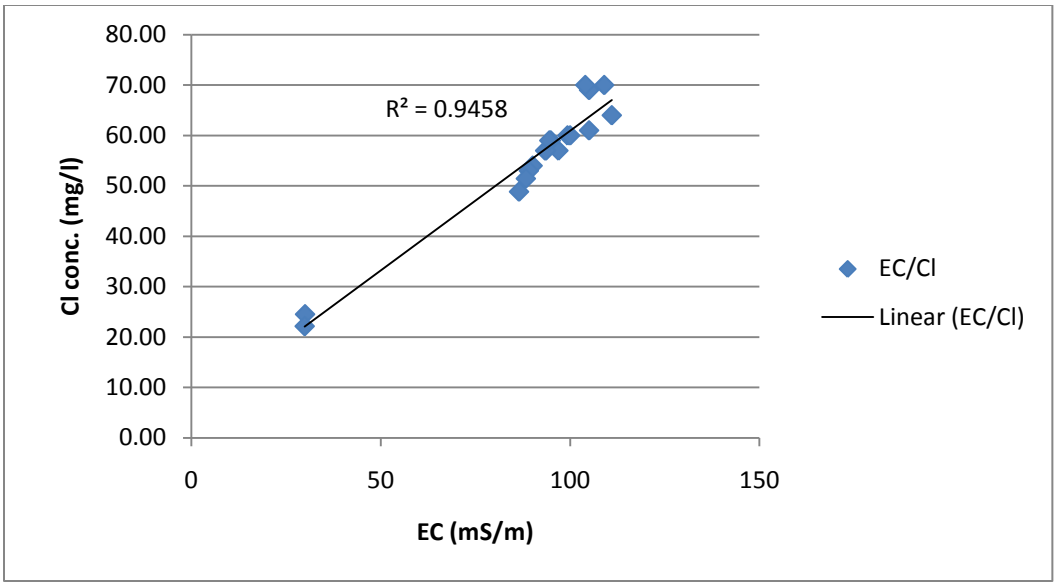

Figure 6-9: Correlation of chloride concentrations with EC values.

Figure 6-9 shows a correlation of 95 % between chloride concentrations and electric conductivity of groundwater and river water. 95 % is a high correlation and based on that, it can be concluded that there is a good relationship between the EC and chloride concentrations on the study site. The EC values are due to the presence of chlorides in water. With this relationship, chloride concentrations can be estimated by extrapolation on the graph in cases where only the EC value is known. This may be useful since it is quicker and easier to measure EC in a borehole than to analyse for chloride concentrations in a laboratory.

Groundwater has lower concentrations of ^{18}O than river water. It therefore means that groundwater did not recharge from a surface water body but from a preferred pathway since it falls far from the evaporation water line but closer to the meteoric water line. River water has a higher concentration of heavy isotopes and therefore falls on the evaporation water line. Tritium concentrations show that groundwater is generally of the type sub-modern water while river water is a mixture of sub-modern and modern water.

With this understanding of the aquifer system in terms of groundwater and seepage sources, it is vital to construct a conceptual model of the area based on the groundwater flow patterns and hydraulics established in the previous and current chapters.

7 CONCLUSIONS AND CONCEPTUAL MODEL

7.1 Introduction

This chapter summarizes the conclusions that answered the aims in the previous chapters. Furthermore, it builds up on the hydrogeological conceptual model of the study area by combining all conclusions that were made in related chapters.

A conceptual model is a representation of the *hydrogeological* system based on the observations made during field investigations (Gomo, 2009).

The conceptualization of the site is made based on the conclusions made in these sections:

- Geology
- Hydraulic parameters
- Chemical analysis
- Natural groundwater behaviour

7.2 Conclusion

7.2.1 Geology

The study site is characterized by hard surface calcrete formation and loose calcrete rich loamy-sand soil which is gradually replaced by loam soil as one approaches the river. The loamy-sand on the river banks is not a calcrete type of soil since it showed no significant response to the acid test, unlike the loamy-sand towards inland which responded positively. The inland loamy-sand was formed as a result of weathering of calcrete formation that blankets the area while the loamy-sand on the river bank edges was located as a result of river deposition.

The profile along the river banks below the loamy-sand shows highly fractured and weathered shale due to exposure to weather elements such as air, water, temperature variations etc. The vertical cross-section is characterized by geology in the order calcrete/loamy-sand, coarse sand/ gravel, and shale. The gravel layer is of approximate thickness of 3 meters and comprises of rounded (indication of flowing water history) pebbles and rough gravel which includes quartz particles which may have been brought by river deposition. It is therefore concluded that the hydrogeology of this area is dominated by flow of groundwater that occurs in the alluvium material at the general depth of 8 mbgl just above the shale bed.

The National Water Act states that an aquifer is a geological formation which has structures or textures that hold water or permit appreciable water movement through them (National Water Act (Act No. 36 of 1998)). Based on this definition, even if there is water flowing in the shale

crevices, if it is not able to supply appreciable amounts of water, then it cannot be termed an aquifer, therefore, between the elevations of 1249 mamsl (surface elevation of the most elevated borehole), and 1213 mamsl (elevation of the bottom of the deepest borehole) there is only one aquifer which is the alluvial aquifer. As to whether there is another *aquifer* (that can produce appreciable amounts) below 1213 mamsl is beyond the scope of this thesis.

7.2.2 Groundwater flow behaviour, discharge and recharge

Groundwater flows in this area is towards the north-easterly direction which is in the direction of the topographic slope while the direction of the river is south-eastwards. In addition to the groundwater direction being due to topography, groundwater flow behaviour may also be influenced by the effect of the seepage at the river bank. This seepage that releases water at an approximate rate of 25 l/s per 100 m width acts as a natural borehole that forms a semi-cone of depression that draws water towards it slightly in the north-eastern direction.

The geometric mean of the percent recharge values obtained using Chloride mass balance method was found to be 1.7 %.

7.2.3 Aquifer parameters

Figure 7-4 shows the transmissivities of the boreholes in relation to their locations. As shown on Figure 7-4, the transmissivity of BH13 is alarmingly low compared to other boreholes in its vicinity. It is postulated that since all the boreholes intersected the same geological formations with similar lithology, water strikes, and that the water level time series is in the same range, the reason behind BH13's unusual behavior is due to the faulty construction.

Excluding BH13's transmissivity, the harmonic mean calculations give the transmissivity range of the aquifer to be from 36 m^2/d (recovery method) to 66 m^2/d (Cooper-Jacob method).

The Darcy velocity as obtained from the point dilution tracer test gave a geometric mean of 6.9 m/d. Under natural systems, groundwater in this aquifer flows at 6.9 m/d.

7.2.4 Hydrochemistry

From a variety of chemical presentation plots, the dominant anion is carbonates and bicarbonates (T.Alk) followed by chloride while the dominant cation is sodium followed by magnesium and calcium. The water is generally of the calcium, magnesium carbonate (Ca, $MgCO_3$) type of water. The chemical composition of the seepage water does not indicate a different source from the borehole water. Both the macro element data analysis and isotope analysis show that seepage water plots with shallow water. This is the reason why flow in the formation was postulated as shown on Figure 7-2.

There is a 95 % correlation between EC and chloride of water samples collected on site. From this it is concluded that the chloride concentration has a high and major influence on the electric conductance of water. The ^{18}O versus ^{2}H plots reveal that groundwater from boreholes is similar to the seepage water at the edges of the river bank. Groundwater plots closer to the GMWL than river water hence it is concluded that it does not have an evaporation history i.e., it does not plot on the evaporation water line. Groundwater recharge must have been dominated by a preferred pathway rather than through a surface water body since surface water is usually water that was left after evaporation of lighter isotopes. Tritium concentrations show that groundwater is generally of the type sub-modern water while river water is a mixture of sub-modern and modern water.

7.3 Conceptual model

Based on the geology of the area and other parameters that were determined, a conceptual model was developed which gave a clearer picture of the study area. Figure 7-1 is a geological conceptual model of the study area showing how the geology changes from inland to the river.

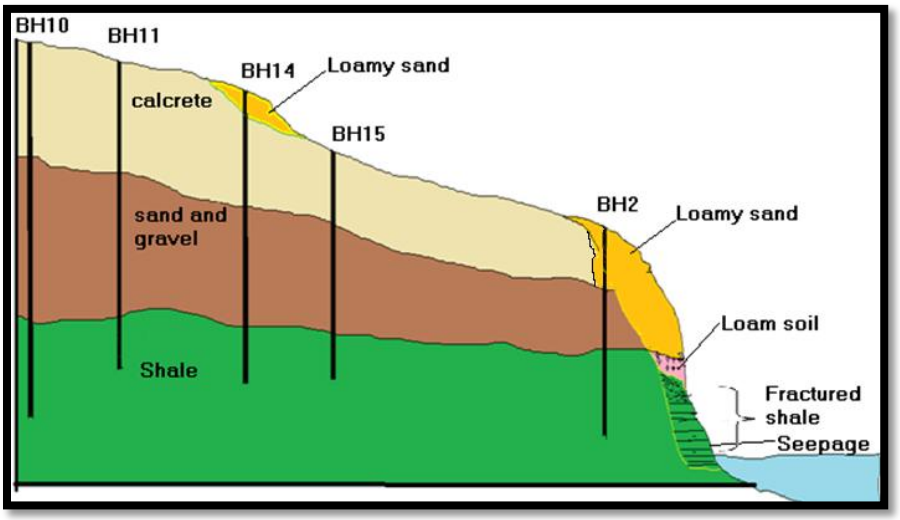

Figure 7-1: Geological conceptual model of the study area showing how geology changes from inland to the river.

Conducted aquifer tests and drill cuttings revealed that the hydrogeology in this area is dominated by flow that occurs in the alluvium aquifer from inland to the river, but the vertical profile on the river bank shows no presence of gravel or calcrete, therefore flow through the gravel formation to the seepage zone was conceptualized as shown on Figure 7-2. The weathered section of shale formation possibly acts as a path through which water seeps from gravel to the seepage phase as shown on Figure 7-2. The blue arrows show groundwater movement in the gravel material while the white arrows show movement in the shale fractures.

The chemistry data analysis shows that groundwater and seepage water have the same source which is possibly the alluvium aquifer, hence the postulated groundwater flow conceptual model. For the purposes of this illustration, the micro-fractures that have been formed by the horizontal cleavages in between shale layers have not been drawn; this is because the main focus was on the fate of groundwater from gravel through the weathered shale to the seepage.

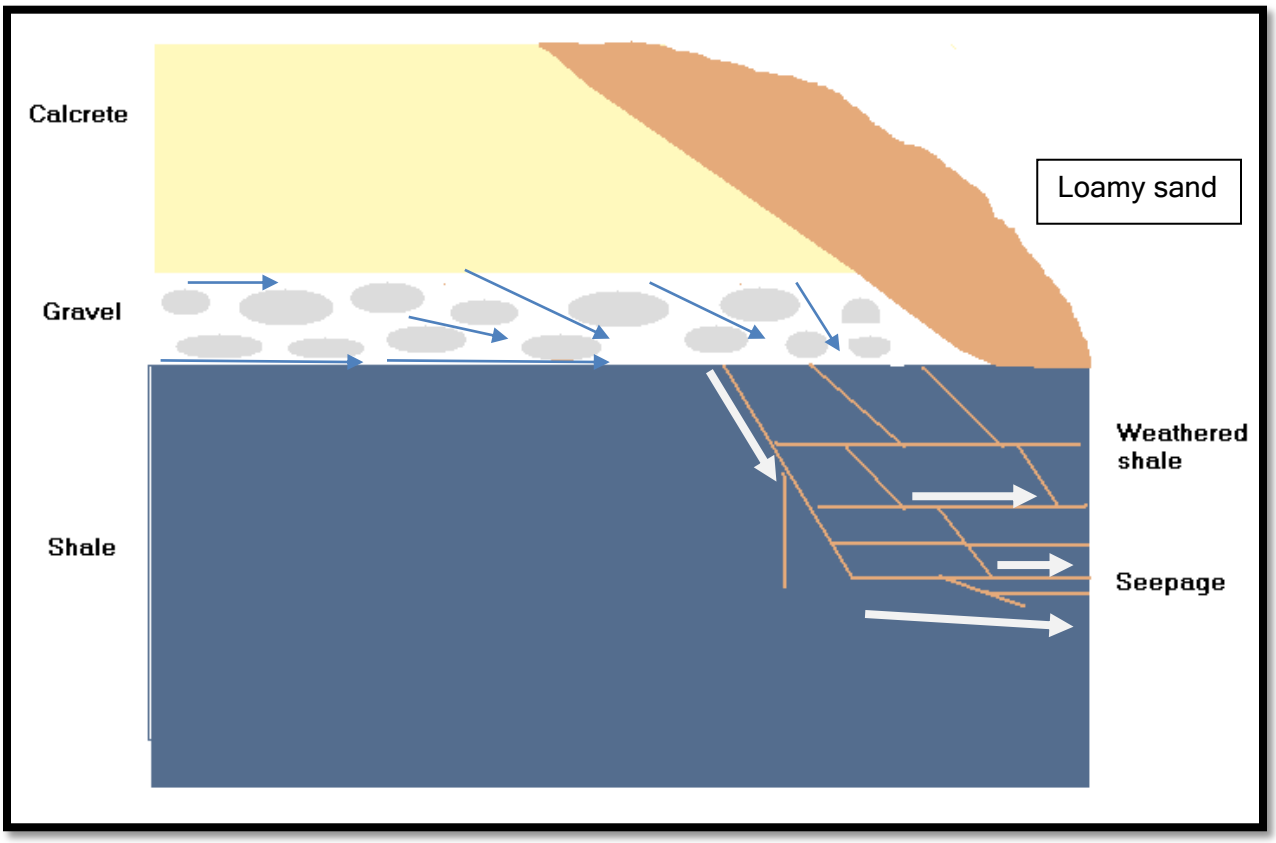

Figure 7-2: Conceptual model seepage flow through gravel and shale formations on the site.

The groundwater flow is towards the north-east direction which is approximately in the direction of the local topographic gradient. Groundwater flow may be due to the direction in which surface topography slopes, in addition to that, studies that were made on the river bank revealed that 25 litres flow through a 100 m section of the river per second. This outcome may be referred to in postulating that the flow direction is due to the seepage since it acts as a natural borehole that makes a semi-cone of depression as conceptualized on Figure 7-3.

In reference to the alluvium aquifer, this section of the river that is adjacent to the study site can be classified as a gaining stream since it gains water from the alluvial aquifer and not the other way round so the conceptualization of hydrogeology does not incorporate depths that are beyond the depth of the drilled boreholes.

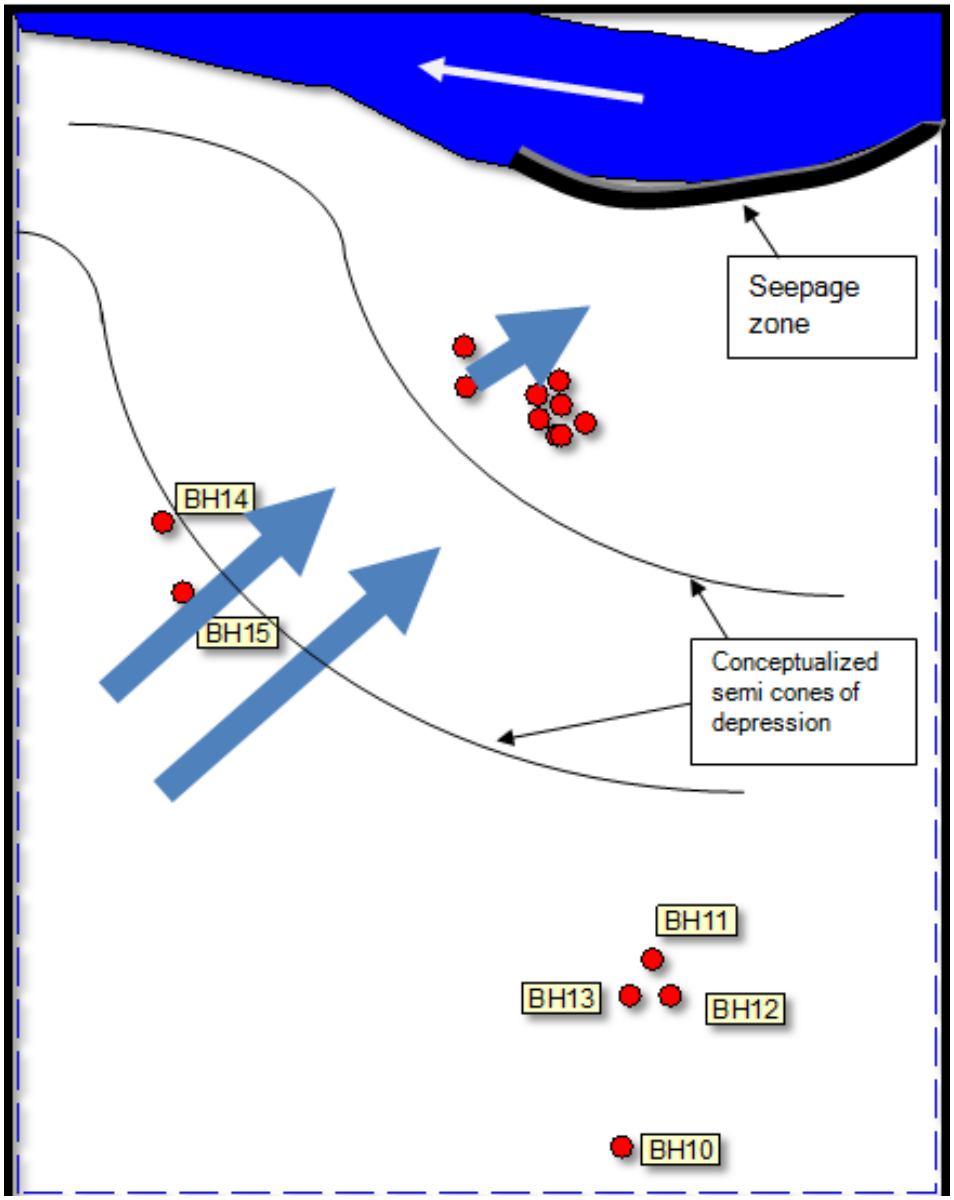

Figure 7-3: Conceptualized groundwater flow in the study system.

A summary of the parameters obtained in hydrogeological characterization of the study area is shown on Figure 7-4 as a special overview of the study area.

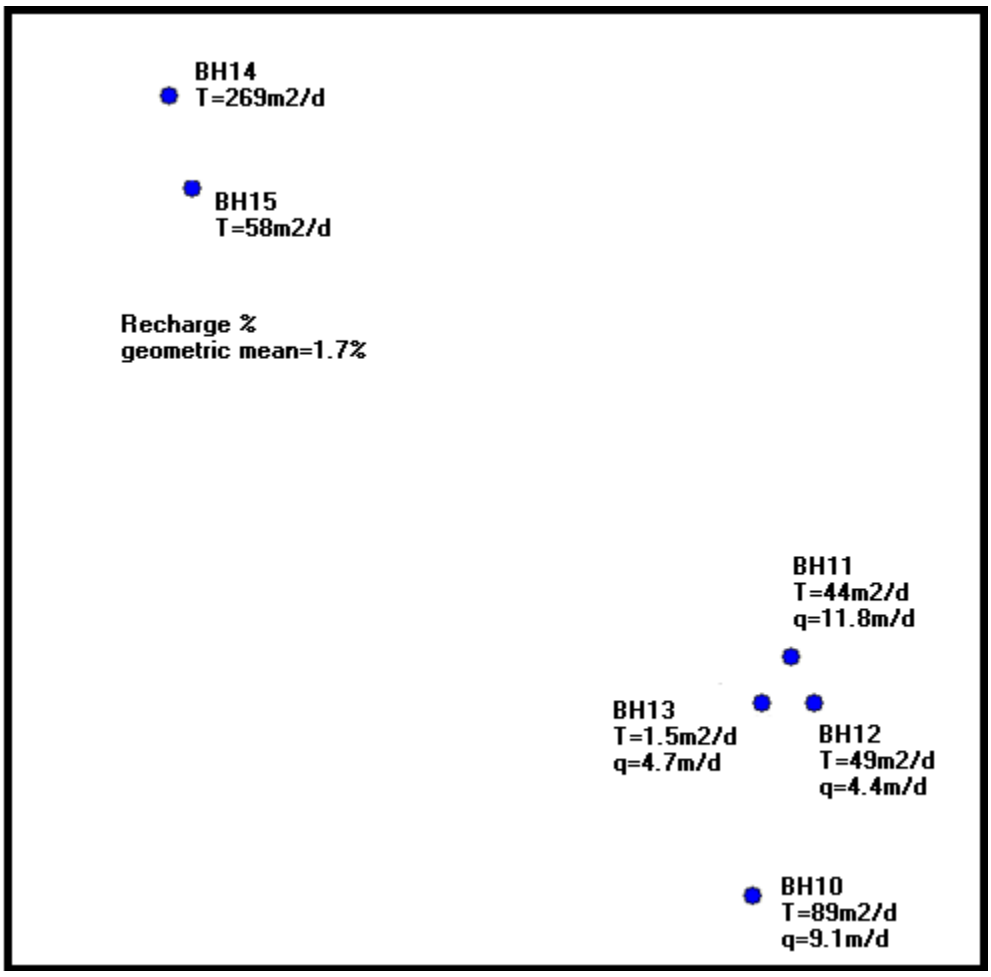

Figure 7-4: Summary of hydraulic parameters (spatial distribution of transmissivity and Darcy velocity over the study area as obtained from the Cooper-Jacob method).

8 REFERENCES

Appello, C A., D, Postma. (2005). *Geochemistry, groundwater and pollution*, 2nd ed. Balkema.

Bear, J. (1979). *Hydraulics of groundwater*. McGraw-Hill. New York.

Botha, J, Van der Voort, I., Vivier, J., Collinston, W., & Loock, J. (1998). *Karoo Aquifers. Their Geology, Geometry, and physical behaviour: WRC487/1/98.* Pretoria: Water Research Commission, P.O Box 824, Pretoria 0001.

Bouwer, H., RC, Rice. (1976). A *slug test for determination of hydraulic conductivity of Unconfined aquifers with completely or partially penetrating wells*. USA Department of Agriculture, Phoenix, USA.

Brassington, R. (1998). *Field Hydrogeology.* London: Geological society of London hand book series, Open University Press.

Cherry, A., A. Freeze. (1979). *Groundwater.* New York: Prentice hall, Inc.

Dennis R. (2006). Flow direction. Unpublished groundwater flow direction spreadsheet. University of the Free State, Institute for Groundwater Studies, South Africa.

DEAT, D. O (2001). *Environmental Potential Atlas of South Africa.* Pretoria: DEAT.

Driscoll, F. (1986). *Ground water and wells.* St Paul, Minnesota: Johnson Division .

Ebbing D, D. S. D Gammon. (1999). General chemistry (6th Ed.). Houghton Mifflin company. USA

Fetter, C. (2001). *Applied Hydrogeology.* New Jersey: Prentice Hall,Inc.

Fourie, F.D. (2003). Applications of electro-seismic techniques in geohydrological investigations. Un-published PhD thesis. University of the Free State

Gat, J.R. (1996). Oxygen and hydrogen isotopes in the hydrologic cycle. Unpublished paper, Department of Environment Sciences and energy research, Weizmann Institute of Science, 76100 Rehovot, Israel.

Geoscience, C. f. (2006). *Summary of Economic geology of provinces: Free State Province*. Retrieved 08 26, 2010, from Summary of Economic geology of provinces: Free State Province: http://www.geoscience.org.za

GHR 611: Aquifer mechanics lecture notes. (2009). Institute for Groundwater Studies, University of the Free State Bloemfontein, South Africa.

Gomo, M. (2009). *Site characterization of LNAPL-contaminated fractured rock-aquifer.* Un-Published MSc Thesis. University of the Free State, Institute for Groundwater studies.

Heath, R. C. (2004). *Basic groundwater hydrology.* Denver C0800225: U.S Geological survey, Information services, P.O Box 25286, Denver Federal centre .

Kinyua, J., Welderufael, W., & Woyessa, Y. (July 2008). Conceptualization of the consequenses of land use descitions on waterresources in the central region of South Africa: An agent based modelling perspective. *The Journal for transdisciplinary research in South Africa, Vol 4* , 237-250.

Kotze, DJC. (2001). Hydrogeology of the Table Mountain sandstone aquifer-Klein Karoo. Un-Published PhD Thesis. University of the Free State, Institute for Groundwater Studies.

Kruseman, G.P. N A de Ridder. (1994). Analysis and evaluation of pumping test data (2nd Ed.). Amsterdam. International Institute for Land Reclamation and Improvement, P.O Box 45, 6700 AA Wageningen, The Netherlands.

Laker, MC. Dupreez, CC (1982). An investigation into the accuracy of hydrometers for soil particle size distribution. Agroplantae.

Mook, W.G. (1980). Chapter-2.Carbon-14 hydrogeological studies. In P.Fritz and J.C Fontess(eds.), Handbook of environmental Isotope Geochemistry,v. 1, Elsevier, Amsterdam, P.49-74

Peyton, G. R, ET al. (1986). *Effective porosity of geologic materials. Proceedings of the Twelfth Annual Research Symposium.* U.S. Environmental Protection Agency, EPA/6009-86:21-8.

Raboroko, R. (2005). *An evaluation of the spatial variability of sediment sources along the banks of modder river free state province south africa.* Bloemfontein: Unpublished thesis: University of the Free State.

Readon. E. J, P. Fritz. (1978). Computer modeling of groundwater 13C and 14C isotope compositions. J. Hydrol., v.36, p 201-224.

Riemann, K. (2002). *New Developments in conducting and analyzing Tracer Tests in Fractured Rock Aquifers*. Unpublished PhD Thesis at the Institute for Groundwater Studies, University of the Free State, South Africa.

Riemann, K., Van Tonder Gerrit, J and Dennis, I., 2002. *Interpretation of single - well tracer tests using fractional-flow dimensions.* Part 1: theory and mathematical models, pp 352 - 355.

Rudolph, D.C. Kirchner, J. and Botha, J.F. (1992) *Investigation into variable head tests for the determination of aquifer constants.* Water Research Commission Report no. 272/1/92

Schwartz. F.W, H. Zhang (2003). Fundamentals of Groundwater. New York. Donnelley Willard

Thatcher, LL, Janzer, V.J, and Edwards, R.W. (1977). Methods for determination of radioactive substances in water and fluvial sediments. In: Techniques of water resources investigations of the US Geological Survey. US Government Printing Office, Washington

Thomas, C. Judson, W. Lehn, F. William, M. (1998*). Groundwater and surface water a single resource*. Denver Colorado: U.S Geological survey.

Usher, B. J. (2005). *Management of a Karoo fractured-rock aquifer system -Kalkveld water user association (WUA).* Institute for Groundwater Studies, University of the Free State, PO Box 339, Bloemfontein 9300, South Africa.

Vacher, H. L. (1989). *The three point problem in the context of elementary vector analysis*. Journal of Geological Education 37:280-87.

Van Der Voort, I. (1995). *An investigation of the geometry of Karoo aquifers and the effect this has on the ability to yield water.* Bloemfontein 9300: unpublished thesis, University of the Free State.

Van Tonder, G.J, Kunstmann, H., Xu, Y. (2001). *FC Program*. Software developed for DWAF by the Institute for Groundwater Studies. IGS, University of the Free State, South Africa.

Van Tonder, G., Bardenhagen, I., Rieman, K., van Bosch, J., Dzanga, P. And Xu, Y. (2002). *Manual on Pumping test analysis in fractured-rock aquifers*. WRC Report No 1116/1/02

Van Tonder, G.J. and Vermeulen, P.D. (2005). *The applicability of slug tests in fractured rock formations*. Water SA, Vol. 31,No. 2,pp157, April 2005. ISSN 0378-4738.

Van Tonder, G.J. (2011). Personal communication

Vermeulen, PD. (2006). *The impact of irrigation with coal mine water on groundwater resources. Bloemfontein*: Unpublished PhD thesis: University of Free State

Vivier, J. J. P., van Tonder, G.J. and Botha, J.F. (1995). *The use of slug tests to predict borehole yields: correlation between the recession time of slug tests and borehole yields*. In comference proceedings: Groundwater'95: Groundwater Recharge and Rural Water Supply, Midrand, South Africa.

Weaver, J.M.C., Conrad, J.E. and Eskes, S.J.T., (1993*) Valley calcretes: another Karoo ground water exploration target*. Proc. Convention: Africa needs ground water. Ground Water Division, GSSA, Univ. of the Witwatersrand, Johannesburg, Volume. I, Paper 8.

Weight, W. D. (2008). *Hydrogeology Field Manual* (2nd ed.). New York: McGraw-Hill Companies.

Wigley, T.M.L., L.N. Plummer, F.J. Pearson Jr. (1978). *Mass transfer and Carbon isotope evolution in natural water systems*. Geochim. Cosmochim. Acta, v. 42, P 1117-1137.

Woodford, A., & Chevallier, L. (2002). *Hydrogeology of the Main Karoo Basin: Current knowledge and fiture research needs TT179/02.RSA.*

Internet resources

http://www.geoafrica.co.za/reddog/groundwater/aquachem/aquachem.htm. (date accessed 27/10/2010)

(AquaChem: http://www.geoafrica.co.za/reddog/groundwater/aquachem/aquachem.htm.

(date accessed 27/10/2010)

IDEQ-Idaho Division of Environmental Quality. *How to Determine the Direction of Ground water flow*. http://imnh.isu.edu/digitalatlas/hydr/concepts/gwater/gflow.htm. (Accessed 12th October 2010)

William, E. Age dating groundwater. 2200 Powell Street, Suite 225 Emeryville, CA9460. www.grac.org/agedating **groundwater. PDF** (May 2011)

9 APPENDIXES

9.1 Appendix A: Geology

Figure 9-1 to Figure 9-8 show the geological cuttings and the manner in which they were logged in WISH (Windows Interpretation Systems for Hydrogeologists).

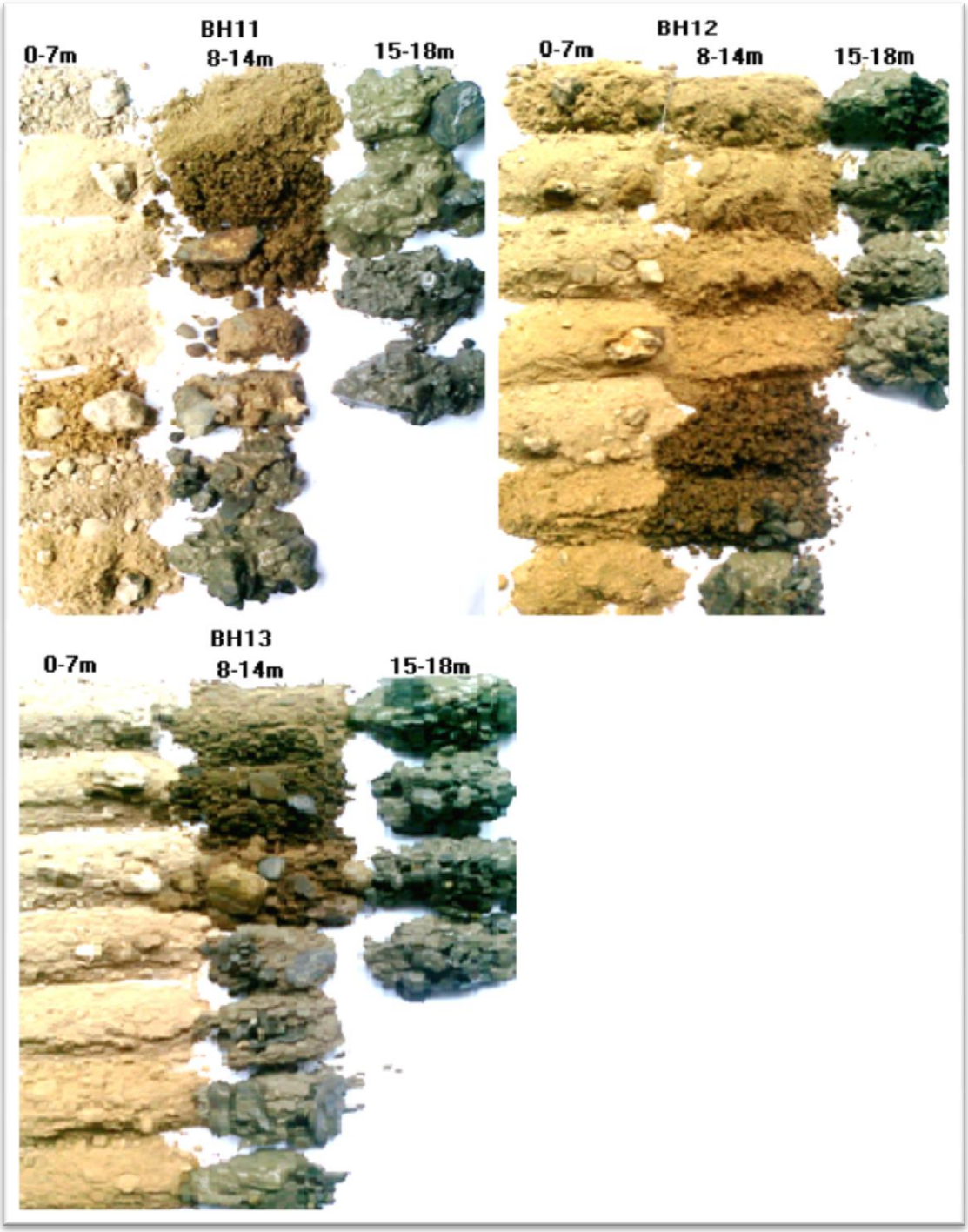

Figure 9-1: Geological cuttings collected during drilling of BH 11, BH12 and BH13.

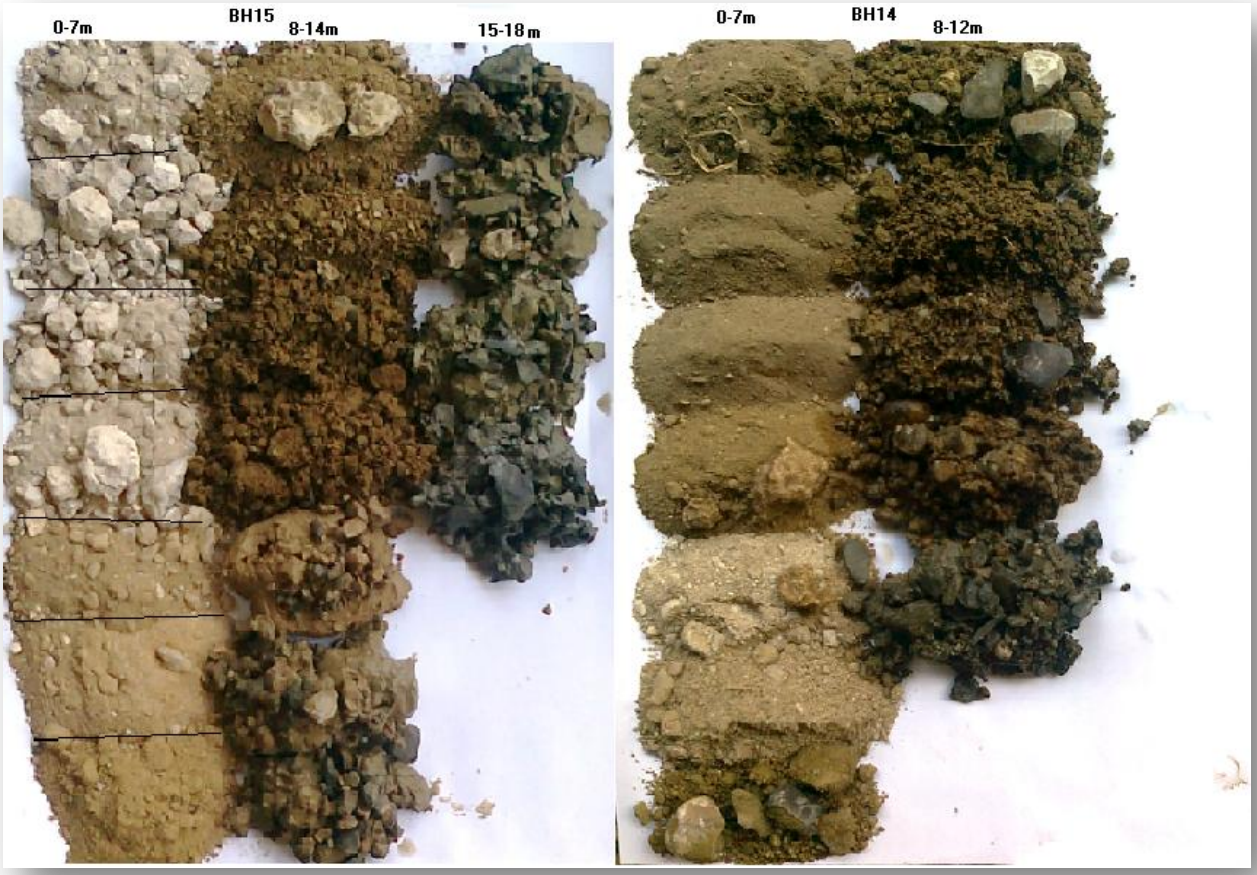

Figure 9-2: Geological cuttings collected during drilling of BH14 and BH15.

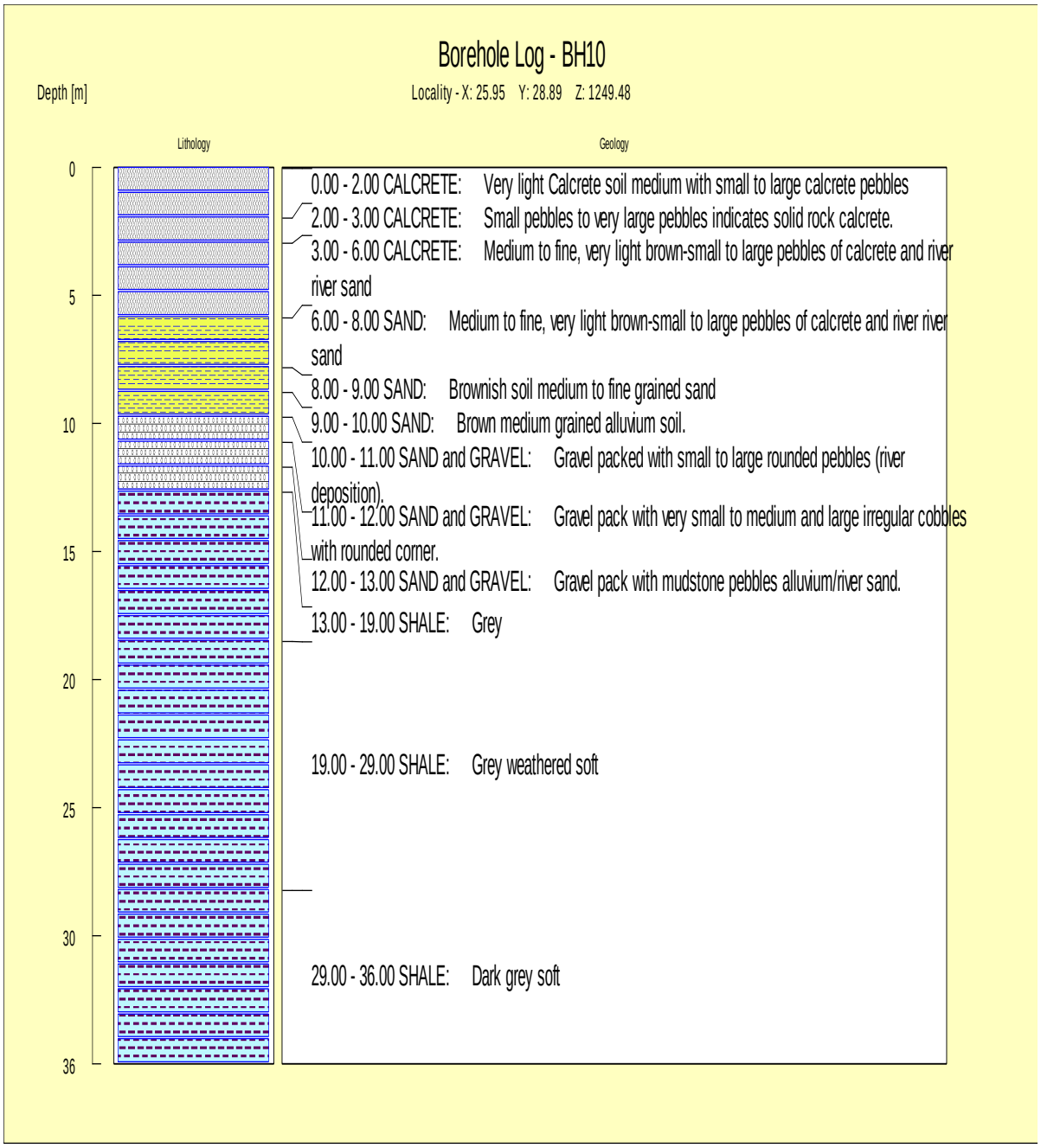

Figure 9-3: BH10 Core geological log.

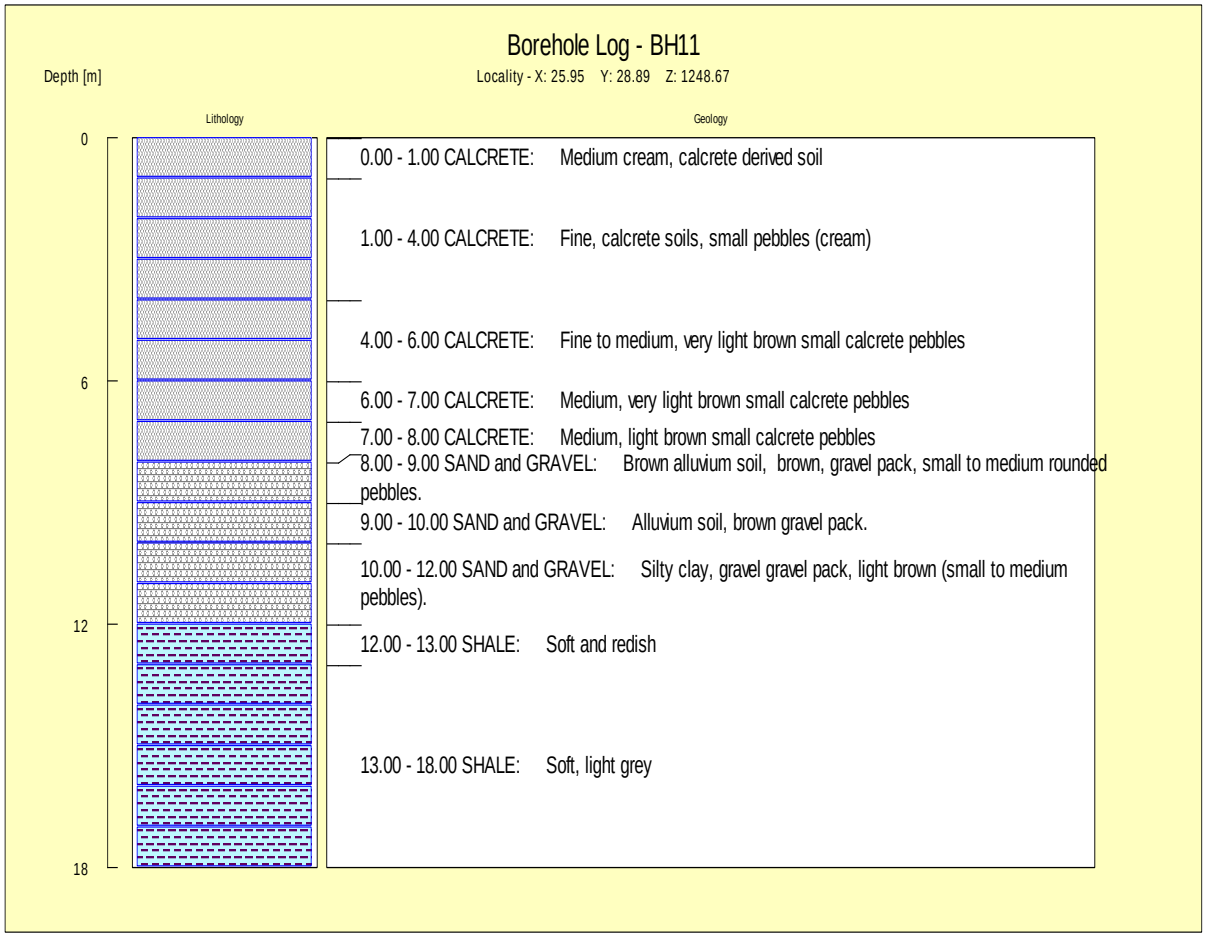

Figure 9-4: BH11 core geological log.

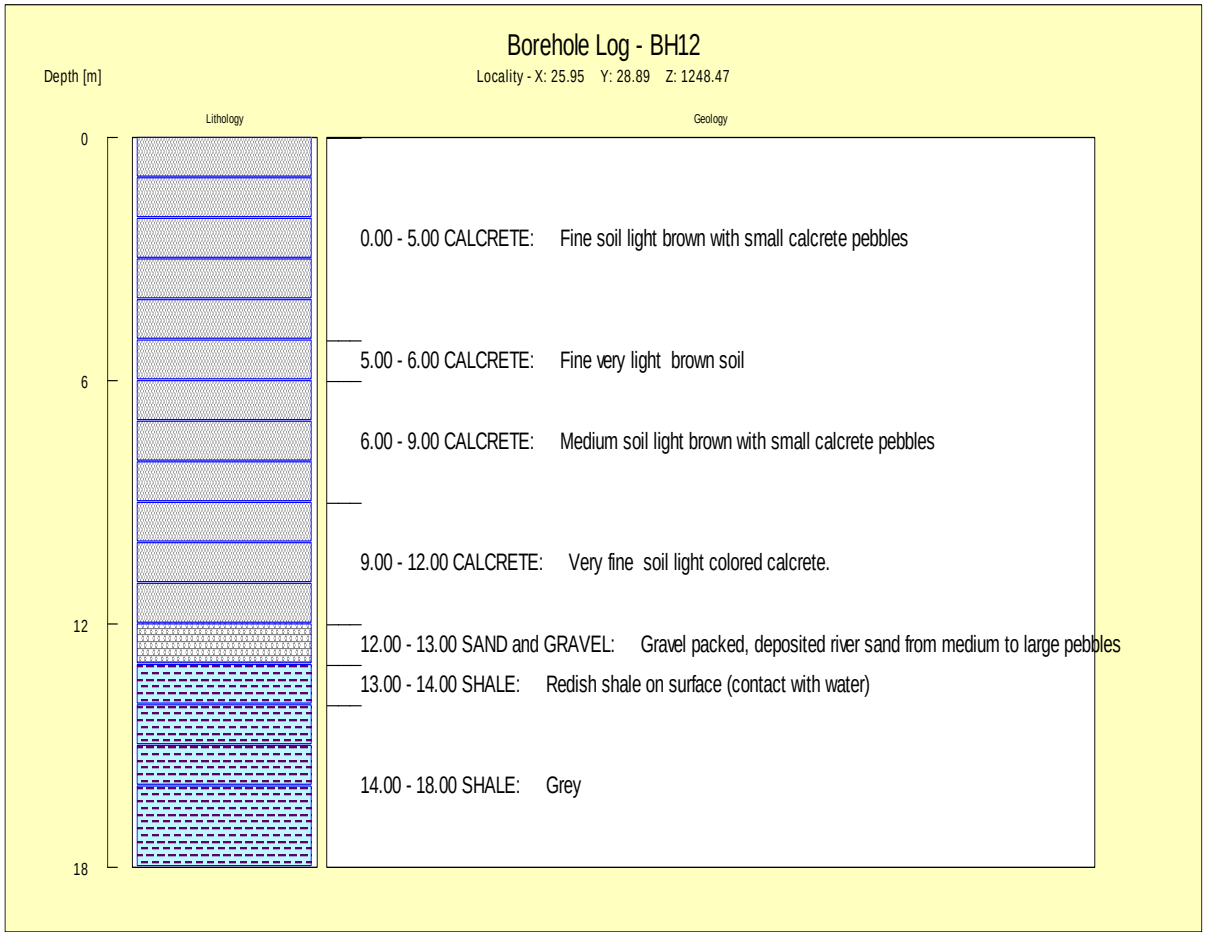

Figure 9-5: BH12 core geological log.

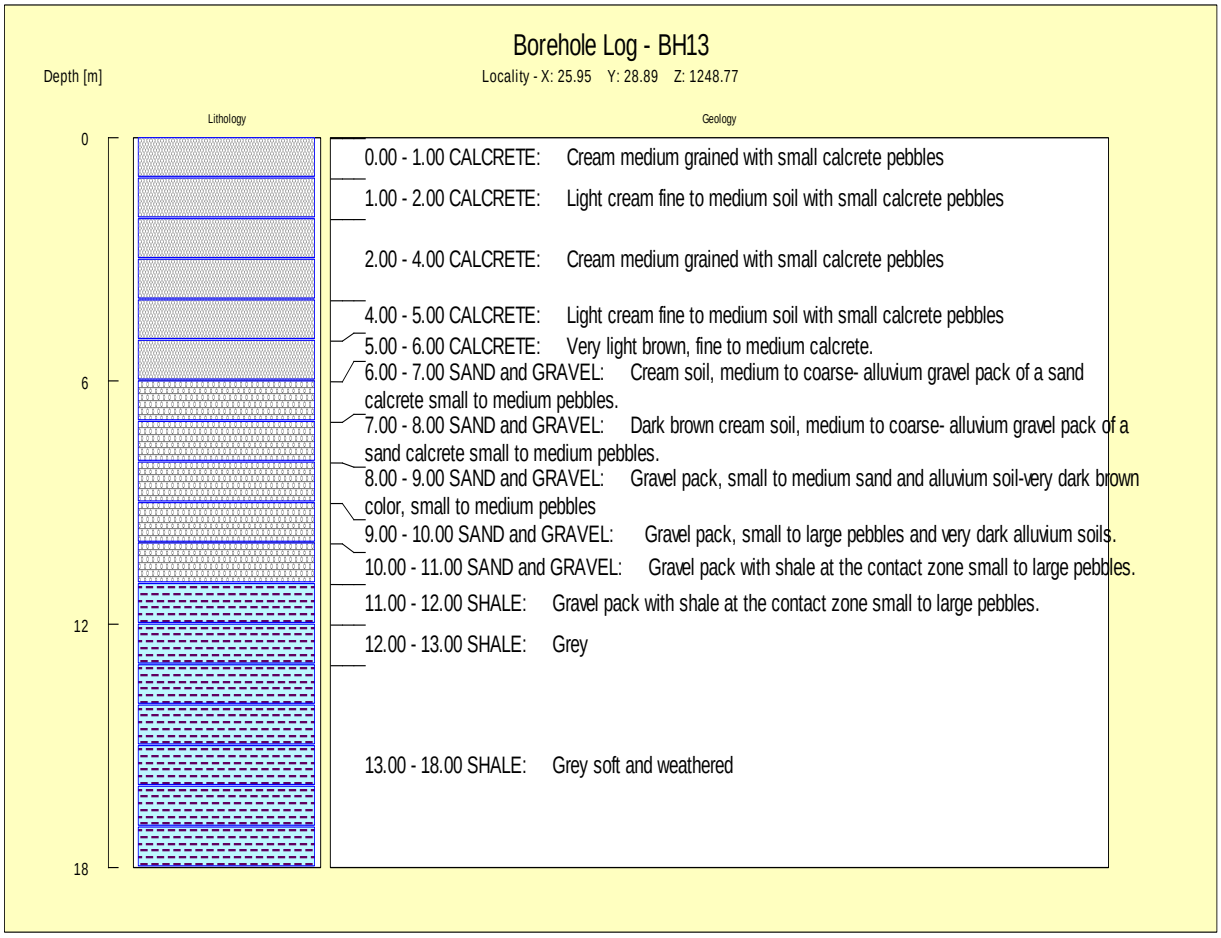

Figure 9-6: BH13 core geological log.

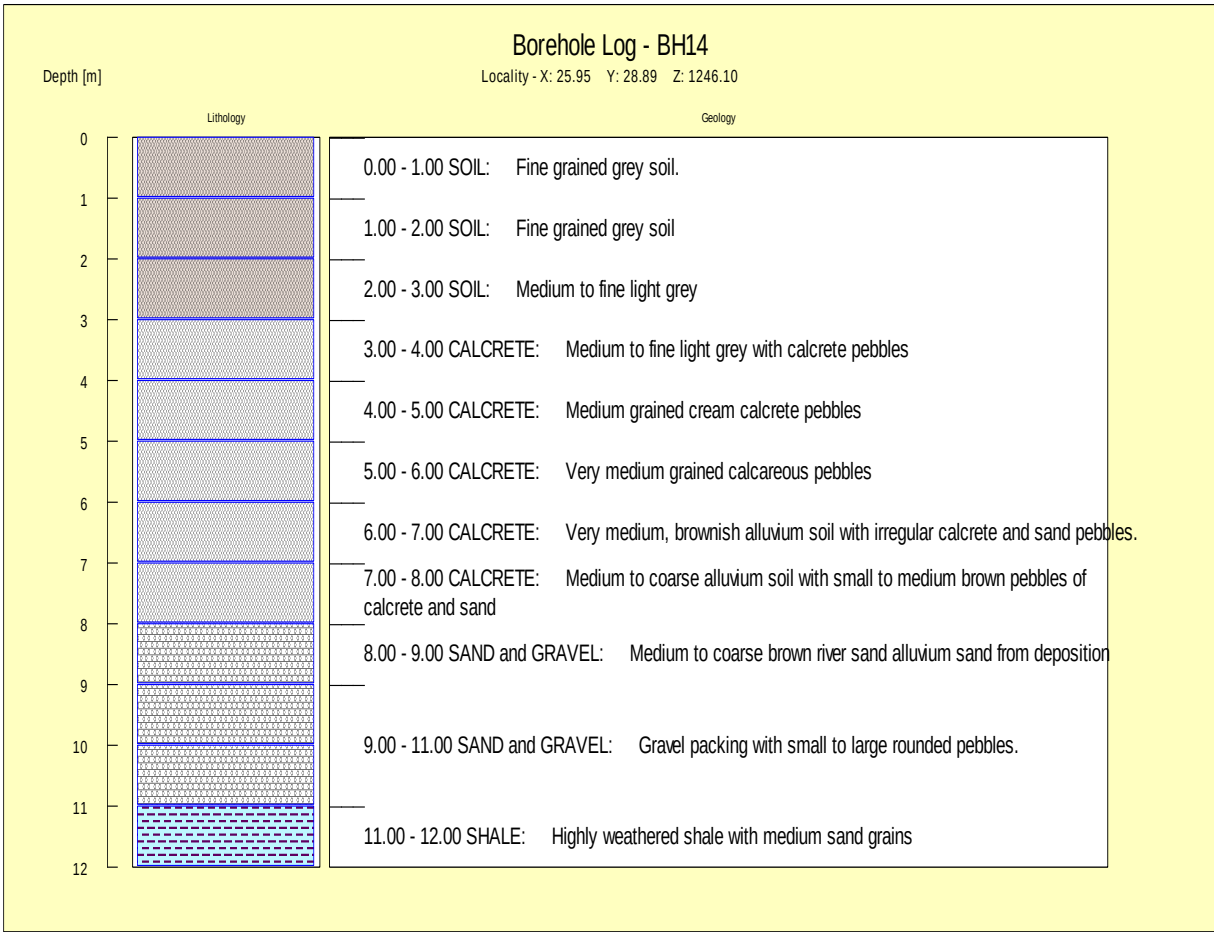

Figure 9-7: BH14 core geological log.

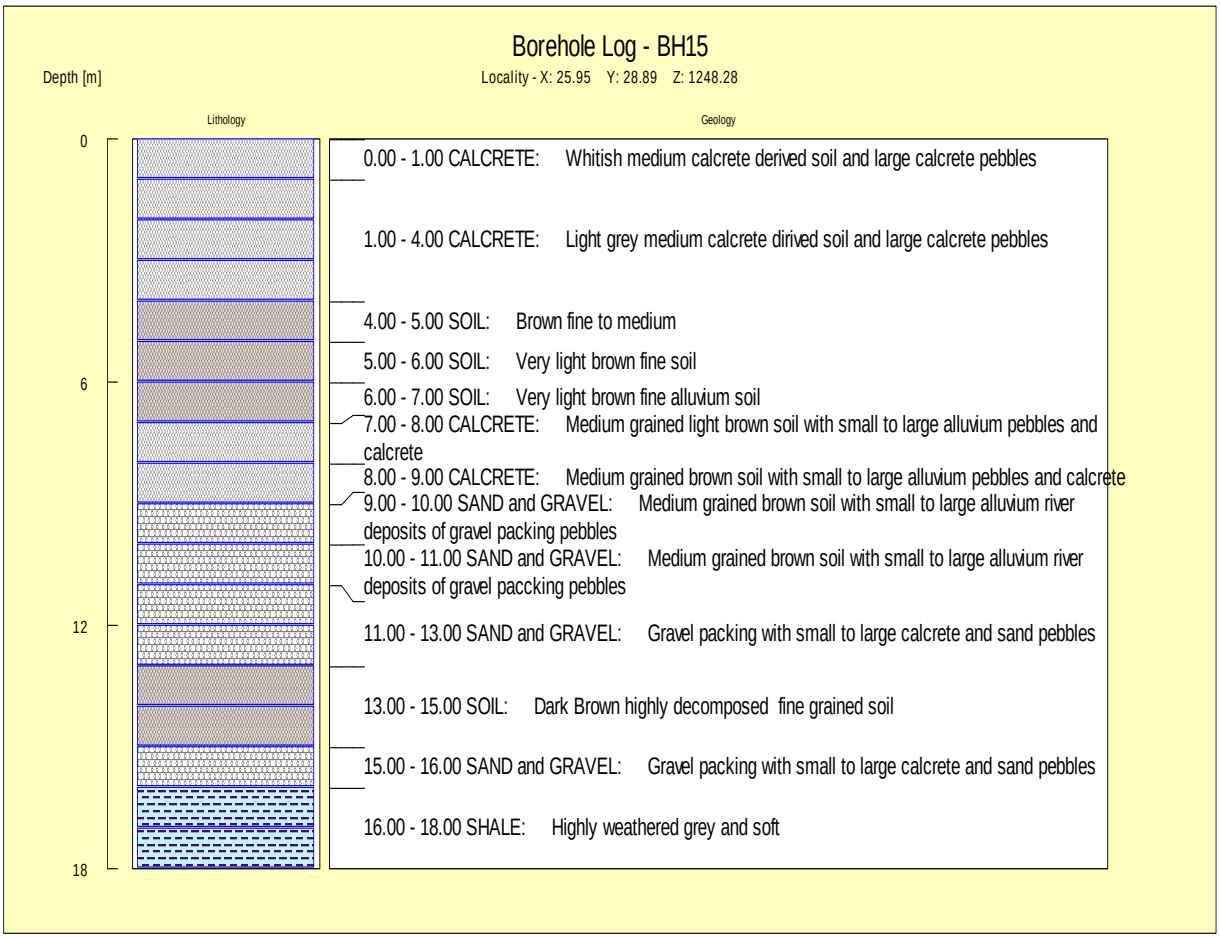

Figure 9-8: BH15 core geological log.

9.2 Appendix B: Hydraulic tests

Aquifer tests

Aquifer test data and FC programmes can be found in the provided spread sheets in the Appendix Disc.

Point dilution tracer test

Table 9-1 to Table 9-4 show the standardized concentrations of NaCl while Figure 9-9 to Figure 9-12 show the decay of standardized concentrations of NaCl in BH10, BH11, BH12 and BH13.

Table 9-1: Standardized concentration of NaCl during point dilution tracer test.

r (m)	0.16	Borehole radius		
L (m)	2	Length of tested section		
α	2	Distortion factor		
pi	3.142			
BH10		BH ID		
BV	43.5	Background value		
t (mins)	**t (days)**	**mS/m**	**standardized concentration**	**q m/d**
0	0	296.7	1	
1	0.000694	107.7	0.25	79.04
2	0.001389	90.1	0.18	48.75
3	0.002083	86.7	0.17	33.95
4	0.002778	84.2	0.16	26.32
5	0.003472	84	0.16	21.11
11	0.007639	84.7	0.16	9.51
12	0.008333	85.4	0.17	8.63
13	0.009028	84.7	0.16	8.05
14	0.009722	84.7	0.16	7.47
15	0.010417	84.7	0.16	6.97
20	0.013889	82.8	0.16	5.37
26	0.018056	81.4	0.15	4.21
30	0.020833	80.7	0.15	3.68
40	0.027778	79.1	0.14	2.83
50	0.034722	76.8	0.13	2.34
60	0.041667	74.7	0.12	2.01
77	0.053472	64.3	0.08	1.87
90	0.0625	59.9	0.06	12.16
120	0.083333	51	0.03	24.34
	geometric mean			9.1

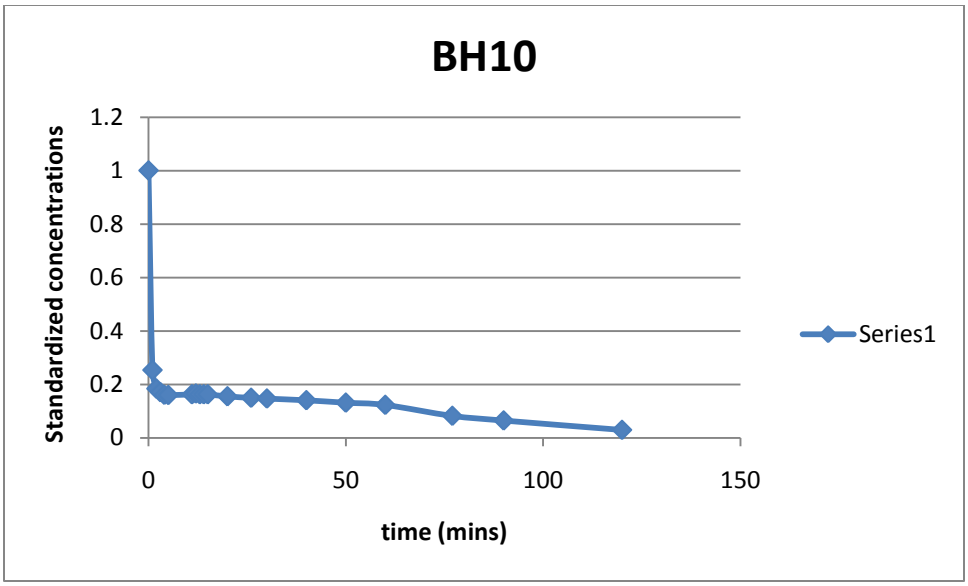

Figure 9-9: Decay of standardized concentration in BH10 during point dilution tracer test.

Table 9-2: Standardized concentrations of NaCl during a point dilution tracer test in BH11

r (m)	0.16		Borehole radius	
L (m)	2		Length of tested section	
α	2		Distortion factor	
pi	3.142		pie	
BH11			BH ID	
BV mS/m	79.7		Background Value	
t (mins)	**t (days)**	**ms/m**	**standardized concentration**	**q m/d**
0	0	194.9	1	
1	0.000694	182.1	0.89	6.78
2	0.001389	145.4	0.57	16.17
3	0.002083	120.4	0.35	19.98
4	0.002778	115.7	0.31	16.75
5	0.003472	99.5	0.17	20.29
6	0.004167	93.5	0.12	20.37
7	0.004861	93.3	0.18	17.58
8	0.005556	92.9	0.11	15.60
9	0.00625	93.3	0.12	13.67
14	0.009722	90.9	0.10	9.59
15	0.010417	90.4	0.09	9.13
16	0.011111	89.9	0.09	8.73
17	0.011806	89.5	0.09	8.35
18	0.0125	89.1	0.08	8.02

19	0.013194	88.6	0.08	7.76
20	0.013889	87.4	0.07	7.79
25	0.017361	82	0.02	9.02
	Geometric mean			11.8

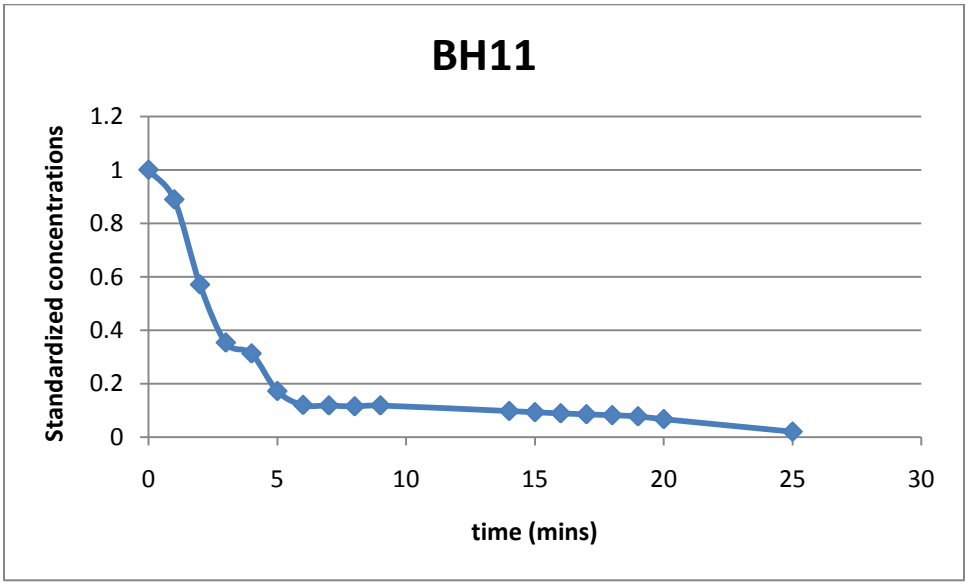

Figure 9-10: Decay of standardized concentrations in BH11 during a point dilution tracer test.

Table 9-3: Standardized concentrations of NaCl during a point dilution tracer test in BH12.

r (m)	0.165	Borehole radius	
L (m)	1	Length of tested section	
α	2	Distortion factor	
pi	3.142		
BH12		BH ID	
BV	56.3	Background value	
t (days)	**ms/m**	**standardized concentration**	**q m/d**
0	100.6	1	
0.000694	97.7	0.93	4.02
0.001389	93.9	0.85	4.87
0.002083	88.8	0.73	6.13
0.002778	81.7	0.57	8.26
0.003472	80.9	0.56	6.99

0.004167	80.9	0.56	5.82
0.004861	79.5	0.52	5.49
0.005556	76.2	0.45	5.94
0.00625	73.9	0.40	6.09
0.006944	73.7	0.39	5.55
0.007639	73.7	0.39	5.05
0.008333	73.7	0.39	4.63
0.009028	73.4	0.39	4.35
0.010417	70.9	0.33	4.40
0.011111	70.7	0.33	4.17
0.011806	69.9	0.31	4.13
0.0125	68.6	0.28	4.23
0.013194	68.5	0.28	4.03
0.013889	68.5	0.28	3.83
0.017361	66.8	0.24	3.42
0.020833	64.9	0.19	3.25
0.027778	63.7	0.17	2.66
0.034722	62.2	0.13	2.40
0.041667	61	0.11	2.22
Geometric mean			4.4

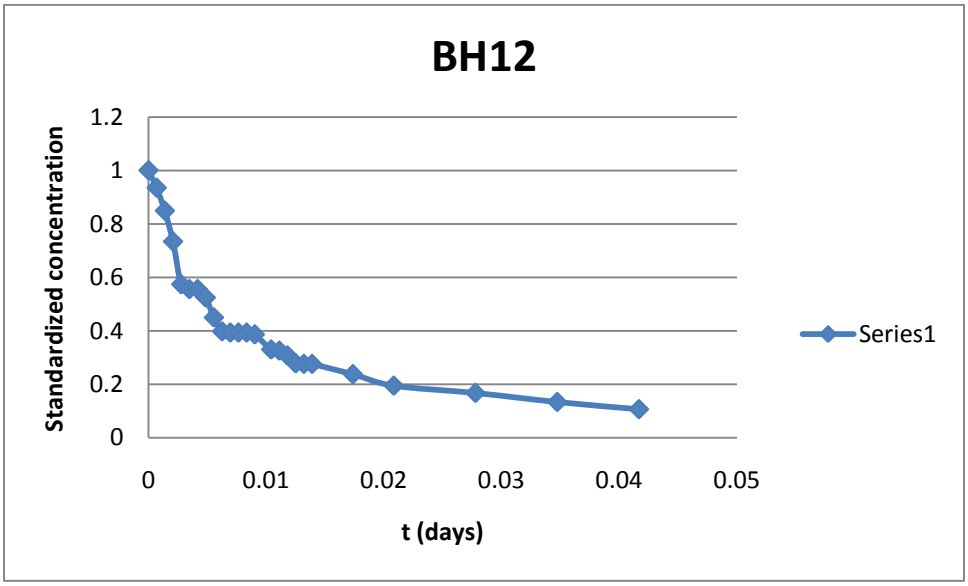

Figure 9-11: Decay of standardized concentrations in BH12 during a point dilution tracer test.

Table 9-4: Standardized concentrations of NaCl during a point dilution tracer test in BH13.

r (m)	0.16	Borehole radius		
L (m)	2	Length of tested section		
α	2	Distortion factor		
pi	3.142			
BH13		BHID		
BV	51.5	Background Value		
t (mins)	**t (days)**	**ms/m**	**standardized concentration**	**q m/d**
0	0	149	1	
1	0.000694	136.7	0.87	7.77
2	0.001389	125.6	0.76	7.90
3	0.002083	118.9	0.69	7.09
4	0.002778	114	0.64	6.40
5	0.003472	110	0.60	5.88
6	0.004167	106.8	0.57	5.44
7	0.004861	104.9	0.55	4.95
8	0.005556	102.1	0.52	4.72
9	0.00625	99.2	0.49	4.58
10	0.006944	97.4	0.47	4.34
11	0.007639	94.7	0.44	4.26
12	0.008333	92	0.42	4.22
13	0.009028	90.2	0.40	4.09
14	0.009722	88.8	0.38	3.95
15	0.010417	86.3	0.36	3.96
16	0.011111	85.1	0.34	3.84
17	0.011806	83.1	0.32	3.82
18	0.0125	81.6	0.31	3.76
19	0.013194	79	0.28	3.84
25	0.017361	67.9	0.17	4.11
30	0.020833	64.1	0.13	3.93
40	0.027778	57.6	0.06	3.99
50	0.034722	54.6	0.03	3.97
Geometric mean				4.7

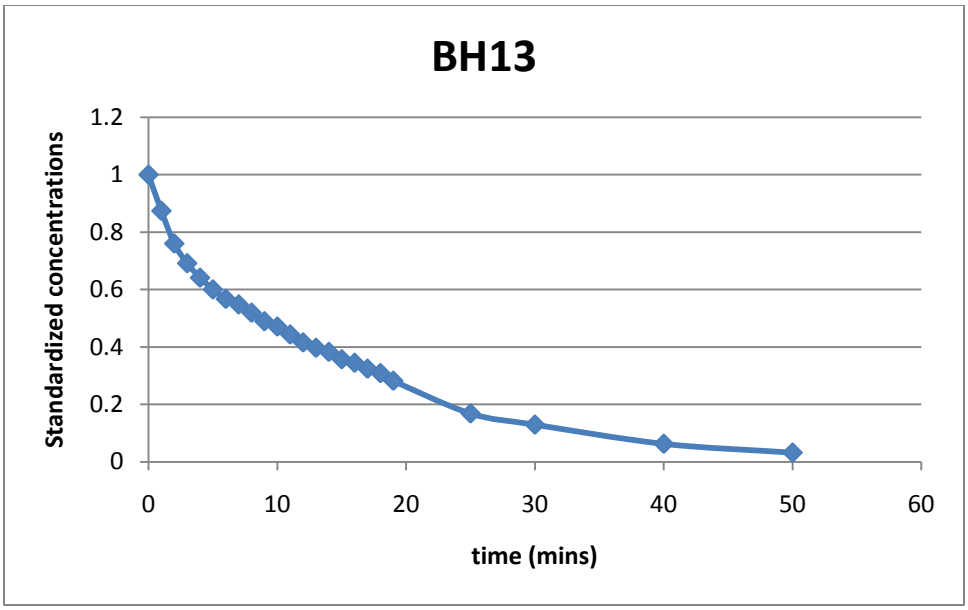

Figure 9-12: Decay of standardized concentrations of NaCl during a point dilution tracer test in BH13.

9.3 Appendix C: Natural Groundwater Behaviour

Figure 9-13: Illustration of how groundwater flow directions are being determined manually (IDEQ, 2010).

Determining the Direction Ground Water Flows

Ground water usually flows toward, and eventually drains into, streams, rivers, and lakes. The flow of ground water in aquifers does not always mirror the flow of water on the surface. The following steps show how to determine the direction ground water is flowing and the hydraulic gradient within an unconfined aquifer:

Step 1. Determine the **water table elevation** at three locations. To do this subtract the **depth to water** from the **surface elevation** at each well. Can you find the water table elevation for each of the three wells shown in figure 1?

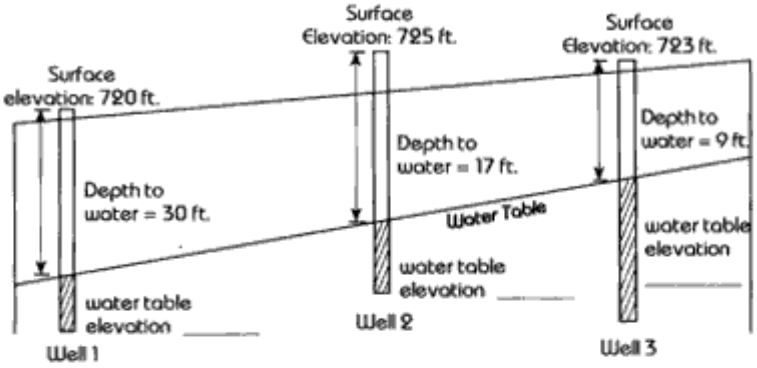

Figure 1.

Step 2. The well locations from step one are shown in figure 2. The difference in **water table elevations** between each of the wells is determined by subtracting the water table elevation of a well with a higher elevation from the water table elevation of a well with a lower elevation on each of the straight lines connecting the wells. These elevation differences are divided up into equal increments as shown in figure 2. Water table elevation levels have been placed on the figure by adding the initial water level to each increment. Draw straight lines connecting the increments which have the same values. These lines represent the water table contours.

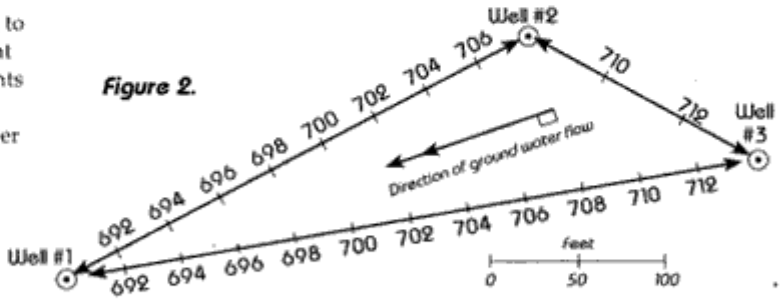

Figure 2.

Step 3. The ground water will flow from higher elevations to lower elevations in the direction of maximum change in elevation. The line perpendicular to the straight lines which connect the elevation increments indicates the direction that ground water flows.

The vertical change in ground water elevation over horizontal distance, in the direction of ground water flow, is called the **hydraulic gradient.** It can be determined for this example using the following equation:

$$\text{Hydraulic Gradient} = \frac{\text{Water Table Elevation Change (in the direction of flow)}}{\text{Horizontal Distance between measurement points}}$$

This means the **water table elevation** decreases by ___ feet for every foot the ground water flows.

The excel spread sheets for groundwater direction determinations have been provided in the Appendix Disc (Appendix C).

Recharge

In addition to the following table, the spreadsheet is provided on Appendix Disc (Appendix C).

Table 9-5: Recharge calculations using Chloride method.

Cl.rainfall (mg/l)	1			
Rfav (mm/a)	559	annual rainfall		
Krugersdrift 24 Jan				
Number	**Cl**	**a (recharge coefficient)**	**% recharge**	**Rf.av(mm/a)**
BH1	57.00	1.75E-02	1.8	9.81
BH2	54.00	1.85E-02	1.9	10.4
BH3	70.00	1.43E-02	1.4	7.99
BH4	53.00	1.89E-02	1.9	10.5
BH5	61.00	1.64E-02	1.6	9.16
BH6	60.00	1.67E-02	1.7	9.32
BH7	60.00	1.67E-02	1.7	9.32
BH8	69.00	1.45E-02	1.4	8.10
BH9	70.00	1.43E-02	1.4	7.99
BH10	57.00	1.75E-02	1.8	9.81
BH11	59.00	1.69E-02	1.7	9.47
BH12	57.00	1.75E-02	1.8	9.81
BH13	59.00	1.69E-02	1.7	9.47
BH14	51.44	1.94E-02	1.9	10.9
BH15	48.84	2.05E-02	2.0	11.4
S1	64.00	1.56E-02	1.6	8.73
Geometric mean			1.69	

9.4 Appendix D: Chemistry

Table 9-6 and Table 9-7 show the chemistry and isotope data for groundwater samples on the 24th January 2011.

Macro and trace element data

Table 9-6: Groundwater chemistry as analyzed in the IGS laboratory.

Sampling date	24 January 2011								
BH Number	**pH**	**EC**	**Ca**	**Mg**	**Na**	**K**	**PAlk**	**MAlk**	**F**
BH1	7.45	96.9	39.32	40.65	113.10	5.10	0	411	0.56
BH2	7.36	90.1	39.42	40.09	93.29	8.23	0	381	0.49
BH3	7.57	109	36.31	50.06	157.34	5.59	0	589	0.67
BH4	7.48	89.1	39.95	43.30	100.12	5.42	0	381	0.51
BH5	7.46	105	35.54	56.60	123.66	5.58	0	462	0.62
BH6	7.45	99.3	41.66	48.91	114.49	5.58	0	426	0.55
BH7	7.43	100	34.35	49.50	111.73	5.70	0	430	0.57
BH8	7.68	105	35.65	47.35	124.83	5.60	0	436	0.55
BH9	7.55	104	37.55	45.18	121.54	5.31	0	424	0.57
BH10	7.52	93.4	37.29	42.37	103.35	5.26	0	394	0.54
BH11	7.61	94.9	34.62	41.43	108.99	5.50	0	398	0.53
BH12	7.63	93.6	36.32	41.59	106.68	5.40	0	395	0.49
BH13	7.63	94.5	35.47	42.21	108.56	5.41	0	396	0.51
BH14	7.46	88.3	40.94	42.28	86.50	4.75	0	380	0.41
BH15	7.49	86.5	40.45	41.53	84.14	4.85	0	373	0.36
Seepage	7.57	111	44.02	58.28	119.83	5.85	0	485	0.65
River water Cys2 BH1	7.31	30	16.2	7.3	27.0	6.5	0	99	0.17
100m from Weir	7.26	29.9	22.0	8.9	23.5	6.6	0	99.7	0.16

Table 9-6 continued.

BH Number	Cl	NO_2(N)	Br	NO_3(N)	PO_4	SO_4	Al	Fe	Mn
BH1	57.00	0.01	0.19	0.37	-0.10	25.65	0.033	0.044	0.002
BH2	54.00	0.30	0.24	0.82	-0.10	21.87	0.031	0.058	0.002
BH3	70.00	-0.01	0.30	0.18	-0.10	31.27	0.031	0.039	0.002
BH4	53.00	-0.01	0.29	0.37	-0.10	21.32	0.049	0.067	0.002
BH5	61.00	-0.01	0.31	0.00	-0.10	26.31	0.031	0.036	0.090
BH6	60.00	-0.01	0.32	0.23	-0.10	25.76	0.033	0.044	0.002
BH7	60.00	-0.01	0.36	0.08	-0.10	26.05	0.040	0.045	0.005
BH8	69.00	-0.01	0.36	0.25	-0.10	32.02	0.026	0.033	0.002
BH9	70.00	-0.01	0.34	0.32	-0.10	34.05	0.032	0.039	0.002
BH10	57.00	-0.01	0.20	0.34	-0.10	24.82	0.032	0.034	0.002
BH11	59.00	-0.01	0.28	0.33	-0.10	26.41	0.032	0.038	0.002
BH12	57.00	-0.01	0.28	0.31	-0.10	24.87	0.030	0.054	0.002
BH13	59.00	-0.01	0.27	0.37	-0.10	26.56	0.027	0.034	0.002
BH14	51.44	0.02	0.25	0.51	-0.10	20.56	0.032	0.036	0.005
BH15	48.84	0.02	0.31	0.51	-0.10	20.02	0.027	0.034	0.003
Seepage	64.00	-0.01	0.33	0.07	-0.10	29.16	0.032	0.041	0.002
River water near Cys2 BH1	24.53	-0.01	0.03	0.40	-0.10	16.15	0.096	0.107	0.031
100m from Weir	22.16	-0.01	0.08	0.46	-0.10	15.08	0.089	0.110	0.020

Table 9-7: Isotope data as analysed by Ithemba laboratory.

Laboratory Number	Sample Identification	δ D‰	$\delta^{18}0$
IGS 043	BH1	-32.8	-4.97
IGS 044	BH2	-33.9	-4.97
IGS 045	BH3	-33.7	-5.02
IGS 046	BH4	-34.4	-5.01
IGS 047	BH5	-34.1	-5.09
IGS 048	BH6	-32.5	-5.09
IGS 049	BH7	-33.3	-5.00
IGS 050	BH8	-32.7	-5.01
IGS 051	BH9	-32.9	-4.95
IGS 052	BH10	-32.4	-4.97
IGS 053	BH11	-32.8	-5.02
IGS 054	BH12	-32.9	-5.06
IGS 055	BH13	-32.5	-5.04
IGS 056	BH14	-33.1	-5.12
IGS 057	BH15	-33.7	-5.12
IGS 058	S1	-33.7	-5.12
IGS 059	RIVER WATER 4.7KM	-17.7	-2.86
IGS 060	RIVER WATER 5KM	-17.4	-2.78

Summary

The Institute for Groundwater Studies (IGS) undertook a groundwater surface water interaction project under the funding of Water Research Commission starting July 2010. The Modder River was identified as an appropriate study area since it is located downstream of Krugersdrift Dam and has only been impacted by farming activities.

This thesis aims at investigating the hydraulic parameters and flow characteristics of groundwater in the study area aquifer so as to have a preliminary picture of the groundwater systems of the site prior to the groundwater surface water interaction project takeoff.

The field procedures were performed starting with site inspection, drilling, water level monitoring, pumping tests, tracer tests, and chemical sampling. Geological classification was performed during site inspection and drilling, while soil cover was analysed for texture analysis in the soil science laboratory. Water level monitoring was performed to study the groundwater fluctuations and flow directions with time. Constant rate tests were performed together with recovery tests to determine the transmissivity of the aquifer in the study area while point dilution tracer tests were done to determine the Darcy velocity of the section of maximum flow in the aquifer. In chemical analysis, micro and macro analysis were performed while tritium ^{3}H, Deuterium ^{2}H, and 18-Oxygen were analysed for in isotope analysis. Chemistry and isotope analysis were done to classify water in terms of its source, fate and age.

From all boreholes, at the average depth of 8 meters, an alluvial material was obtained in between the top calcareous soil material and the bottom shale formation. The water level fluctuation trend was similar in all boreholes indicating possibilities of a common aquifer intercepted by all boreholes. Using water level time series, groundwater flow direction was determined to be towards the North-Eastern direction slightly in the direction of local topography while the river flow is westwards. The geometric mean of transmissivity values obtained from a Cooper-Jacob plot is 66 m^2/d and the geometric mean for the recharge value from chloride method is 1.7 %. The geometric mean of the Darcy velocity value obtained from different boreholes in the aquifer is 6.9 m/d. These mean values are representative of the whole aquifer.

In addition to flow direction being due to topography, it is hypothesized that the unusual flow direction behaviour is due to the seepage that acts like a natural borehole at the river bank such that a semi-cone of depression is formed towards the North East. In hydrochemistry, the most abundant cation is sodium followed by magnesium and the most abundant anion is T.Alk (carbonates). From a Piper diagram, groundwater was characterized to be calcium magnesium

bicarbonate type of water. The SAR of groundwater is low and within the recommended value for irrigation agriculture while the EC is so high that the water is recommended strictly for crops that are not sensitive to brackish water. According to the isotope analysis, the water from the boreholes and seepage seem to have the same isotopic fingerprint. Needless to say that, the water that seeps on the banks is the same water as that from the aquifer that is intercepted by the boreholes. Groundwater plots closer to the global meteoric water line than river water which plots on the evaporation water line, needless to say that, river water is evaporation water rich in 18-oxygen while groundwater experiences less evaporation hence high 16-oxygen content.

The hydrogeology of the area is therefore characterized by the presence of major flow in the gravel material at the average depth of 8 meters.